Analysis of Virulence-Associated Petrobactin Reacquisition in *Bacillus anthracis*

by

Shandee Dawn Dixon

A dissertation submitted in partial fulfillment
of the requirements for the degree of
Doctor of Philosophy
(Microbiology and Immunology)
in The University of Michigan
2013

Doctoral Committee:

Professor Philip C. Hanna, Chair
Professor Carol A. Fierke
Associate Professor Maria B. Sandkvist
Professor David H. Sherman

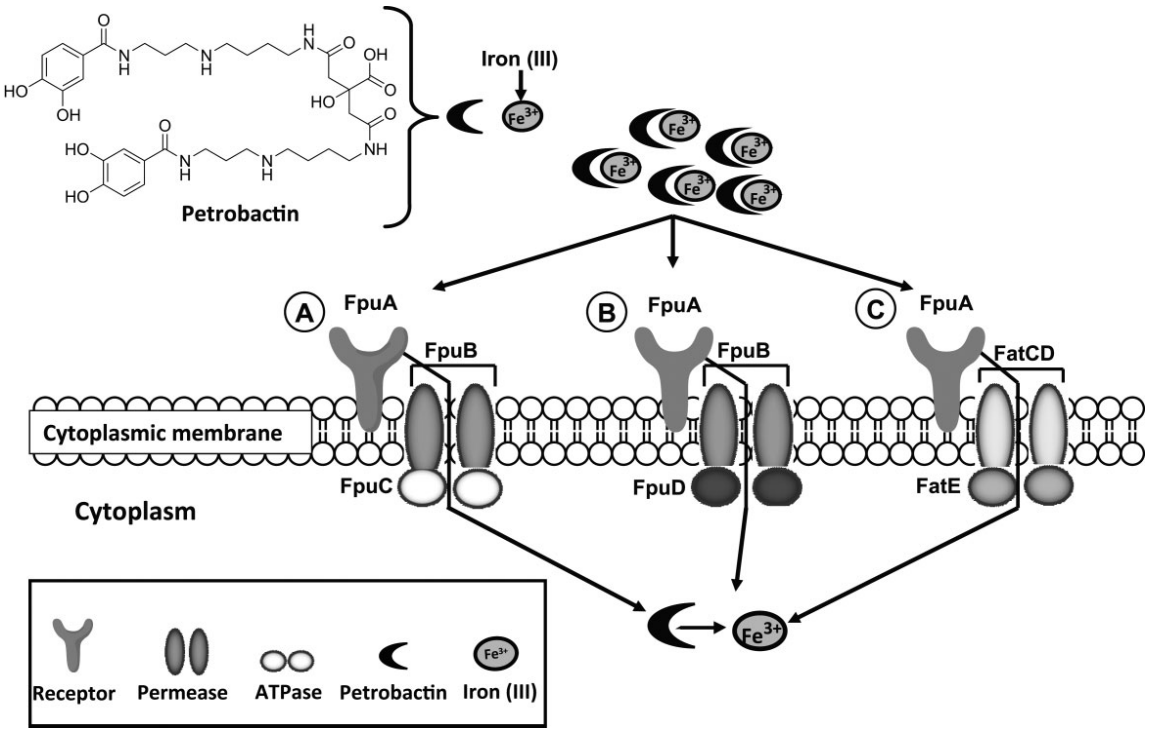

The Bacillus anthracis Petrobactin ATP-Binding Cassette (ABC) Import System

DEDICATION

For my Family

PREFACE

This written dissertation summarizes the labor and thought invested in my graduate studies to develop a better understanding of how *Bacillus anthracis* reacquires the vital siderophore petrobactin back into the cytoplasm after sequestering iron from its host. The identification of this system and the elucidation of the mechanisms involved in the reacquisition of iron-bound petrobactin will greatly improve our current knowledge of *Bacillus anthracis* pathogenesis.

This body of work is divided into four chapters. Chapter 1 introduces the general importance of iron in microbial biology and aspects of iron acquisition in *Bacillus anthracis*. An emphasis is placed on current research surrounding the virulence-associated siderophore petrobactin and introduces the uptake mechanisms employed by bacteria to reacquire iron-bound siderophores. Additionally, Chapter 1 describes work I performed along with my colleagues during my first year in the Hanna laboratory which provides the first description of the only receptor protein required for the reacquisition of petrobactin. This research has been published as an article in the journal Molecular Microbiology (Carlson PE Jr, Dixon SD, Janes BK, Carr KA, Nusca TD, Anderson EC, Keene SE, Sherman DH, and Hanna PC 2008. "Genetic analysis of petrobactin transport in *Bacillus anthracis*." *Mol Microbiol.* 2010 Feb;75(4):900-9).

Chapter 2 describes work performed to identify the remaining components of the petrobactin import system. Mutants of candidate permease and ATPase genes were

generated allowing for characterization of multiple petrobactin ATP-binding cassette (ABC)-import systems. The research put forth in Chapter 3 has been published in the journal of Molecular Microbiology (Dixon SD, Janes BK, Bourgis A, Carlson PE Jr, and Hanna PC. 2012. "Multiple ABC transporters are involved in the acquisition of petrobactin in *Bacillus anthracis*". *Mol Microbiol.* 2012 Apr;84(2):370-82.)

Findings in Chapter 2 directed my focus onto designing a biochemical assay to identify small molecule inhibitors of petrobactin ABC-import machinery. The identified ABC-transport proteins described in Chapter 2 are essential in cell viability, virulence and pathogenicity, and have conserved sequences across all bacterial species, making these proteins intriguing targets for therapeutics. Because active ATPases can be easily purified and only requires ATP as a substrate, these enzymes are prime candidates for a high-throughput inhibitor search. Chapter 3 describes my efforts to design and implement a high-throughput screen (HTS) at the University of Michigan Center for Chemical Genomics (CCG) to search for novel molecules capable of inhibiting the activity of these crucial ATPase proteins. By investigating methods to inhibit the activity of these ATPases, my overall goal was to devise a strategy to shut down siderophore import and thus the necessary act of iron acquisition by *B. anthracis* and other dangerous pathogens.

As a closing section, Chapter 4 aims to summarize the research presented in Chapters 2 and 3 as well as its possible implications in the fields of microbial iron-acquisition and the development of novel therapeutics against bacterial infection. Generally, Chapter 4 encompasses hypothetical and future avenues of experimentation that were made more apparent by the body of this dissertation; however, in some instances, preliminary data is presented.

TABLE OF CONTENTS

LIST OF FIGURES

Figure

LIST OF TABLES

Table

ABSTRACT

In Bacillus anthracis the siderophore petrobactin is vital for iron acquisition and virulence. The petrobactin-binding receptor FpuA is required for these processes. FpuA has high homology to the receptors associated with ATP-binding Cassette (ABC) transporter complexes, indicating that the mechanism of petrobactin reacquisition requires an ABC transport system. ABC transporters are used by bacteria for cross-membrane transport of many small molecules. Recently, the additional components of petrobactin reacquisition have been identified. We have shown that either of two distinct permeases, FpuB or FatCD, are required for iron acquisition and play redundant roles in petrobactin transport. Additionally, three ATPase proteins are sufficient to provide the energy required for petrobactin reacquisition. These results provide the first description of the permease and ATPase proteins required for the import of petrobactin in *B. anthracis*. Furthermore, these ABC-transport proteins are essential in cell viability, virulence and pathogenicity. The ABC ATPases share conserved sequences across all bacterial species, and only requires ATP as a substrate, making these proteins prime candidates for a high-throughput inhibitor search for small molecules that can potentially block siderophore import and thus the necessary act of iron acquisition by *B. anthracis* and other dangerous pathogens. Sixteen top ATPase inhibitor hits were identified in a pilot high-throughput screen at the University of Michigan Center for Chemical

Genomics. Eight of which were reconfirmed at the bench-top to reveal three compounds as promising leads in the development of therapeutics or tools to probe ATPase activity.

Chapter 1

Introduction

1.1 Introduction

Bacillus anthracis is a member of the *Bacillus cereus* group species which are a collection of Gram-positive, rod shaped, spore-forming bacteria that typically exist in the soil (Hanna, 1998a). Despite the fact that members of the *B. cereus* group are closely related in genetics and physiology, there are very distinct species-specific phenotypes displayed by each, and importantly, a number of these are related to pathogenicity (Hanna, 1998a). This is the case with *B. anthracis,* in which respiratory, gastrointestinal, or cutaneous entry of spores into a mammalian host can lead to anthrax infection. Each of these routes results in a different disease manifestation with the inhalational form being most severe (Hanna, 1998b, Dixon *et al.*, 1999, Doganay & Welsby, 2006). In the inhalational route of infection, the spore is the infectious form of the organism (Bartrand *et al.*, 2008, Dutz & Kohout, 1971, Dutz & Kohout-Dutz, 1981, Guidi-Rontani *et al.*, 1999)**.** Once latent spores make their way to the lung epithelium, host antigen-presenting cells, primarily macrophages and dendritic cells, phagocytose the infectious spore and shuttle it to other parts of the lymphatic system (Dixon et al., 1999, Doganay & Welsby, 2006, Dutz & Kohout, 1971, Moayeri *et al.*, 2012). It is at this later stage of host ingress where the spore finally germinates into vegetative cells and begins to rapidly replicate to extremely high titers, up to 10^8 organisms per milliliter in the blood and, through the

effects of secreted toxins, cause severe edema that directly contributes to lethality (Frankel *et al.*, 2009, H onsa & Maresso). The rapid and high lethality of anthrax, combined with the resilience of latent spores both in the environment and in a weaponized form, have made *B. anthracis* a practical system in which to study mechanisms of bacterial pathogenesis (Sweeney *et al.*, 2011).

It has been demonstrated that the metal iron facilitates activities including DNA replication, amino acid synthesis, electron transport and lipid conversion that can be associated with the extensive cell division observed by *B. anthracis* in the blood. Furthermore, the secondary metabolite petrobactin, nearly unique to *B. anthracis* and closely related species in the *B. cereus* group, is required for necessary levels of iron acquisition in the host. Despite the importance of petrobactin, and having had its biosynthetic pathways elucidated, little was known regarding how this molecule was recognized and transported by *B. anthracis*. Based on t his, I describe in this thesis studies identifying the key components of the petrobactin-iron import machinery in *B. anthracis*, and explore how these proteins may be inhibited with the goal of shutting down requisite iron acquisition of dangerous and problematic bacterial pathogens.

1.2 Importance of Iron during Anthrax Infection

For pathogenic bacteria, including *B. anthracis*, iron acquisition is essential for survival under iron limited conditions (Ratledge & Dover, 2000). The transition metal, iron, is involved in multiple biological phenomena essential to life that include a variety of metabolic and signaling functions such as oxygen transport and respiration, electron transfer, and DNA synthesis and repair (Latunde-Dada, 2009). The roles of iron in these

vital processes make this metal a necessary nutrient for the growth and proliferation of bacteria (Ratledge & Dover, 2000, Faraldo-Gomez & Sansom, 2003, Wandersman & Delepelaire, 2004). Bacteria must acquire iron from the extracellular milieu they occupy by employing dedicated mechanisms for iron acquisition, transport and storage (Schaible & Kaufmann, 2004). This includes within the context of a host, in which ability of a microorganism to sequester iron is one of the major determinants of its survival and virulence (Andrews *et al.*, 2003, Barclay & Ratledge, 1986, Garénaux *et al.*, 2011, Ratledge, 2007, Ratledge & Dover, 2000, Ratledge & Winder, 1964, Wandersman & Delepelaire, 2004).

Iron is typically found in the +2 (ferrous) and +3 (ferric) oxidation states in biological systems (Ratledge, 2007, Ratledge & Dover, 2000, Miethke & Marahiel, 2007, Davidson *et al.*, 2008). Free ferric iron has inherent toxicity arising from the tendency of the metal to cycle between the Fe^{3+} / Fe^{2+} oxidation states thereby generating damaging hydroxyl radicals through Fenton chemistry (Wardman & Candeias, 1996). Because of this, the majority of free iron in the mammalian host is bound to carrier proteins such as lactoferrin, transferrin and ferritin, or the protoporphyrin ring in hemoproteins such as hemoglobin (Ratledge & Dover, 2000, Glanfield *et al.*, 2007, Nemeth & Ganz, 2006, Ganz & Nemeth, 2006). This tight regulation results in a free iron concentration of virtually zero in extracellular body fluids (Andrews et al., 2003). The limited availability of free iron serves as a barrier against bacterial infection, an example of a strategy often referred to as "nutritional immunity" (Hood & Skaar, 2012, Cassat & Skaar, 2012, Dragomirescu *et al.*, 1979, Weinberg, 1975), as bacteria that are unable to obtain iron are rendered helpless against host defenses as a result of iron starvation (Lewin, 1984).

During early stages of infection, iron is also necessary for mounting specific bacterial countermeasures against host immune defenses. The release of reactive oxygen species by neutrophils and other immune cells has a strong antibacterial effect, and infection by *B. anthracis* is highly reliant on proteins requiring iron as a cofactor, including cystathionine β-synthase, responsible for accumulation of reductive H_2S (Shatalin *et al.*), and a suite of redundant superoxide dismutases (SODs) to combat oxidative stress (Cybulski *et al.*, 2009, Passalacqua *et al.*, 2006). In fact, copies of SOD constitute one of the three main iron reservoirs in *B. anthracis* along with the bacterioferritin Dps2 and ferredoxin (Tu *et al.,* Passalacqua *et al.*, 2007a).

Faced with this strict iron shortage, *B. anthracis* and several other bacterial species have evolved a variety of iron acquisition mechanisms to sequester the metal from host proteins and compete with other organisms sharing the same biological niche. There are two primary mechanisms of iron-acquisition in *B. anthracis* which include siderophore-mediated iron sequestration and import and heme uptake, both of which are elaborated on further in following sections (Dixon et al., 1999, Passalacqua & Bergman, 2006).

1.3 Heme-iron Acquisition

Approximately 80% of mammalian iron is bound in its ferrous state to iron-protoporphyrin IX, or heme (Mazmanian *et al.*, 2003, Maresso *et al.*, 2008). A large amount of this is further bound to the oxygen-carrier protein hemoglobin found in red blood cells, making this protein an obvious target for bacterial iron acquisition during replication in the extracellular environment (Wandersman & Delepelaire, 2004, Nobles &

Maresso, 2011, Honsa & Maresso, 2011). The heme iron acquisition system is depicted in Figure 1-1. Since heme is bound in hemoglobin, which is packaged at high levels within red blood cells, a multi-step process is required for *B. anthracis* to utilize this iron source. One mechanism that is thought to facilitate heme release involves the secretion of hemolysins that lyse red blood cells to expose hemoglobin, followed by the secretion of bacterial hemophores, namely IsdX1 and IsdX2, which sequester heme from hemoglobin, and subsequently pass it off to the cell wall anchored IsdC proteins (Honsa *et al.*, 2011, Maresso *et al.*, 2006, Maresso & Schneewind, 2006). These cell surface proteins are part of an iron-regulated surface determinant (Isd) network that uses receptors to specifically recognize heme and subsequently transfer it to the heme-specific IsdEFD ABC transport system in the cell membrane which consists of NEAr-iron transporter (NEAT) domains (Gat *et al.*, 2008, Maresso et al., 2006, Maresso & Schneewind, 2006, Honsa et al., 2011). Once inside the bacterial cytoplasm, iron is then released from heme by the action of the bacterial heme monooxygenase, IsdG (Skaar *et al.*, 2006).

Using this system, *B. anthracis* is able to grow *in vitro* with only heme as its iron source; however the complete role of heme acquisition in the life cycle or pathogenesis of *B. anthracis*, remains to be elucidated. It is hypothesized that acquisition of iron from heme would occur during later stages of infection, when *B. anthracis* is growing extracellularly in the host bloodstream (Honsa & Maresso, 2011). When directly tested, some *B. anthracis* strains lacking the ability to utilize heme retain wild-type levels of virulence in mice, while mutant strains lacking other NEAT domain containing proteins have exhibited only a mild attenuation (Honsa et al., 2011, Gat et al., 2008). While these data do not strongly support a major role for iron acquisition from heme during anthrax

infection in mice, it is possible that iron acquisition from heme is necessary for infection of more common mammalian hosts such as large herbivores, or rare hosts such as humans. Future experimentation with different experimental systems will be necessary to determine the role of heme-iron acquisition in the pathogenesis of *B. anthracis* as it is highly possible that current animal models of inhalational anthrax do not accurately portray late stage infection.

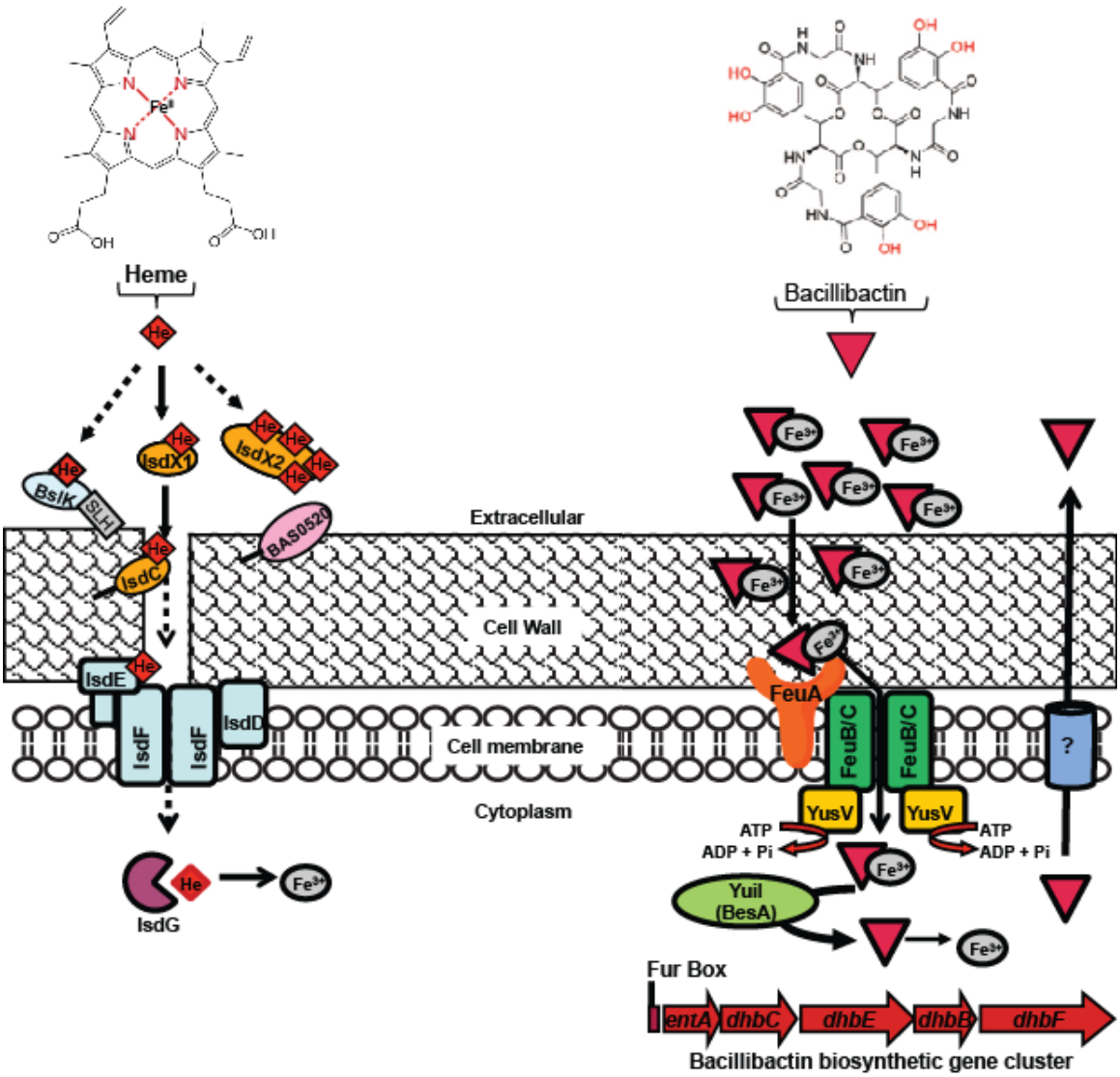

Figure 1-1. Known mechanisms of iron acquisition from heme or bacillibactin in *Bacillus anthracis*. The pathways for iron acquisition using heme (left), and bacillibactin (right) are shown here. S tructure of each molecule is shown above its respective transport system (red residues interact directly with iron). Iron binding molecules are represented by red squares (heme), and maroon triangles (bacillibactin). A ll known components of these two specific transport systems are represented. Specific components and functions of each iron acquisition system are discussed within the text. C artoon representation of the genes in the biosynthetic operon for bacillibactin is shown beneath its transport system.

1.4 *Bacillus anthracis* Siderophores

The second and primary mechanism of iron acquisition in *B. anthracis* is the production and secretion of siderophores. Siderophores are high-affinity iron chelating molecules that are secreted into the extracellular environment where they are able to scavenge ferric iron from host sources (Raymond *et al.*, 2003, Honsa & Maresso, 2011, Koster, 2001, Miethke & Marahiel, 2007, Ratledge & Dover, 2000, Neilands, 1995). Briefly, within the low iron environment of the host, siderophores' extremely high affinity for iron confers the ability to sequester the metal from host proteins (Braun & Braun, 2002). Following the scavenging of host iron, holo-iron-siderophore complexes are recognized by high affinity substrate-binding proteins on the surface of the cell membrane and are transported into the cytoplasm of the bacterium through specific membrane associated ATP Binding Cassette (ABC)-transport systems for utilization (Radnedge *et al.*, 2003, Ratledge & Dover, 2000, Beasley & Heinrichs, 2010). *Bacillus anthracis* is capable of synthesizing two siderophores, bacillibactin and petrobactin (Wilson *et al.*, 2006, H otta *et al.,* Cendrowski *et al.*, 2004c). While both of these molecules exhibit high affinity binding to ferric iron (bacillibactin $K_f = 10^{48}$; petrobactin $K_f = 10^{23}$), they differ significantly in both structure and role in bacterial pathogenesis (Cendrowski et al., 2004c, Koppisch *et al.*, 2005, Lee *et al.*, 2007).

Bacillus anthracis Siderophores

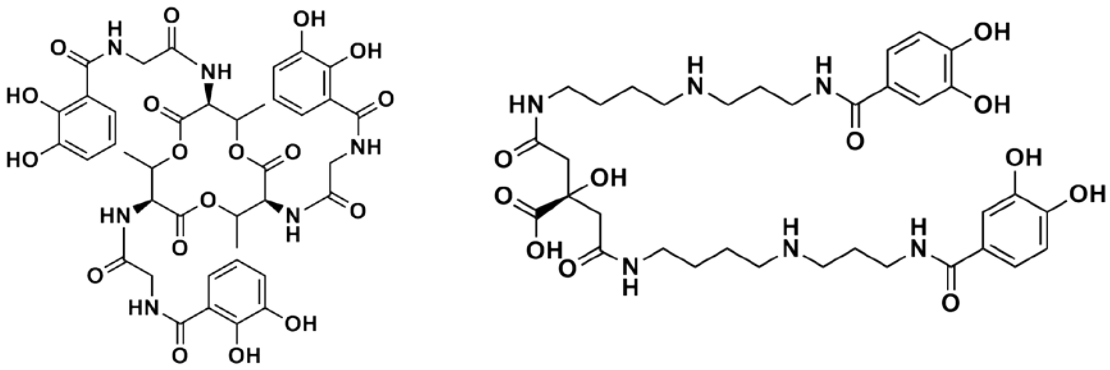

Bacillibactin **Petrobactin**

Figure 1-2. The two siderophores produced by *Bacillus anthracis*.

Bacillibactin is a tris-catecholate siderophore that is generated by a non-ribosomal peptide synthetase (NRPS) pathway encoded by the *dhb* operon (May *et al.*, 2001) and has three dihydroxybenzoate moieties with hydroxyls in a 2,3 (ortho, para) orientation (Koppisch et al., 2005) commonly found in several *Bacillus* species. Most of the data regarding the function of this siderophore is inferred from studies using *B. subtilis*. In this organism, bacillibactin is secreted through the major facilitator-superfamily protein YmfE (Miethke *et al.*, 2008). Following secretion, iron bound bacillibactin is specifically imported by an ABC import system, which is encoded by *feuABC* and *yusV*, (Figure 1-1, right) (Miethke *et al.*, 2006, Dertz *et al.*, 2006a, Dertz *et al.*, 2006b). Once inside the cytoplasm of the cell, the iron-bacillibactin complex is then hydrolyzed by the YuiL esterase (encoded by *besA*), allowing for release of imported iron ions in the cytoplasm for use by the bacterium (Figure 1-1, left) (Miethke et al., 2006, Dertz et al., 2006b).

Although bacillibactin is produced by many *Bacillus* species, it is not required for growth of *B. anthracis* under iron-limited conditions (Cendrowski et al., 2004c) even though the *B. anthracis* genome encodes orthologs of all of the proteins for synthesis and uptake of this siderophore found in other *Bacillus* spp. One possible explanation for this could be altered patterns of bacillibactin secretion. In *B. anthracis*, as compared to *B. subtilis*, secretion of bacillibactin *in vitro* appears to occur late in the life cycle, with measureable amounts of the siderophore only being detected after nearly ten hours of growth in iron limited media (Wilson *et al.*, 2010). The late secretion of this siderophore could be due to the fact that *B. anthracis* has no clear homolog of YmfE, which is largely responsible for bacillibactin secretion in *B. subtilis* (Miethke et al., 2008, Wilson et al., 2006). Similar to our current knowledge of heme-iron acquisition, there are currently no

data associating bacillibactin with virulence, suggesting that it plays, at most, a minor role during infection (Cendrowski *et al.*, 2004a). It is possible, however, that bacillibactin plays some role in the colonization of *B. anthracis* in a host organism or other niche that has yet to be studied.

1.5 Petrobactin Identification and Biosynthesis

A second siderophore, petrobactin, is found only in select strains of the *Bacillus* genus, predominantly limited to members of the *B. cereus* sensu lato group (Wilson et al., 2006). This catacholate siderophore was first isolated from the oil-degrading, Gram-negative marine microbe *Marinobacter hydrocarbonoclasticus* (Koppisch *et al.*, 2008a, Hickford *et al.*, 2004, Barbeau *et al.*, 2002, Homann *et al.*, 2009). It was in this organism that the chemical structure of petrobactin was first determined and is in fact identical to that of petrobactin produced by *B. anthracis*. Transcriptional analysis of *B. anthracis* mutants deficient for growth in iron-depleted conditions enabled identification of the pathway responsible for siderophore biosynthesis and enzymatic machinery encoded by the *B. anthracis* siderophore biosynthesis (*asb*) operon (Fig. 1-3, A) (Cendrowski *et al.*, 2004b, Koppisch et al., 2005, Liu *et al.*, 2007). The symmetrical petrobactin molecule is comprised of a central citric acid and two selectively-oriented spermidine arms, each bound by an amide bond to a unique 3,4-dihydroxybenzoic acid (3,4-DHBA) chelating moiety, to this point unknown in any other siderophore (Fig. 1-3, B) (Koppisch *et al.*, 2008b, Abergel *et al.*, 2008b, Pfleger *et al.*, 2007, Pfleger *et al.*, 2008, Lee et al., 2007).

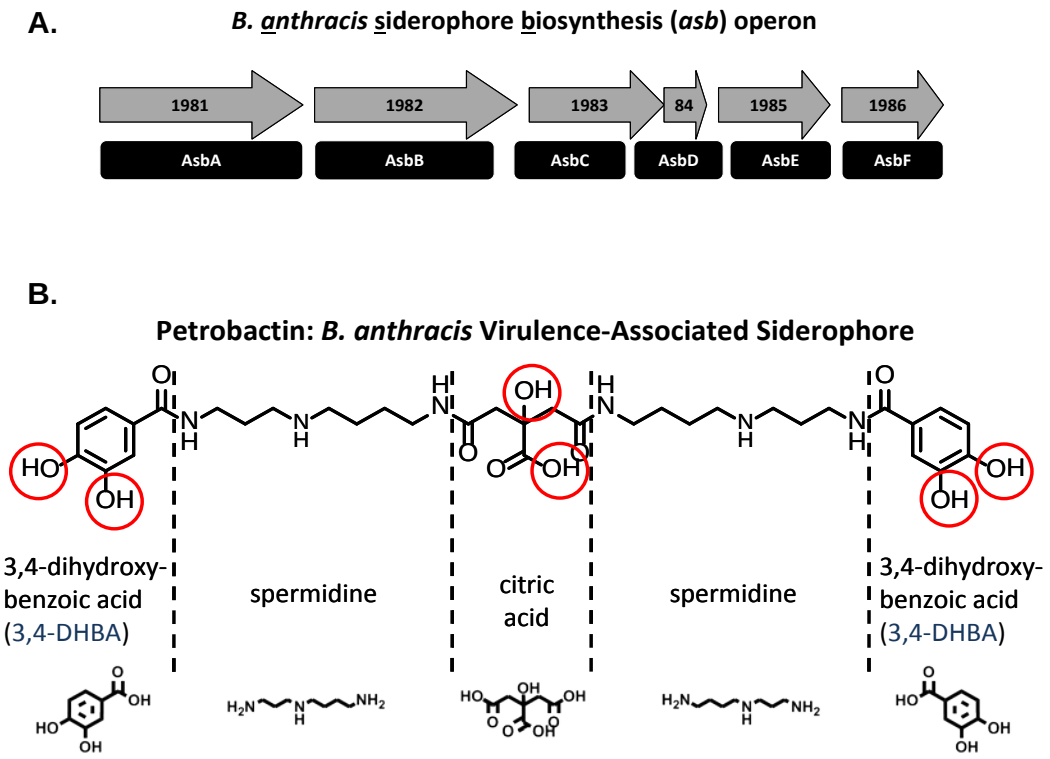

Figure 1-3. *B. anthracis* virulence-associated siderophore petrobactin biosynthetic operon and molecular structure. (A) The *anthracis* siderophore biosynthesis (*asb*) operon which encodes all of the enzymes necessary for the synthesis of petrobactin. There are 6 genes, *asbA-F*, and listed above them are their designated locus numbers in *B. anthracis* str. Ames. (B) Petrobactin is comprised of three precursors, the central citrate, two spermidine arms, and the outer catechol moieties produced by 3,4-dihydroxybenzoic acid (3,4-DHBA). Citrate and spermidine are found naturally in most bacteria, but 3,4-DHBA is a unique secondary metabolite. The orientation of the hydroxyl groups is unique and the source of petrobactin's "stealth" abilities during host infection. Petrobactin forms a hexadentate complex with an iron atom and has six chelation points circled in red (two on each catechol and two on each citrate).

Previous genetic experiments have shown that products of the polycistronic operon consisting of the six genes *asbABCDEF* contribute to assembly of petrobactin in bacteria (Lee et al., 2007). Work done in David Sherman's and Philip Hanna's lab at the University of Michigan, has shown that mutation of individual *asb* genes allowed for the assignment of function to the encoded biosynthetic polypeptides, and confirmation of the metabolites that constitute the starting components of petrobactin biosynthesis (Pfleger et al., 2007, Pfleger et al., 2008). All products of the *asb* operon have been heterologously purified and described individually *in vitro* through enzymatic assays. AsbA and AsbB are both members of the non-ribosomal peptide synthetase - independent siderophore (NIS) synthetase family (Oves-Costales *et al.*, 2007, Oves-Costales *et al.*, 2009b, Challis, 2005). Incorporation of the unique 3,4-DHBA to the spermidine "arms" of petrobactin is facilitated by interactions of AsbC, -D, and –E (Pfleger et al., 2007). These polypeptides share homology with aryl-transferase modules of many NRPS pathways, including those for mycobactin, enterobactin, and vibriobactin; such similarity in mechanism and structure has characterized petrobactin biosynthesis as a mixed NRPS/NIS pathway (Oves-Costales *et al.*, 2009a, Barry & Challis, 2009, Schmelz *et al.*, 2009, Kim *et al.*, 2008, Harrison *et al.*, 2006, Challis, 2005, Crosa & Walsh, 2002).

Pathogenic *Bacillus* species, including *B. anthracis*, *B. cereus*, and some isolates of *B. thuringiensis*, can produce petrobactin (Koppisch et al., 2005). For *B. anthracis* under iron-starved conditions *in vitro*, the level of petrobactin secretion into culture supernatants is nearly five times greater than that of bacillibactin (Koppisch et al., 2005, Wilson *et al.*, 2009a, Wilson et al., 2010). There is also a significant difference in the production of siderophore secretion, with measureable levels of petrobactin present five

hours before detection of bacillibactin *in vitro* (Wilson et al., 2010, Wilson et al., 2009a). Unlike bacillibactin, petrobactin is required for normal growth rates in low iron media and growth in macrophages (La Scola *et al.*, 2003, Lee et al., 2007, Pfleger et al., 2007). Furthermore, mutant strains lacking the ability to synthesize or import this siderophore are severely attenuated in murine models of anthrax infection (Carlson *et al.*, 2010, Cendrowski et al., 2004c, Dixon *et al.*, 2012) In fact, the level of attenuation observed for these mutants (approximately 1,000 fold) is similar to what has been observed for toxin-deficient *B. anthracis* strains (Pezard *et al.*, 1991).

1.6 Petrobactin is a "Stealth" Siderophore

Mammalian species protect themselves from invading pathogens through a vast array of host-defense mechanisms including the production of anti-microbial peptides and defensins which act on t he bacterial cell wall or disrupt bacterial cell membranes, respectively (Fleming 1992, Yang et al. 2007). Additionally, there is a group of host-defense proteins that act on invading bacteria by preventing them from sequestering iron. Some of these proteins include lactoferrin and lipocalin-2, both of which keep host iron concentrations low and unavailable to bacteria. Lipocalin-2 proteins are secreted by neutrophils during infection and are capable of binding to ferric-siderophore complexes, preventing iron reuptake into the bacterial cell (Abergel *et al.*, 2006b, Abergel *et al.*, 2008a, Abergel *et al.*, 2006a, Lee et al., 2007). Since these proteins bind to siderophores, they have also been termed siderocalins (Hoette *et al.*, 2008). Siderocalin proteins can bind catecholate siderophores containing 2,3-dihydroxybenzoic acid (DHBA) subunits, including the *B. anthracis* siderophore bacillibactin, which is effectively neutralized by

this protein during the host response to infection (Goetz *et al.*, 2002, Fischbach *et al.*, 2006b, Fischbach *et al.*, 2006a). However, siderocalin cannot accommodate the unique structure of petrobactin, specifically the presence of 3,4-dihydroxybenzoate moieties, leaving the siderophore free to function in iron acquisition in vivo and essentially making this molecule invisible to the human immune system (Abergel et al., 2006a, Abergel et al., 2006b). This lack of immune recognition by a mammalian host led to petrobactin being defined as a "stealth" siderophore (Abergel et al., 2006b, Pfleger et al., 2008, Zawadzka *et al.*, 2009a). Other organisms have also evolved methods to evade siderocalin sequestration including decoration of 2,3-DHBA moieties with sugars in the case of salmochelin produced by *E. coli* (Muller *et al.*, 2009), or by not having catechols at all, as is the case with many other siderophores that use hydroxamate or carboxylate groups as their main chelating functionalities (Abergel et al., 2008a, Abergel et al., 2006a, Abergel et al., 2006b, Abergel *et al.*, 2009, Abergel et al., 2008b).

The utility of petrobactin as a stealth siderophore and virulence factor has been shown thus far only in *B. anthracis*. What's more, a survey of genetically similar strains showed that a large subset of *Bacillus* species contain genes homologous to *asb* on their genome, and though not all were reported to be pathogenic, the ability to synthesize petrobactin appeared essential for virulence in some of these strains (Abergel et al., 2008b). Rather than evolving mechanisms to facilitate iron scavenging during mammalian infection *de novo*, it seems plausible that the *asb* gene cluster may have been acquired by *Bacillus* through horizontal transfer from another unrelated species. Thus, the selective advantage gained during host infection by production of the stealth 3,4-DHBA component of petrobactin was an opportune advancement in iron acquisition lending to

pathogenesis. To further highlight this, the *asb* biosynthetic gene cluster appears to be conserved in several different species that have had their genomes sequenced, including Gram-negative microbes like the above mentioned *Marinobacter hydrocarboniclasticus*, most of which are not regarded as pathogens (Homann et al., 2009, Koppisch et al., 2008a). It is unknown if the unique structure of petrobactin serves a higher purpose than simply scavenging iron. While petrobactin biosynthesis is limited to bacterial species possessing homologs of *asbA-F*, "xenosiderophore" studies have shown that the pathogens *S. aureus* and *B. subtilis,* which lack *asbABCDEF,* are able to recognize petrobactin with their own siderophore receptors (Zawadzka *et al.*, 2009b, Beasley & Heinrichs, 2010). This is not surprising considering the structural similarity between NIS synthetase-derived siderophores like aerobactin (from *E. coli*), staphyloferrins (from *S. aureus*), and petrobactin, among others, and the selective advantage that may be acquired through the high-jacking of another species' iron chelator (Grigg *et al.*, 2010, Maresso & Schneewind, 2006, Wyatt *et al.*, 2010, Wooldridge *et al.*, 1992). This cross-recognition combined with the ubiquity of virulence associated NIS pathways makes petrobactin, due to its well-characterized pathway and unique stealth structure, useful in further understanding iron acquisition in bacterial pathogens (Tanabe *et al.*, 2012).

1.7 Iron Response Regulation

The bacterial response to iron starvation is largely mediated by the ferric uptake response (Fur) regulator (Venturi *et al.*, 1995, Ollinger *et al.*, 2006b, Torres *et al.*, 2010, de Lorenzo *et al.*, 1988). The actual Fur protein is a dimeric AraC-like repressor that undergoes a conformational change in the absence of iron, resulting in release of bound

DNA (Friedman & O'Brian, 2003, Pohl *et al.*, 2003, Stojiljkovic & Hantke, 1995). A canonical AT-rich DNA sequence constituting the "Fur box" precedes many iron acquisition genes in *Bacillus* spp., including *dhb*, responsible for bacillibactin biosynthesis, the elemental iron importer Ywb, and multiple ABC transporters hypothesized to be responsible for siderophore and heme uptake (Ollinger *et al.*, 2006a, Honsa & Maresso). In *E. coli*, an additional Fur-regulated gene constitutes a second level in low-iron response through expression of the siRNA RyhB, and the product FsrA appears to serve the analogous role in some *Bacillus* species (Gaballa *et al.*, 2008, Smaldone *et al.*). These polynucleotides post-transcriptionally affect multiple mRNAs with the end result of increasing precursor pools for siderophore biosynthesis, repressing translation of iron-dependent proteins, and repression of further expression of *fur* (Gaballa et al., 2008, Smaldone et al., MassÃ© *et al.*, 2007). While an exact homolog of FsrA does not show up in the *B. anthracis* genome, remnants of the recognition sequence for this small RNA are present near ORFs whose regulation is associated with iron starvation including chorismate biosynthesis and iron-sulfur enzyme gene clusters (NCBI-BLAST, unpublished data). Considering this, it seems plausible that some undefined RNA mechanism would contribute to low-iron response in *B. anthracis*.

Genetic and chemical analysis of *B. anthracis* revealed that the *asb* biosynthetic operon responsible for petrobactin biosynthesis is critical for infection of macrophages and in a mouse model (Lee *et al.*, 2011, Koppisch et al., 2005, Cendrowski et al., 2004b). Interestingly, while petrobactin production is induced in iron-deficient conditions, there is no canonical Fur-box preceding any *asb* genes. While there is some upstream sequence that may confer Fur-like regulator binding, multiple studies suggest additional factors

may control *asb* expression (Lee et al., 2011, Wilson *et al.*, 2009b, Passalacqua *et al.*, 2007b). Petrobactin production is also affected by paraquat- and H_2O_2-induced oxidative stress, variation in temperature, and oxygen availability (Lee et al., 2011, Passalacqua et al., 2007b, Wilson et al., 2010, Garner *et al.*, 2004). Reinforcing this, global expression studies of *Bacillus* species demonstrate an overlap in expression profiles between response to oxidative stress and iron starvation (Passalacqua et al., 2007b, Pohl *et al.,* Lee et al., 2011). In addition to the requirement for iron-containing enzymes like catalase to prevent redox damage, an oxidative environment directly contributes to a loss of cytoplasmic and protein-bound ferrous (Fe^{2+}) iron (Cornelis *et al.*).

1.8 Siderophore Recognition

Since petrobactin plays such an important role in *B. anthracis* pathogenesis, early work in the Hanna lab sought to elucidate the role of two proteins implicated in petrobactin binding. Deletion mutants lacking two putative siderophore binding proteins, FatB and FpuA, encoded by GBAA5330 and GBAA4766, respectively, were generated. Purified *B. cereus* homologs of these proteins were shown by others to have the ability to bind multiple forms of petrobactin, however their role in the pathogenesis of the bacterium remained untested (Zawadzka et al., 2009a). Extensive work in our laboratory was done to demonstrate the role of these genes during growth in iron limited conditions *in vitro* as well as to determine their effect on murine virulence.

Despite the ability of both FpuA and FatB derived from *B. cereus* to bind petrobactin *in vitro*, only FpuA was shown to be important for the growth of *B. anthracis* under iron limiting conditions (Carlson et al., 2010). Importantly, mutants lacking the

FpuA substrate binding protein exhibited a severe growth defect when either vegetative bacteria or spores were tested for growth in iron depleted media (IDM) (Fig. 1-4, A). These cultures exhibited growth kinetics nearly identical to those of *B. anthracis* strains unable to synthesize petrobactin, Δ*asbABCDEF* (Dixon et al., 2012, Cendrowski et al., 2004c, Lee et al., 2007, Carlson et al., 2010). Furthermore, a *B. anthracis* strain with deletions in both putative petrobactin binding proteins (Δ*fpuA* Δ*fatB*) grew to the same levels as Δ*fpuA* single mutants, while mutants lacking the single FatB protein were not impaired in their ability to grow in IDM (Carlson et al., 2010). These data showed that the substrate binding protein, FatB does not play a critical role in petrobactin uptake by *B. anthracis*. Additionally, we showed that strains lacking the petrobactin binding protein, FpuA were severely attenuated in a murine inhalational anthrax infection model, with an LD_{50} nearly 3,000 times that of wild-type *B. anthracis* Sterne $34F_2$ (Fig. 1-4, B)(Carlson et al., 2010). This finding further emphasized the significance of petrobactin-associated iron acquisition and the importance of FpuA in *B. anthracis* pathogenesis. The observed attenuation of the Δ*fpuA* strain is consistent with published reports on the attenuation of petrobactin biosynthesis mutants (Cendrowski et al., 2004c, Pfleger et al., 2008), and although the growth phenotypes of these two strains appear very similar in IDM, slight differences in murine virulence were observed at higher doses, with LD_{50} of Δ*asbABCDEF* mutants approximately eight fold lower than that of the Δ*fpuA* strain. These results indicate that Δ*fpuA* mutants are slightly less virulent than even the petrobactin biosynthesis mutant, leading to the hypothesis that this receptor protein plays a secondary function during mammalian infection. It is possible that this receptor is able to recognize exogenous siderophore-like molecules, or other ligands

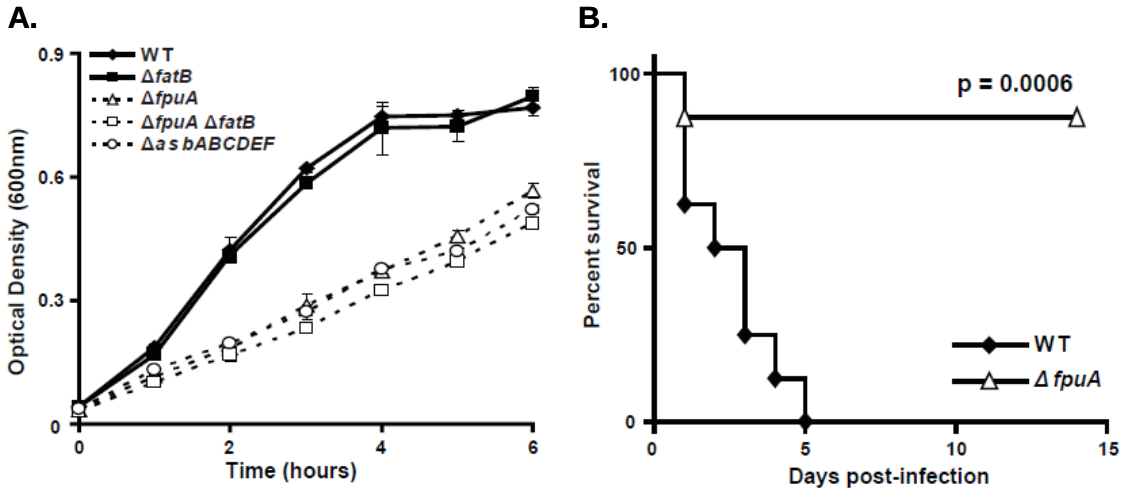

Figure 1-4. Growth of *B. anthracis* mutant strains in iron depleted media and attenuation of virulence of the Δ*fpuA* strain in a murine model of infection. (A) Wild-type (solid diamonds), Δ*fatB* (solid squares), Δ*fpuA* (open triangles), Δ*fpuA* Δ*fatB* (open squares), and Δ*asbABCDEF* (open circles) were grown in iron depleted media. All cultures were inoculated with vegetative bacilli at an initial OD600 = 0.05 and growth was monitored by measuring change in OD600 over time. Data presented are representative of four individual experiments. (B) DBA/2J mice were infected by intratracheal infection with WT (filled diamonds) or Δ*fpuA* (open triangles) spores at 1x105 spores per mouse. Mice were monitored for fourteen days. Survival curves for Δ*fpuA* were significantly different from wild-type by the log-rank test (p value is indicated above) (Figure adapted from Carlson and Dixon *et al*., 2010)

providing the bacterium with an increased survival advantage during infection. Uptake of exogenous siderophores has been shown in other bacterial species including *B. cereus* and *Pseudomonas aeruginosa* (Greenwald *et al.*, 2009, Ollinger et al., 2006b), however an exact mechanism for this in *B. anthracis* remains to be elucidated and will be discussed in Chapter 4.

Taken together, these results provided the first genetic evidence demonstrating the role of FpuA in petrobactin uptake. Because FpuA has significant homology to the substrate binding proteins associated with the ATP binding cassette (ABC) transport systems used in other bacterial species for the import of iron-siderophore complexes, we hypothesized that petrobactin-associated iron acquisition in *B. anthracis* also occurs through an ABC-transport system (Quentin *et al.*, 1999, Miethke & Marahiel, 2007, Koppisch et al., 2005, Koster, 2001).

1.9 ATP-Binding Cassette Transport Systems

ATP-binding cassette (ABC) transporters play a crucial role in the life cycles of bacteria, archaea and eukaryotes and constitute one of the largest and most ancient superfamilies (Fuellen *et al.*, 2005, Guidotti, 1996, Koster, 2001, Schneider & Hunke, 1998, Lewis *et al.*, 2012, Davidson et al., 2008). ATP systems couple the energy provided by ATP hydrolysis to drive the translocation of solutes (allocrites) across lipid membranes against a concentration gradient (Davidson et al., 2008, Davidson, 2002, Holland & Holland, 2005). Interestingly, there is phylogenetic evidence to support the notion that the ABC transport family may have diversified before the divergence of bacteria, archaea and eukaryotes on separate evolutionary paths (Lewis et al., 2012,

Albers *et al.*, 2004, Annilo *et al.*, 2003). Given the importance of these ABC systems in selective permeability to nutrients and metabolites, their development may have been one of the first distinctive properties of primitive cells (Schneider & Hunke, 1998, Seeger & van Veen, 2009, Higgins, 1992). Eukaryotic ABC transport systems have more recently gained attention due to their role in several severe human diseases, however bacterial ABC transport systems were first identified and characterized in detail in the 1970's (Ames & Lever, 1970, Ferenci *et al.*, 1977, Kellermann & Szmelcman, 1974). Examples of these include the histidine and maltose importers of *Salmonella enterica* serovar *typhimurium* and *E. coli*, respectively (Morbach *et al.*, 1993, Gilson *et al.*, 1982, Saurin *et al.*, 1989, Walter *et al.*, 1992, Nikaido *et al.*, 1997, Liu & Ames, 1997). Almost 20 years ago now, following the completion of the nucleotide sequencing of these two systems, it became obvious that these ABC transport systems exhibited high similarity in the overall nature of their components (Davidson et al., 2008, Ames & Lecar, 1992). Furthermore, the components thought to be involved in driving translocation through the cell membrane via ATP hydrolysis shared up to 32% amino acid sequence identity (Gilson et al., 1982). Importantly, later work showed that bacterial proteins functioning in a wide array of translocation processes such as nutrient uptake, toxin export, DNA repair, etc., all shared similar sequences (Higgins *et al.*, 1986, Doolittle *et al.*, 1986). These findings suggested that conserved "ATP-binding" proteins provide the energy required to drive the transport of various substances in the systems mentioned above (Doolittle et al., 1986).

ABC systems can be divided into three main functional categories, as follows. The first of these are importers which mediate the uptake of nutrients in prokaryotes. A

schematic of typical iron uptake in Gram-positive bacteria using siderophore secretion and ABC-transport is illustrated in Figure 1-5. The list of substrates that are transported via ABC importers includes, but is not limited to, amino acids, peptides, organic and inorganic ions, mono- and oligosaccharides, metals, vitamins and iron-siderophore complexes (Davidson et al., 2008). Second are the exporters that are involved in secretion of various molecules such as toxins, hemolysins, hydrophobic drugs, and lipids just to name a few (Fath & Kolter, 1993). The third group of ABC systems is not actually involved in transport at all, and is instead required in other important cellular processes such as DNA repair and the translation of mRNA (Higgins, 1992). Bacterial ABC transport systems are associated with the inner membrane and are involved in both import and export of a variety of diverse secreted substrates as mentioned above (Davidson & Maloney, 2007). In eukaryotes, however, these transporters are found in the plasma membranes as well as intracellular membranes, and unlike ABC transport systems of prokaryotes, these transporters are unidirectional out of the cytoplasm (Gottesman & Ambudkar, 2001, Higgins, 1992).

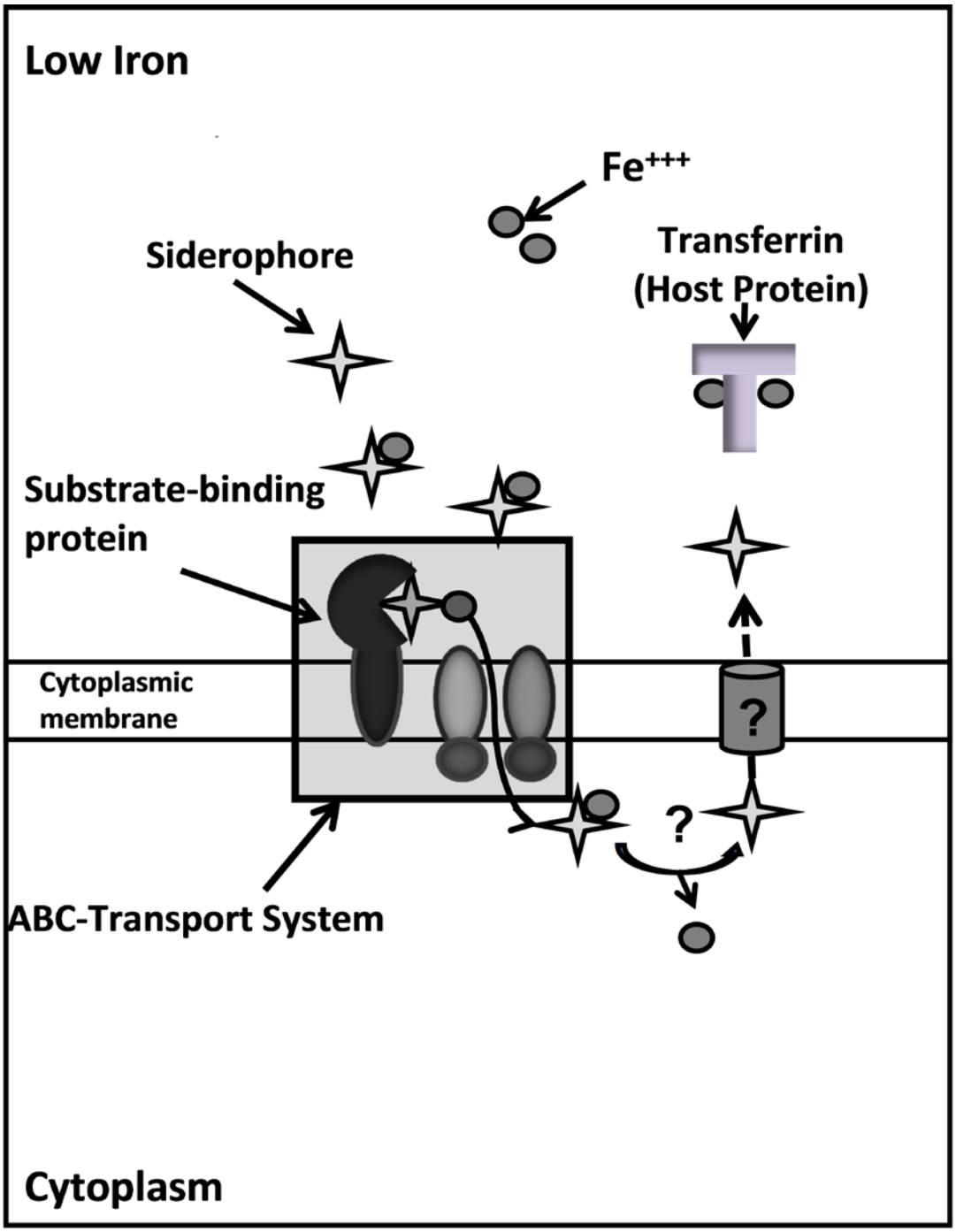

Figure 1-5. Iron acquisition in Gram-positive bacteria using siderophore secretion and ABC-transport. Following the scavenging of iron from host proteins, such as transferrin, iron-siderophore complexes are recognized by a high affinity substrate-binding protein on the surface of the cell membrane and are transported into the cytoplasm of the bacterium through membrane associated ABC-transport systems for utilization.

ABC Transporter Structure

Despite the extremely diverse population of substrates and differences that exist in transport polarity, all ABC transporters share a common, prototypical structure containing four distinct domains: two membrane-spanning domains, or permease proteins, and two nucleotide-binding domains (NBDs), or ATPase proteins (Fig. 1-6, A) (Eitinger *et al.*, 2011, Davidson et al., 2008, Kerr, 2002, Moody & Thomas, 2005). These domains, however, can be organized in a variety of ways. In importers, these four domains are almost always found in distinct polypeptide chains that come together to form a multimeric complex (Chen *et al.*, 2003). Meanwhile, some ABC transporters can be encoded in a single polypeptide, where the permease and the ATPase subunits are fused and allow for the formation of a homodimer protein in the active form (Locher, 2009). Alternatively, bacterial ABC transporters can be encoded by two separate polypeptides, one permease and one ATPase, this would allow for a homodimer of heterodimers to form. More complex versions can also exist where one or more of either of the subunits, permease or ATPase, are distinct and come together to form an active transport complex (Jones *et al.*, 2009). Conversely, in many eukaryotic ABC transport systems, all four domains are typically found in a single polypeptide (Higgins, 1992).

The permease components of ABC transporters form the channel across the bacterial membrane through which the allocrite is translocated (Hollenstein *et al.*, 2007). The diversity of these transported elements is immense and has been reflected in the relatively low sequence similarities found amongst the permeases of various transporters. Inspection of the crystal structures of ABC permeases that have been determined so far reveals that some structural flexibility exists as demonstrated with the identification of

three different folds (types I, II, and III) (Chen et al., 2003). Yet, there is one conserved characteristic that has been found in some bacterial import permease subunits, this is the EEA motif or L-loop, which provides a point of interaction between the ATPase and the permease subunits (Mourez *et al.*, 1997, Schmitt *et al.*, 2003).

ATPase Domains

ATPase subunits of ABC transporters, unlike the permease subunits, have highly conserved "cassette" domains, or characteristic sequences that span a ~200 amino acid region (Higgins, 1992, Higgins, 2001, Higgins & Linton, 2001). In fact, all functional ATPases have a two-domain architecture that consists of a RecA-like catalytic domain and a second, smaller helical domain (Story & Steitz, 1992, Story *et al.*, 1992, Ames & Lecar, 1992), with the overall appearance of an ATPase having an L-shape. The signature motif, which is found between the Walker A and Walker B motifs (Fig. 1-6, B), is also known as the linker peptide or LSSGQ motif, and is traditionally used to identify ABC transporters of different species (Jones et al., 2009). It is only when an ATPase dimer is formed that the signature sequence comes into play allowing for interaction with ATP (Mourez et al., 1997). Two ATPase monomers orient in a "head-to-tail" fashion forming a sandwich where opposing Walker A and Walker B motifs come together to form the ATP binding pocket (Locher, 2009). The Walker A motif is common to several ATP- and GTP-hydrolyzing proteins and interacts with the phosphate moieties of ATP (Walker *et al.*, 1982, Saraste *et al.*, 1990). Approximately 25 residues downstream of the Walker A motif is the A-Loop, which contains a well conserved tyrosine residue that is involved in interactions with the adenine moiety of ATP (Ambudkar *et al.*, 2006, Kim *et al.*, 2006).

The Walker B motif also interacts with ATP and forms a contact between the γ-phosphate and the Mg^{2+} cofactor through water molecules (Schneider & Hunke, 1998). Immediately following the Walker B motif is a highly conserved glutamate residue that has been shown to act as a general base in the ATP hydrolysis reaction (Lomovskaya *et al.*, 2007). Approaching the C-terminal end of the ATPase domain, another motif called the D-loop contains the consensus sequence SALD and functions in communication between the ATP-binding sites of the two ATPase monomers by forming contacts between both *cis* and *trans* residues (Fig. 1-6, B)(Jones et al., 2009). The Q-loop, like the Walker B motif, contacts γ-phosphate of ATP through its single conserved glutamine reside (Fig. 1-6, B) (Schneider & Hunke, 1998).

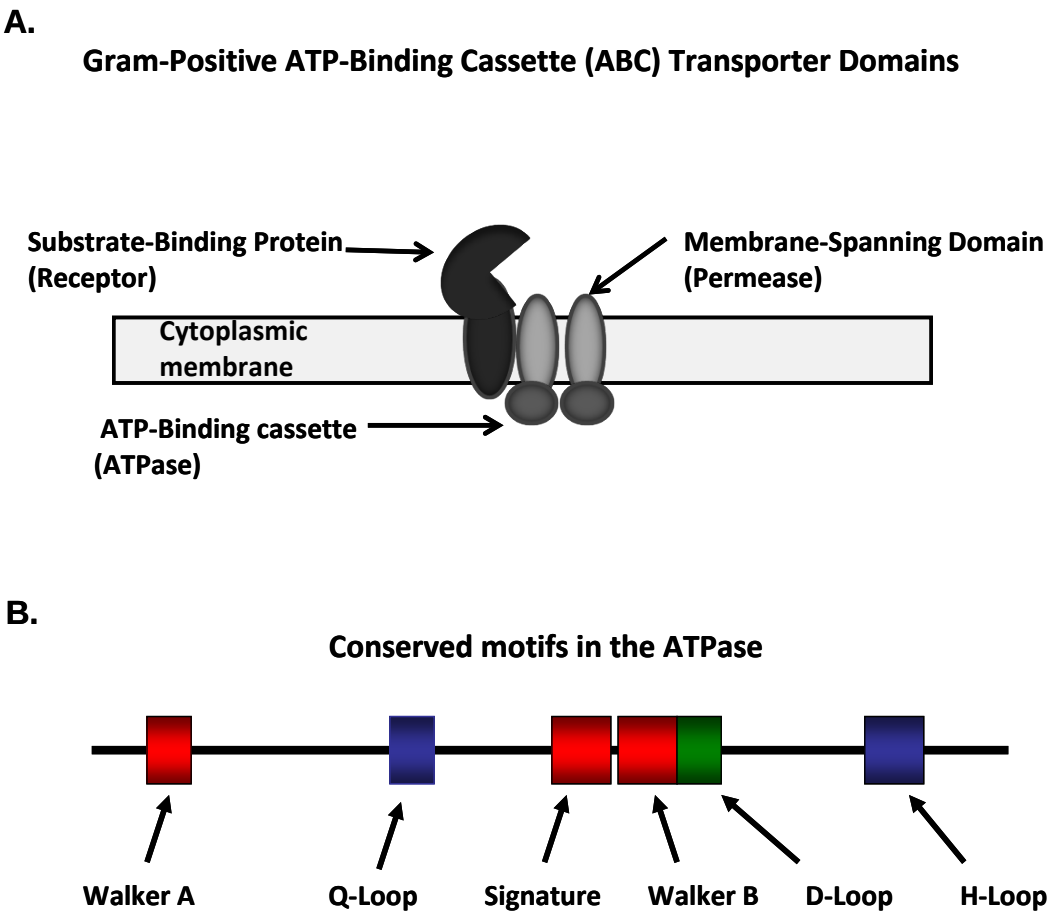

Figure 1-6. Gram-Positive ATP-Binding Cassette (ABC) Transporter Domains and Conserved motifs in the ATPase. A. The structural organization of ABC- transporter consists of two hydrophobic membrane-spanning domains, or permeases, and two hydrophilic ATPase domains on t he inner surface of the cytoplasmic membrane that couple the energy of ATP hydrolysis to transport across the membrane-spanning permease channel. Gram-positive bacteria lack an outer membrane and periplasmic space ,thus their importers rely on high-affinity substrate-binding proteins bound to the external side of the cytoplasmic membrane. Three characteristic motifs found in all ABC ATPases are represented by red boxes. B. The Walker A motif and the Walker B motif form the nucleotide binding fold of the P-Loop ATPase family. The signature motif is unique to ABC ATPase proteins and interacts with ATP. Other characteristic motifs including the Q-Loop and H-Loop, contain just one highly conserved residue and are represented by blue boxes. These residues make contacts with the γ-phosphate of ATP. In the formation of the ATP dimer, the D-Loop makes contacts with the Walker A motif of the opposing monomer and is represented by a green box. The structurally diverse region (SDR) is located between the Q-Loop and the Signature sequence and constitutes a helical domain important for the formation of contacts between ATPases and their permease partners.

ABC Transporter Assembly

In bacteria, a vast number of ABC proteins with various transport roles exist, and as mentioned above, several of these have their ATPase and permease subunits expressed as separate polypeptides. This brings forth the dilemma of molecular recognition and the ability to dock to the correct counterpart for the formation of a functional ABC transport complex. For that reason, specificity and diversity in the primary and tertiary structures of these proteins helps to ensure the correct "fit". Between the Q-Loop and the signature sequence lays a structurally diverse region (SDR) that is thought to facilitate the correct pairing of permeases to their cognate ATPase subunits (Fig. 1-6, B) (Schmitt et al., 2003, Schneider & Hunke, 1998).

In short, the ATPase components of the ABC transport complexes are highly conserved among bacterial species and provide the "motor" of the translocation process through the binding and hydrolyzing of ATP, while the Walker A and B motifs, H-Loop, and signature motif are responsible for the binding and hydrolysis of ATP (Fig. 1-6, B) (Smith *et al.*, 2002). Furthermore the Q-and D-Loops are thought to couple the substrate binding sites of the permease proteins to the ATP-binding sites of the ATPases and assists in forming dimer interactions (Fig. 1-6, B) (Davidson et al., 2008, Davidson & Maloney, 2007). Much investigation has gone into showing that the free energy change provided by ATP hydrolysis is coupled to the translocation of solutes across the membrane, however there is still some debate as to whether ATP is actually necessary to drive the initial transport events or whether its role is to merely reset the permease channel configuration to an open, solute-accepting "ready" state (Higgins & Linton,

2004). Nevertheless, the action of coupling ATPase activity to a change in the conformation of the permease channel to drive transport is key.

The majority of bacterial ABC transport systems relies on the presence of high-affinity extracytoplasmic substrate binding proteins (SBP) and can be referred to as binding protein dependent (BPD) transport systems (Fig. 1-6, A) (Wolters *et al.*, 2010, Berntsson *et al.*, 2010). In gram-positive bacteria, such as in the case of *B. anthracis*, which lack a periplasm, the SBP are often lipoproteins that are found bound to the external face of the cytoplasmic membrane by N-terminal acyl-glyceryl cysteines (Davidson et al., 2008). SBP typically bind their substrates with extremely high affinities in the range of 0.01 to 1 μM allowing for high transport efficiency even at very low substrate concentrations (Koster, 2001, Dippel & Boos, 2005). In fact, many cells can actually concentrate translocated nutrients up to 10^6-fold when found at submicromolar levels in the extracellular environment (Dippel & Boos, 2005). While most transporters are specific for a single type of substrate, it is possible that a single SBP can have wide substrate specificity as is the case in the multiple-sugar transporter Msm of *Streptococcus mutans,* which can recognize five diverse sugar molecules (Russell *et al.*, 1992, Tao *et al.*, 1993). It is also possible for multiple SBP's to have different binding specificities and interact with a single transporter. An example of this is illustrated by the histidine, lysine, and arginine transport system of *Enterobacteriaceae* (Higgins & Ames, 1981).

ABC Transport and Petrobactin Utilization

FpuA, the virulence associated petrobactin-recognition protein characterized by my early work in the Hanna lab, has significant homology to the substrate binding

proteins found in the ATP-binding cassette transport systems referred to above. Since this mechanism is used in other bacterial species for the import of iron-siderophore complexes (Miethke & Marahiel, 2007), it was hypothesized that petrobactin-associated iron acquisition in *B. anthracis* also occurs through an ABC-transport mechanism. With key aspects of the structure and function of these vital transport systems now introduced, the remaining chapters in this thesis will demonstrate the importance of specific ABC transport components in *B. anthracis* pathogenesis, particularly iron acquisition, and the utility of these systems in anthrax therapeutic design.

1.10 References

Abergel, R. J., M. C. Clifton, J. C. Pizarro, J. A. Warner, D. K. Shuh, R. K. Strong & K. N. Raymond, (2008a) The siderocalin/enterobactin interaction: a link between mammalian immunity and bacterial iron transport. *Journal of the American Chemical Society* **130**: 11524-11534.

Abergel, R. J., E. G. Moore, R. K. Strong & K. N. Raymond, (2006a) Microbial evasion of the immune system: structural modifications of enterobactin impair siderocalin recognition. *Journal of the American Chemical Society* **128**: 10998-10999.

Abergel, R. J., M. K. Wilson, J. E. Arceneaux, T. M. Hoette, R. K. Strong, B. R. Byers & K. N. Raymond, (2006b) Anthrax pathogen evades the mammalian immune system through stealth siderophore production. *Proceedings of the National Academy of Sciences of the United States of America* **103**: 18499-18503.

Abergel, R. J., A. M. Zawadzka, T. M. Hoette & K. N. Raymond, (2009) Enzymatic hydrolysis of trilactone siderophores: where chiral recognition occurs in enterobactin and bacillibactin iron transport. *J Am Chem Soc* **131**: 12682-12692.

Abergel, R. J., A. M. Zawadzka & K. N. Raymond, (2008b) Petrobactin-mediated iron transport in pathogenic bacteria: coordination chemistry of an unusual 3,4-catecholate/citrate siderophore. *Journal of the American Chemical Society* **130**: 2124-2125.

Albers, S. V., S. M. Koning, W. N. Konings & A. J. Driessen, (2004) Insights into ABC transport in archaea. *J Bioenerg Biomembr* **36**: 5-15.

Ambudkar, S. V., I. W. Kim, D. Xia & Z. E. Sauna, (2006) The A-loop, a novel conserved aromatic acid subdomain upstream of the Walker A motif in ABC transporters, is critical for ATP binding. *FEBS letters* **580**: 1049-1055.

Ames, G. F. & H. Lecar, (1992) ATP-dependent bacterial transporters and cystic fibrosis: analogy between channels and transporters. *FASEB journal : official publication of the Federation of American Societies for Experimental Biology* **6**: 2660-2666.

Ames, G. F. & J. Lever, (1970) Components of histidine transport: histidine-binding proteins and hisP protein. *Proceedings of the National Academy of Sciences of the United States of America* **66**: 1096-1103.

Andrews, S. C., A. K. Robinson & F. Rodriguez-Quinones, (2003) Bacterial iron homeostasis. *FEMS microbiology reviews* **27**: 215-237.

Annilo, T., Z. Q. Chen, S. Shulenin & M. Dean, (2003) Evolutionary analysis of a cluster of ATP-binding cassette (ABC) genes. *Mammalian genome : official journal of the International Mammalian Genome Society* **14**: 7-20.

Barbeau, K., G. Zhang, D. H. Live & A. Butler, (2002) Petrobactin, a photoreactive siderophore produced by the oil-degrading marine bacterium Marinobacter hydrocarbonoclasticus. *Journal of the American Chemical Society* **124**: 378-379.

Barclay, R. & C. Ratledge, (1986) Participation of iron on t he growth inhibition of pathogenic strains of mycobacterium avium and M. paratuberculosis in serum. *Zentralblatt fur Bakteriologie, Mikrobiologie, und Hygiene. Series A, Medical microbiology, infectious diseases, virology, parasitology* **262**: 189-194.

Barry, S. M. & G. L. Challis, (2009) Recent advances in siderophore biosynthesis. *Curr Opin Chem Biol* **13**: 205-215.

Bartrand, T. A., M. H. Weir & C. N. Haas, (2008) Dose-Response Models for Inhalation of Bacillus anthracis Spores: Interspecies Comparisons. *Risk Analysis* **28**: 1115-1124.

Beasley, F. C. & D. E. Heinrichs, (2010) Siderophore-mediated iron acquisition in the staphylococci. *J Inorg Biochem* **104**: 282-288.

Berntsson, R. P., S. H. Smits, L. Schmitt, D. J. Slotboom & B. Poolman, (2010) A structural classification of substrate-binding proteins. *FEBS letters* **584**: 2606-2617.

Braun, V. & M. Braun, (2002) Active transport of iron and siderophore antibiotics. *Curr Opin Microbiol* **5**: 194-201.

Carlson, P. E., Jr., S. D. Dixon, B. K. Janes, K. A. Carr, T. D. Nusca, E. C. Anderson, S. E. Keene, D. H. Sherman & P. C. Hanna, (2010) Genetic analysis of petrobactin transport in Bacillus anthracis. *Molecular microbiology* **75**: 900-909.

Cassat, J. E. & E. P. Skaar, (2012) Metal ion acquisition in Staphylococcus aureus: overcoming nutritional immunity. *Seminars in immunopathology* **34**: 215-235.

Cendrowski, S., W. MacArthur & P. Hanna, (2004) Bacillus anthracis requires siderophore biosynthesis for growth in macrophages and mouse virulence. *Mol Microbiol* **51**: 407-417.

Challis, G. L., (2005) A widely distributed bacterial pathway for siderophore biosynthesis independent of nonribosomal peptide synthetases. *Chembiochem* **6**: 601-611.

Chen, J., G. Lu, J. Lin, A. L. Davidson & F. A. Quiocho, (2003) A tweezers-like motion of the ATP-binding cassette dimer in an ABC transport cycle. *Molecular cell* **12**: 651-661.

Cornelis, P., Q. Wei, S. C. Andrews & T. Vinckx, (2011) Iron homeostasis and management of oxidative stress response in bacteria. *Metallomics* **3**: 540-549.

Crosa, J. H. & C. T. Walsh, (2002) Genetics and assembly line enzymology of siderophore biosynthesis in bacteria. *Microbiol Mol Biol Rev* **66**: 223-249.

Cybulski, R. J., P. Sanz, F. Alem, S. Stibitz, R. L. Bull & A. D. O'Brien, (2009) Four Superoxide Dismutases Contribute to Bacillus anthracis Virulence and Provide Spores with Redundant Protection from Oxidative Stress. *Infection and Immunity* **77**: 274-285.

Davidson, A. L., (2002) Mechanism of coupling of transport to hydrolysis in bacterial ATP-binding cassette transporters. *J Bacteriol* **184**: 1225-1233.

Davidson, A. L., E. Dassa, C. Orelle & J. Chen, (2008) Structure, function, and evolution of bacterial ATP-binding cassette systems. *Microbiol Mol Biol Rev* **72**: 317-364, table of contents.

Davidson, A. L. & P. C. Maloney, (2007) ABC transporters: how small machines do a big job. *Trends in microbiology* **15**: 448-455.

de Lorenzo, V., F. Giovannini, M. Herrero & J. B. Neilands, (1988) Metal ion regulation of gene expression. Fur repressor-operator interaction at the promoter region of the aerobactin system of pColV-K30. *J Mol Biol* **203**: 875-884.

Dertz, E. A., A. Stintzi & K. N. Raymond, (2006a) Siderophore-mediated iron transport in Bacillus subtilis and Corynebacterium glutamicum. *J Biol Inorg Chem* **11**: 1087-1097.

Dertz, E. A., J. Xu, A. Stintzi & K. N. Raymond, (2006b) Bacillibactin-mediated iron transport in Bacillus subtilis. *J Am Chem Soc* **128**: 22-23.

Dippel, R. & W. Boos, (2005) The maltodextrin system of Escherichia coli: metabolism and transport. *Journal of bacteriology* **187**: 8322-8331.

Dixon, S. D., B. K. Janes, A. Bourgis, P. E. Carlson, Jr. & P. C. Hanna, (2012) Multiple ABC transporters are involved in the acquisition of petrobactin in Bacillus anthracis. *Molecular microbiology* **84**: 370-382.

Dixon, T. C., M. Meselson, J. Guillemin & P. C. Hanna, (1999) Anthrax. *N Engl J Med* **341**: 815-826.

Doganay, L. & P. D. Welsby, (2006) Anthrax: a disease in waiting? *Postgrad Med J* **82**: 754-756.

Doolittle, R. F., M. S. Johnson, I. Husain, B. Van Houten, D. C. Thomas & A. Sancar, (1986) Domainal evolution of a prokaryotic DNA repair protein and its relationship to active-transport proteins. *Nature* **323**: 451-453.

Dragomirescu, T., M. Antonescu & V. Apateanu, (1979) [Iron and infection. I. Iron and "nutritional immunity". The leukocytic endogenous mediator]. *Revista de igiena, bacteriologie, virusologie, parazitologie, epidemiologie, pneumoftiziologie. Bacteriologia, virusologia, parazitologia, epidemiologia* **24**: 1-14.

Dutz, W. & E. Kohout-Dutz, (1981) Anthrax. *Int J Dermatol* **20**: 203-206.

Dutz, W. & E. Kohout, (1971) Anthrax. *Pathol Annu* **6**: 209-248.

Eitinger, T., D. A. Rodionov, M. Grote & E. Schneider, (2011) Canonical and ECF-type ATP-binding cassette importers in prokaryotes: diversity in modular organization and cellular functions. *FEMS Microbiol Rev* **35**: 3-67.

Faraldo-Gomez, J. D. & M. S. Sansom, (2003) Acquisition of siderophores in gram-negative bacteria. *Nat Rev Mol Cell Biol* **4**: 105-116.

Fath, M. J. & R. Kolter, (1993) ABC transporters: bacterial exporters. *Microbiol Rev* **57**: 995-1017.

Ferenci, T., W. Boos, M. Schwartz & S. Szmelcman, (1977) Energy-coupling of the transport system of Escherichia coli dependent on m altose-binding protein. *European journal of biochemistry / FEBS* **75**: 187-193.

Fischbach, M. A., H. Lin, D. R. Liu & C. T. Walsh, (2006a) How pathogenic bacteria evade mammalian sabotage in the battle for iron. *Nat Chem Biol* **2**: 132-138.

Fischbach, M. A., H. Lin, L. Zhou, Y. Yu, R. J. Abergel, D. R. Liu, K. N. Raymond, B. L. Wanner, R. K. Strong, C. T. Walsh, A. Aderem & K. D. Smith, (2006b) The pathogen-associated iroA gene cluster mediates bacterial evasion of lipocalin 2. *Proc Natl Acad Sci U S A* **103**: 16502-16507.

Frankel, A. E., S. R. Kuo, D. Dostal, L. Watson, N. S. Duesbery, C. P. Cheng, H. J. Cheng & S. H. Leppla, (2009) Pathophysiology of anthrax. *Front Biosci* **14**: 4516-4524.

Friedman, Y. E. & M. R. O'Brian, (2003) A novel DNA-binding site for the ferric uptake regulator (Fur) protein from Bradyrhizobium japonicum. *J Biol Chem* **278**: 38395-38401.

Fuellen, G., M. Spitzer, P. Cullen & S. Lorkowski, (2005) Correspondence of function and phylogeny of ABC proteins based on a n automated analysis of 20 model protein data sets. *Proteins* **61**: 888-899.

Gaballa, A., H. Antelmann, C. Aguilar, S. K. Khakh, K.-B. Song, G. T. Smaldone & J. D. Helmann, (2008) The Bacillus subtilis iron-sparing response is mediated by a Fur-regulated small RNA and three small, basic proteins. *Proceedings of the National Academy of Sciences* **105**: 11927-11932.

Ganz, T. & E. Nemeth, (2006) Regulation of iron acquisition and iron distribution in mammals. *Biochim Biophys Acta* **1763**: 690-699.

Garénaux, A., M. Caza & C. M. Dozois, (2011) The Ins and Outs of siderophore mediated iron uptake by extra-intestinal pathogenic Escherichia coli. *Veterinary Microbiology* **153**: 89-98.

Garner, B. L., J. E. Arceneaux & B. R. Byers, (2004) Temperature control of a 3,4-dihydroxybenzoate (protocatechuate)-based siderophore in Bacillus anthracis. *Curr Microbiol* **49**: 89-94.

Gat, O., G. Zaide, I. Inbar, H. Grosfeld, T. Chitlaru, H. Levy & A. Shafferman, (2008) Characterization of Bacillus anthracis iron-regulated surface determinant (Isd) proteins containing NEAT domains. *Mol Microbiol* **70**: 983-999.

Gilson, E., C. F. Higgins, M. Hofnung, G. Ferro-Luzzi Ames & H. Nikaido, (1982) Extensive homology between membrane-associated components of histidine and

maltose transport systems of Salmonella typhimurium and Escherichia coli. *J Biol Chem* **257**: 9915-9918.

Glanfield, A., D. P. McManus, G. J. Anderson & M. K. Jones, (2007) Pumping iron: a potential target for novel therapeutics against schistosomes. *Trends Parasitol* **23**: 583-588.

Goetz, D. H., M. A. Holmes, N. Borregaard, M. E. Bluhm, K. N. Raymond & R. K. Strong, (2002) The neutrophil lipocalin NGAL is a bacteriostatic agent that interferes with siderophore-mediated iron acquisition. *Mol Cell* **10**: 1033-1043.

Gottesman, M. M. & S. V. Ambudkar, (2001) Overview: ABC transporters and human disease. *Journal of bioenergetics and biomembranes* **33**: 453-458.

Greenwald, J., M. Nader, H. Celia, C. Gruffaz, V. Geoffroy, J. M. Meyer, I. J. Schalk & F. Pattus, (2009) FpvA bound to non-cognate pyoverdines: molecular basis of siderophore recognition by an iron transporter. *Mol Microbiol* **72**: 1246-1259.

Grigg, J. C., J. Cheung, D. E. Heinrichs & M. E. Murphy, (2010) Specificity of Staphyloferrin B recognition by the SirA receptor from Staphylococcus aureus. *J Biol Chem* **285**: 34579-34588.

Guidi-Rontani, C., M. Weber-Levy, E. Labruyere & M. Mock, (1999) Germination of Bacillus anthracis spores within alveolar macrophages. *Mol Microbiol* **31**: 9-17.

Guidotti, G., (1996) ATP transport and ABC proteins. *Chem Biol* **3**: 703-706.

Hanna, P., (1998a) Anthrax pathogenesis and host response. *Curr Top Microbiol Immunol* **225**: 13-35.

Hanna, P., (1998b) How anthrax kills. *Science* **280**: 1671, 1673-1674.

Harrison, A. J., M. Yu, T. Gardenborg, M. Middleditch, R. J. Ramsay, E. N. Baker & J. S. Lott, (2006) The structure of MbtI from Mycobacterium tuberculosis, the first enzyme in the biosynthesis of the siderophore mycobactin, reveals it to be a salicylate synthase. *J Bacteriol* **188**: 6081-6091.

Hickford, S. J., F. C. Kupper, G. Zhang, C. J. Carrano, J. W. Blunt & A. Butler, (2004) Petrobactin sulfonate, a new siderophore produced by the marine bacterium Marinobacter hydrocarbonoclasticus. *J Nat Prod* **67**: 1897-1899.

Higgins, C. F., (1992) ABC transporters: from microorganisms to man. *Annu Rev Cell Biol* **8**: 67-113.

Higgins, C. F., (2001) ABC transporters: physiology, structure and mechanism--an overview. *Research in microbiology* **152**: 205-210.

Higgins, C. F. & G. F. Ames, (1981) Two periplasmic transport proteins which interact with a common membrane receptor show extensive homology: complete nucleotide sequences. *Proc Natl Acad Sci U S A* **78**: 6038-6042.

Higgins, C. F., I. D. Hiles, G. P. Salmond, D. R. Gill, J. A. Downie, I. J. Evans, I. B. Holland, L. Gray, S. D. Buckel, A. W. Bell & et al., (1986) A family of related ATP-binding subunits coupled to many distinct biological processes in bacteria. *Nature* **323**: 448-450.

Higgins, C. F. & K. J. Linton, (2001) Structural biology. The xyz of ABC transporters. *Science* **293**: 1782-1784.

Higgins, C. F. & K. J. Linton, (2004) The ATP switch model for ABC transporters. *Nature structural & molecular biology* **11**: 918-926.

Hoette, T. M., R. J. Abergel, J. Xu, R. K. Strong & K. N. Raymond, (2008) The role of electrostatics in siderophore recognition by the immunoprotein Siderocalin. *Journal of the American Chemical Society* **130**: 17584-17592.

Holland, K. A. & I. B. Holland, (2005) Adventures with ABC-proteins: highly conserved ATP-dependent transporters. *Acta Microbiol Immunol Hung* **52**: 309-322.

Hollenstein, K., R. J. Dawson & K. P. Locher, (2007) Structure and mechanism of ABC transporter proteins. *Current opinion in structural biology* **17**: 412-418.

Homann, V. V., K. J. Edwards, E. A. Webb & A. Butler, (2009) Siderophores of Marinobacter aquaeolei: petrobactin and its sulfonated derivatives. *Biometals : an international journal on the role of metal ions in biology, biochemistry, and medicine* **22**: 565-571.

Honsa, E. S., M. Fabian, A. M. Cardenas, J. S. Olson & A. W. Maresso, (2011) The five near-iron transporter (NEAT) domain anthrax hemophore, IsdX2, scavenges heme from hemoglobin and transfers heme to the surface protein IsdC. *J Biol Chem* **286**: 33652-33660.

Honsa, E. S. & A. W. Maresso, Mechanisms of iron import in anthrax. *Biometals : an international journal on the role of metal ions in biology, biochemistry, and medicine* **24**: 533-545.

Honsa, E. S. & A. W. Maresso, (2011) Mechanisms of iron import in anthrax. *Biometals* **24**: 533-545.

Hood, M. I. & E. P. Skaar, (2012) Nutritional immunity: transition metals at the pathogen-host interface. *Nature reviews. Microbiology* **10**: 525-537.

Hotta, K., C. Y. Kim, D. T. Fox & A. T. Koppisch, (2010) Siderophore-mediated iron acquisition in Bacillus anthracis and related strains. *Microbiology* **156**: 1918-1925.

Jones, P. M., M. L. O'Mara & A. M. George, (2009) ABC transporters: a riddle wrapped in a mystery inside an enigma. *Trends in biochemical sciences* **34**: 520-531.

Kellermann, O. & S. Szmelcman, (1974) Active transport of maltose in Escherichia coli K12. Involvement of a "periplasmic" maltose binding protein. *European journal of biochemistry / FEBS* **47**: 139-149.

Kerr, I. D., (2002) Structure and association of ATP-binding cassette transporter nucleotide-binding domains. *Biochim Biophys Acta* **1561**: 47-64.

Kim, I. H., J. I. Shim, K. E. Lee, W. Hwang, I. J. Kim, S. H. Choi & K. S. Kim, (2008) Nonribosomal peptide synthase is responsible for the biosynthesis of siderophore in Vibrio vulnificus MO6-24/O. *J Microbiol Biotechnol* **18**: 35-42.

Kim, I. W., X. H. Peng, Z. E. Sauna, P. C. FitzGerald, D. Xia, M. Muller, K. Nandigama & S. V. Ambudkar, (2006) The conserved tyrosine residues 401 and 1044 in ATP sites of human P-glycoprotein are critical for ATP binding and hydrolysis: evidence for a conserved subdomain, the A-loop in the ATP-binding cassette. *Biochemistry* **45**: 7605-7616.

Koppisch, A. T., C. C. Browder, A. L. Moe, J. T. Shelley, B. A. Kinkel, L. E. Hersman, S. Iyer & C. E. Ruggiero, (2005) Petrobactin is the primary siderophore synthesized by Bacillus anthracis str. Sterne under conditions of iron starvation. *Biometals : an international journal on the role of metal ions in biology, biochemistry, and medicine* **18**: 577-585.

Koppisch, A. T., S. Dhungana, K. K. Hill, H. Boukhalfa, H. S. Heine, L. A. Colip, R. B. Romero, Y. Shou, L. O. Ticknor, B. L. Marrone, L. E. Hersman, S. Iyer & C. E. Ruggiero, (2008a) Petrobactin is produced by both pathogenic and non-

pathogenic isolates of the Bacillus cereus group of bacteria. *Biometals* **21**: 581-589.

Koppisch, A. T., K. Hotta, D. T. Fox, C. E. Ruggiero, C. Y. Kim, T. Sanchez, S. Iyer, C. C. Browder, P. J. Unkefer & C. J. Unkefer, (2008b) Biosynthesis of the 3,4-dihydroxybenzoate moieties of petrobactin by Bacillus anthracis. *The Journal of organic chemistry* **73**: 5759-5765.

Koster, W., (2001) ABC transporter-mediated uptake of iron, siderophores, heme and vitamin B12. *Research in microbiology* **152**: 291-301.

La Scola, B., P. E. Fournier & D. Raoult, (2003) Searching for Bacillus anthracis in suspect powders: a French experience. *J Clin Microbiol* **41**: 524; author reply 524-525.

Latunde-Dada, G. O., (2009) Iron metabolism: microbes, mouse, and man. *Bioessays* **31**: 1309-1317.

Lee, J. Y., B. K. Janes, K. D. Passalacqua, B. F. Pfleger, N. H. Bergman, H. Liu, K. Hakansson, R. V. Somu, C. C. Aldrich, S. Cendrowski, P. C. Hanna & D. H. Sherman, (2007) Biosynthetic analysis of the petrobactin siderophore pathway from Bacillus anthracis. *Journal of bacteriology* **189**: 1698-1710.

Lee, J. Y., K. D. Passalacqua, P. C. Hanna & D. H. Sherman, (2011) Regulation of petrobactin and bacillibactin biosynthesis in Bacillus anthracis under iron and oxygen variation. *PloS one* **6**: e20777.

Lewin, R., (1984) How Microorganisms Transport Iron: In the midst of plenty, microorganisms are often in danger of iron-starvation; the mechanism by which they transport iron has now been elucidated. *Science* **225**: 401-402.

Lewis, V. G., M. P. Ween & C. A. McDevitt, (2012) The role of ATP-binding cassette transporters in bacterial pathogenicity. *Protoplasma* **249**: 919-942.

Liu, C. E. & G. F. Ames, (1997) Characterization of transport through the periplasmic histidine permease using proteoliposomes reconstituted by dialysis. *J Biol Chem* **272**: 859-866.

Liu, H., K. Hakansson, J. Y. Lee & D. H. Sherman, (2007) Collision-activated dissociation, infrared multiphoton dissociation, and electron capture dissociation

of the Bacillus anthracis siderophore petrobactin and its metal ion complexes. *J Am Soc Mass Spectrom* **18**: 842-849.

Locher, K. P., (2009) Review. Structure and mechanism of ATP-binding cassette transporters. *Philosophical transactions of the Royal Society of London. Series B, Biological sciences* **364**: 239-245.

Lomovskaya, O., H. I. Zgurskaya, M. Totrov & W. J. Watkins, (2007) Waltzing transporters and 'the dance macabre' between humans and bacteria. *Nature reviews. Drug discovery* **6**: 56-65.

Maresso, A. W., T. J. Chapa & O. Schneewind, (2006) Surface protein IsdC and Sortase B are required for heme-iron scavenging of Bacillus anthracis. *J Bacteriol* **188**: 8145-8152.

Maresso, A. W., G. Garufi & O. Schneewind, (2008) Bacillus anthracis secretes proteins that mediate heme acquisition from hemoglobin. *PLoS Pathog* **4**: e1000132.

Maresso, A. W. & O. Schneewind, (2006) Iron acquisition and transport in Staphylococcus aureus. *Biometals* **19**: 193-203.

Mass Ã, E., H. Salvail, G. Desnoyers & M. l. Arguin, (2007) Small RNAs controlling iron metabolism. *Current Opinion in Microbiology* **10**: 140-145.

May, J. r. J., T. M. Wendrich & M. A. Marahiel, (2001) The dhb Operon of Bacillus subtilisEncodes the Biosynthetic Template for the Catecholic Siderophore 2,3-Dihydroxybenzoate-Glycine-Threonine Trimeric Ester Bacillibactin. *The Journal of biological chemistry* **276**: 7209-7217.

Mazmanian, S. K., E. P. Skaar, A. H. Gaspar, M. Humayun, P. Gornicki, J. Jelenska, A. Joachmiak, D. M. Missiakas & O. Schneewind, (2003) Passage of heme-iron across the envelope of Staphylococcus aureus. *Science* **299**: 906-909.

Miethke, M., O. Klotz, U. Linne, J. J. May, C. L. Beckering & M. A. Marahiel, (2006) Ferri-bacillibactin uptake and hydrolysis in Bacillus subtilis. *Mol Microbiol* **61**: 1413-1427.

Miethke, M. & M. A. Marahiel, (2007) Siderophore-based iron acquisition and pathogen control. *Microbiol Mol Biol Rev* **71**: 413-451.

Miethke, M., S. Schmidt & M. A. Marahiel, (2008) The major facilitator superfamily-type transporter YmfE and the multidrug-efflux activator Mta mediate

bacillibactin secretion in Bacillus subtilis. *Journal of bacteriology* **190**: 5143-5152.

Moayeri, M., I. Sastalla & S. H. Leppla, (2012) Anthrax and the inflammasome. *Microbes Infect* **14**: 392-400.

Moody, J. E. & P. J. Thomas, (2005) Nucleotide binding domain interactions during the mechanochemical reaction cycle of ATP-binding cassette transporters. *J Bioenerg Biomembr* **37**: 475-479.

Morbach, S., S. Tebbe & E. Schneider, (1993) The ATP-binding cassette (ABC) transporter for maltose/maltodextrins of Salmonella typhimurium. Characterization of the ATPase activity associated with the purified MalK subunit. *J Biol Chem* **268**: 18617-18621.

Mourez, M., M. Hofnung & E. Dassa, (1997) Subunit interactions in ABC transporters: a conserved sequence in hydrophobic membrane proteins of periplasmic permeases defines an important site of interaction with the ATPase subunits. *The EMBO journal* **16**: 3066-3077.

Muller, S., M. Valdebenito & K. Hantke, (2009) Salmochelin, the long-overlooked catecholate siderophore of Salmonella. *Biometals* **22**: 691-695.

Neilands, J. B., (1995) Siderophores: structure and function of microbial iron transport compounds. *The Journal of biological chemistry* **270**: 26723-26726.

Nemeth, E. & T. Ganz, (2006) Regulation of iron metabolism by hepcidin. *Annu Rev Nutr* **26**: 323-342.

Nikaido, K., P. Q. Liu & G. F. Ames, (1997) Purification and characterization of HisP, the ATP-binding subunit of a traffic ATPase (ABC transporter), the histidine permease of Salmonella typhimurium. Solubility, dimerization, and ATPase activity. *J Biol Chem* **272**: 27745-27752.

Nobles, C. L. & A. W. Maresso, (2011) The theft of host heme by Gram-positive pathogenic bacteria. *Metallomics* **3**: 788-796.

Ollinger, J., K.-B. Song, H. Antelmann, M. Hecker & J. D. Helmann, (2006a) Role of the Fur Regulon in Iron Transport in Bacillus subtilis. *Journal of bacteriology* **188**: 3664-3673.

Ollinger, J., K. B. Song, H. Antelmann, M. Hecker & J. D. Helmann, (2006b) Role of the Fur regulon in iron transport in Bacillus subtilis. *Journal of bacteriology* **188**: 3664-3673.

Oves-Costales, D., N. Kadi & G. L. Challis, (2009a) The long-overlooked enzymology of a nonribosomal peptide synthetase-independent pathway for virulence-conferring siderophore biosynthesis. *Chem Commun (Camb)*: 6530-6541.

Oves-Costales, D., N. Kadi, M. J. Fogg, L. Song, K. S. Wilson & G. L. Challis, (2007) Enzymatic logic of anthrax stealth siderophore biosynthesis: AsbA catalyzes ATP-dependent condensation of citric acid and spermidine. *Journal of the American Chemical Society* **129**: 8416-8417.

Oves-Costales, D., L. Song & G. L. Challis, (2009b) Enantioselective desymmetrisation of citric acid catalysed by the substrate-tolerant petrobactin biosynthetic enzyme AsbA. *Chem Commun (Camb)*: 1389-1391.

Passalacqua, K. D. & N. H. Bergman, (2006) Bacillus anthracis: interactions with the host and establishment of inhalational anthrax. *Future Microbiol* **1**: 397-415.

Passalacqua, K. D., N. H. Bergman, A. Herring-Palmer & P. Hanna, (2006) The Superoxide Dismutases of Bacillus anthracis Do Not Cooperatively Protect against Endogenous Superoxide Stress. *Journal of bacteriology* **188**: 3837-3848.

Passalacqua, K. D., N. H. Bergman, J. Y. Lee, D. H. Sherman & P. C. Hanna, (2007a) The global transcriptional responses of Bacillus anthracis Sterne (34F2) and a Delta sodA1 mutant to paraquat reveal metal ion homeostasis imbalances during endogenous superoxide stress. *J Bacteriol* **189**: 3996-4013.

Passalacqua, K. D., N. H. Bergman, J. Y. Lee, D. H. Sherman & P. C. Hanna, (2007b) The Global Transcriptional Responses of Bacillus anthracis Sterne (34F2) and a Î”sodA1 Mutant to Paraquat Reveal Metal Ion Homeostasis Imbalances during Endogenous Superoxide Stress. *Journal of bacteriology* **189**: 3996-4013.

Pezard, C., P. Berche & M. Mock, (1991) Contribution of individual toxin components to virulence of Bacillus anthracis. *Infection and immunity* **59**: 3472-3477.

Pfleger, B. F., Y. Kim, T. D. Nusca, N. Maltseva, J. Y. Lee, C. M. Rath, J. B. Scaglione, B. K. Janes, E. C. Anderson, N. H. Bergman, P. C. Hanna, A. Joachimiak & D. H. Sherman, (2008) Structural and functional analysis of AsbF: origin of the stealth

3,4-dihydroxybenzoic acid subunit for petrobactin biosynthesis. *Proc Natl Acad Sci U S A* **105**: 17133-17138.

Pfleger, B. F., J. Y. Lee, R. V. Somu, C. C. Aldrich, P. C. Hanna & D. H. Sherman, (2007) Characterization and analysis of early enzymes for petrobactin biosynthesis in Bacillus anthracis. *Biochemistry* **46**: 4147-4157.

Pohl, E., J. C. Haller, A. Mijovilovich, W. Meyer-Klaucke, E. Garman & M. L. Vasil, (2003) Architecture of a protein central to iron homeostasis: crystal structure and spectroscopic analysis of the ferric uptake regulator. *Mol Microbiol* **47**: 903-915.

Pohl, S., W. Y. Tu, P. D. Aldridge, C. Gillespie, H. Hahne, U. Mäder, T. D. Read & C. R. Harwood, Combined proteomic and transcriptomic analysis of the response of Bacillus anthracis to oxidative stress. *PROTEOMICS* **11**: 3036-3055.

Quentin, Y., G. Fichant & F. Denizot, (1999) Inventory, assembly and analysis of Bacillus subtilis ABC transport systems. *Journal of molecular biology* **287**: 467-484.

Radnedge, L., P. G. Agron, K. K. Hill, P. J. Jackson, L. O. Ticknor, P. Keim & G. L. Andersen, (2003) Genome differences that distinguish Bacillus anthracis from Bacillus cereus and Bacillus thuringiensis. *Appl Environ Microbiol* **69**: 2755-2764.

Ratledge, C., (2007) Iron metabolism and infection. *Food and nutrition bulletin* **28**: S515-523.

Ratledge, C. & L. G. Dover, (2000) Iron metabolism in pathogenic bacteria. *Annu Rev Microbiol* **54**: 881-941.

Ratledge, C. & F. G. Winder, (1964) Effect of Iron and Zinc on Growth Patterns of Escherichia Coli in Iron-Deficient Medium. *Journal of bacteriology* **87**: 823-827.

Raymond, K. N., E. A. Dertz & S. S. Kim, (2003) Enterobactin: an archetype for microbial iron transport. *Proc Natl Acad Sci U S A* **100**: 3584-3588.

Russell, R. R., J. Aduse-Opoku, I. C. Sutcliffe, L. Tao & J. J. Ferretti, (1992) A binding protein-dependent transport system in Streptococcus mutans responsible for multiple sugar metabolism. *The Journal of biological chemistry* **267**: 4631-4637.

Saraste, M., P. R. Sibbald & A. Wittinghofer, (1990) The P-loop--a common motif in ATP- and GTP-binding proteins. *Trends Biochem Sci* **15**: 430-434.

Saurin, W., E. Francoz, P. Martineau, A. Charbit, E. Dassa, P. Duplay, E. Gilson, A. Molla, G. Ronco, S. Szmelcman & et al., (1989) Periplasmic binding protein dependent transport system for maltose and maltodextrins: some recent studies. *FEMS Microbiol Rev* **5**: 53-60.

Schaible, U. E. & S. H. Kaufmann, (2004) Iron and microbial infection. *Nature reviews. Microbiology* **2**: 946-953.

Schmelz, S., N. Kadi, S. A. McMahon, L. Song, D. Oves-Costales, M. Oke, H. Liu, K. A. Johnson, L. G. Carter, C. H. Botting, M. F. White, G. L. Challis & J. H. Naismith, (2009) AcsD catalyzes enantioselective citrate desymmetrization in siderophore biosynthesis. *Nat Chem Biol* **5**: 174-182.

Schmitt, L., H. Benabdelhak, M. A. Blight, I. B. Holland & M. T. Stubbs, (2003) Crystal structure of the nucleotide-binding domain of the ABC-transporter haemolysin B: identification of a variable region within ABC helical domains. *Journal of molecular biology* **330**: 333-342.

Schneider, E. & S. Hunke, (1998) ATP-binding-cassette (ABC) transport systems: functional and structural aspects of the ATP-hydrolyzing subunits/domains. *FEMS microbiology reviews* **22**: 1-20.

Seeger, M. A. & H. W. van Veen, (2009) Molecular basis of multidrug transport by ABC transporters. *Biochim Biophys Acta* **1794**: 725-737.

Shatalin, K., E. Shatalina, A. Mironov & E. Nudler, (2011) H2S: A Universal Defense Against Antibiotics in Bacteria. *Science* **334**: 986-990.

Skaar, E. P., A. H. Gaspar & O. Schneewind, (2006) Bacillus anthracis IsdG, a heme-degrading monooxygenase. *J Bacteriol* **188**: 1071-1080.

Smaldone, G. T., O. Revelles, A. Gaballa, U. Sauer, H. Antelmann & J. D. Helmann, (2012) A global investigation of the Bacillus subtilis iron-sparing response identifies major changes in metabolism. *Journal of bacteriology*.

Smith, P. C., N. Karpowich, L. Millen, J. E. Moody, J. Rosen, P. J. Thomas & J. F. Hunt, (2002) ATP binding to the motor domain from an ABC transporter drives formation of a nucleotide sandwich dimer. *Molecular cell* **10**: 139-149.

Stojiljkovic, I. & K. Hantke, (1995) Functional domains of the Escherichia coli ferric uptake regulator protein (Fur). *Mol Gen Genet* **247**: 199-205.

Story, R. M. & T. A. Steitz, (1992) Structure of the recA protein-ADP complex. *Nature* **355**: 374-376.

Story, R. M., I. T. Weber & T. A. Steitz, (1992) The structure of the E. coli recA protein monomer and polymer. *Nature* **355**: 318-325.

Sweeney, D. A., C. W. Hicks, X. Cui, Y. Li & P. Q. Eichacker, (2011) Anthrax infection. *American journal of respiratory and critical care medicine* **184**: 1333-1341.

Tanabe, T., T. Funahashi, K. Shiuchi, N. Okajima, H. Nakao, K. Miyamoto, H. Tsujibo & S. Yamamoto, (2012) Characterization of Vibrio parahaemolyticus genes encoding the systems for utilization of enterobactin as a xenosiderophore. *Microbiology* **158**: 2039-2049.

Tao, L., I. C. Sutcliffe, R. R. Russell & J. J. Ferretti, (1993) Transport of sugars, including sucrose, by the msm transport system of Streptococcus mutans. *Journal of dental research* **72**: 1386-1390.

Torres, V. J., A. S. Attia, W. J. Mason, M. I. Hood, B. D. Corbin, F. C. Beasley, K. L. Anderson, D. L. Stauff, W. H. McDonald, L. J. Zimmerman, D. B. Friedman, D. E. Heinrichs, P. M. Dunman & E. P. Skaar, (2010) Staphylococcus aureus fur regulates the expression of virulence factors that contribute to the pathogenesis of pneumonia. *Infect Immun* **78**: 1618-1628.

Tu, W. Y., S. Pohl, J. Gray, N. J. Robinson, C. R. Harwood & K. J. Waldron, (2012) Cellular Iron Distribution in Bacillus anthracis. *Journal of bacteriology* **194**: 932-940.

Venturi, V., C. Ottevanger, M. Bracke & P. Weisbeek, (1995) Iron regulation of siderophore biosynthesis and transport in Pseudomonas putida WCS358: involvement of a transcriptional activator and of the Fur protein. *Mol Microbiol* **15**: 1081-1093.

Walker, J. E., M. Saraste, M. J. Runswick & N. J. Gay, (1982) Distantly related sequences in the alpha- and beta-subunits of ATP synthase, myosin, kinases and other ATP-requiring enzymes and a common nucleotide binding fold. *EMBO J* **1**: 945-951.

Walter, C., K. Honer zu Bentrup & E. Schneider, (1992) Large scale purification, nucleotide binding properties, and ATPase activity of the MalK subunit of

Salmonella typhimurium maltose transport complex. *J Biol Chem* **267**: 8863-8869.

Wandersman, C. & P. Delepelaire, (2004) Bacterial iron sources: from siderophores to hemophores. *Annu Rev Microbiol* **58**: 611-647.

Wardman, P. & L. P. Candeias, (1996) Fenton chemistry: an introduction. *Radiat Res* **145**: 523-531.

Weinberg, E. D., (1975) Nutritional immunity. Host's attempt to withold iron from microbial invaders. *JAMA : the journal of the American Medical Association* **231**: 39-41.

Wilson, M. K., R. J. Abergel, J. E. Arceneaux, K. N. Raymond & B. R. Byers, (2009a) Temporal production of the two Bacillus anthracis siderophores, petrobactin and bacillibactin. *Biometals : an international journal on the role of metal ions in biology, biochemistry, and medicine*.

Wilson, M. K., R. J. Abergel, J. E. Arceneaux, K. N. Raymond & B. R. Byers, (2009b) Temporal production of the two Bacillus anthracis siderophores, petrobactin and bacillibactin. *Biometals : an international journal on the role of metal ions in biology, biochemistry, and medicine* **23**: 129-134.

Wilson, M. K., R. J. Abergel, J. E. Arceneaux, K. N. Raymond & B. R. Byers, (2010) Temporal production of the two Bacillus anthracis siderophores, petrobactin and bacillibactin. *Biometals : an international journal on the role of metal ions in biology, biochemistry, and medicine* **23**: 129-134.

Wilson, M. K., R. J. Abergel, K. N. Raymond, J. E. Arceneaux & B. R. Byers, (2006) Siderophores of Bacillus anthracis, Bacillus cereus, and Bacillus thuringiensis. *Biochem Biophys Res Commun* **348**: 320-325.

Wolters, J. C., R. P. Berntsson, N. Gul, A. Karasawa, A. M. Thunnissen, D. J. Slotboom & B. Poolman, (2010) Ligand binding and crystal structures of the substrate-binding domain of the ABC transporter OpuA. *PloS one* **5**: e10361.

Wooldridge, K. G., J. A. Morrissey & P. H. Williams, (1992) Transport of ferric-aerobactin into the periplasm and cytoplasm of Escherichia coli K12: role of envelope-associated proteins and effect of endogenous siderophores. *J Gen Microbiol* **138**: 597-603.

Wyatt, M. A., W. Wang, C. M. Roux, F. C. Beasley, D. E. Heinrichs, P. M. Dunman & N. A. Magarvey, (2010) Staphylococcus aureus nonribosomal peptide secondary metabolites regulate virulence. *Science* **329**: 294-296.

Zawadzka, A. M., R. J. Abergel, R. Nichiporuk, U. N. Andersen & K. N. Raymond, (2009a) Siderophore-mediated iron acquisition systems in Bacillus cereus: Identification of receptors for anthrax virulence-associated petrobactin. *Biochemistry* **48**: 3645-3657.

Zawadzka, A. M., Y. Kim, N. Maltseva, R. Nichiporuk, Y. Fan, A. Joachimiak & K. N. Raymond, (2009b) Characterization of a Bacillus subtilis transporter for petrobactin, an anthrax stealth siderophore. *Proc Natl Acad Sci U S A.*

Chapter 2

Multiple ABC Transporters are Involved in the Acquisition of Petrobactin by *Bacillus anthracis*

2.1 Introduction

The production and secretion of siderophores is the primary mechanism of iron acquisition by *Bacillus anthracis* (Ratledge & Dover, 2000). *B. anthracis* produces two distinct siderophore molecules, bacillibactin and petrobactin (Wilson *et al.*, 2006, Hotta *et al.,* Cendrowski *et al.*, 2004b, Koppisch *et al.*, 2005, Lee *et al.*, 2007, Pfleger *et al.*, 2007, Pfleger *et al.*, 2008b, Zawadzka *et al.*, 2009b, Zawadzka et al., 2009a); however, in this species, petrobactin is the only siderophore essential for growth in macrophages and murine virulence (Koppisch et al., 2005, Cendrowski et al., 2004b, Garner *et al.*, 2004, Abergel *et al.*, 2006a, Abergel *et al.*, 2008). This compound has a 3,4-hydroxyl orientation on its catecholate moieties (3,4-dihydroxybenzoate) that is unique among siderophores. This uncommon orientation allows petrobactin to evade recognition by the human immune protein siderocalin, thus petrobactin has been termed the "stealth siderophore" of *B. anthracis* (Abergel *et al*., 2006a, Pfleger *et al*., 2008b, Zawadzka *et al*., 2009b).

The stages of petrobactin biosynthesis have been well studied in *B. anthracis* (Abergel et al., 2008, Abergel *et al.*, 2006b, Barbeau *et al.*, 2002, Cendrowski *et al.*,

2004a, Challis, 2005, Fox *et al.*, 2008, Kadi & Challis, 2009, Koppisch *et al.*, 2008a, Koppisch et al., 2005, Koppisch *et al.*, 2008b, Lee et al., 2007, Lee *et al.*, 2011, Liu *et al.*, 2007, Oves-Costales *et al.*, 2009, Oves-Costales *et al.*, 2007, Oves-Costales *et al.*, 2008, Pfleger *et al.*, 2008a, Pfleger et al., 2007, Wilson *et al.*, 2009, Wilson et al., 2006). However, only some of the details about iron-petrobactin import are known. We have previously shown that FpuA is the receptor protein required for normal growth under iron-depleted conditions and for murine virulence (Carlson *et al.*, 2010). Furthermore, FpuA shows high sequence homology with the receptor components of ATP-binding cassette (ABC)-transport systems from other bacteria; therefore transport of iron-petrobactin most likely occurs through an ABC-transport system.

A bioinformatic search produced six candidate permease and seven ATPase genes that were hypothesized to be involved in ferri-siderophore transport based on sequence homology to well-characterized systems in other species. Markerless deletion of these genes were made in a Sterne $34F_2$ background. Through subsequent observation of the mutants for phenotypes in iron-depleted conditions and a mouse model of anthrax, I now present the identification and characterization of all permease and ATPase components of the ABC-import system required for iron uptake via the virulence-associated siderophore petrobactin in *B. anthracis*.

2.2 Results

Identification of two individual permeases involved in petrobactin reacquisition

Seven iron-hydroxamate transporter permeases were identified as putative components of the *B. anthracis* petrobactin import system. Each of these proteins has significant sequence homology to the well characterized ATP-dependent iron (III) hydroxamate permease (FhuB) from *Escherichia coli* (Koster, 2001, Koster, 2005), and all are induced by iron starvation (Carlson *et al.*, 2009). Genetic organization of these putative permeases fall into two classes: those that are encoded by a single gene (GBAA4767, GBAA4596, GBAA4785, and GBAA5630), and those that are encoded by two consecutive genes (GBAA5328-5329, GBAA3865-3866, and GBAA0616-0617) (Fig. 2-1). Of these predicted permeases, the most obvious candidate for a role in petrobactin import was GBAA4767 (*fpuB*), as it is located directly downstream and likely co-transcribed with *fpuA,* which encodes the petrobactin receptor protein (Carlson *et al*., 2010). Another attractive candidate was the heterodimeric permease FatCD (GBAA5328-5329). An orthologue of this permease, YclNO, was previously shown to be required for petrobactin reacquisition in *B. subtilis* (Zawadzka *et al*., 2009b).

To test if any of these putative permease proteins were required for the import of petrobactin, individual mutants lacking each of the seven permeases were constructed and analyzed. Each mutant was examined for the ability to grow in iron-depleted media (IDM). Mutants unable to synthesize or import petrobactin display a severe growth defect under these conditions (Carlson et al., 2010, Cendrowski et al., 2004b). Surprisingly, none of the single permease mutants, including Δ*fpuB* and Δ*fatCD,*

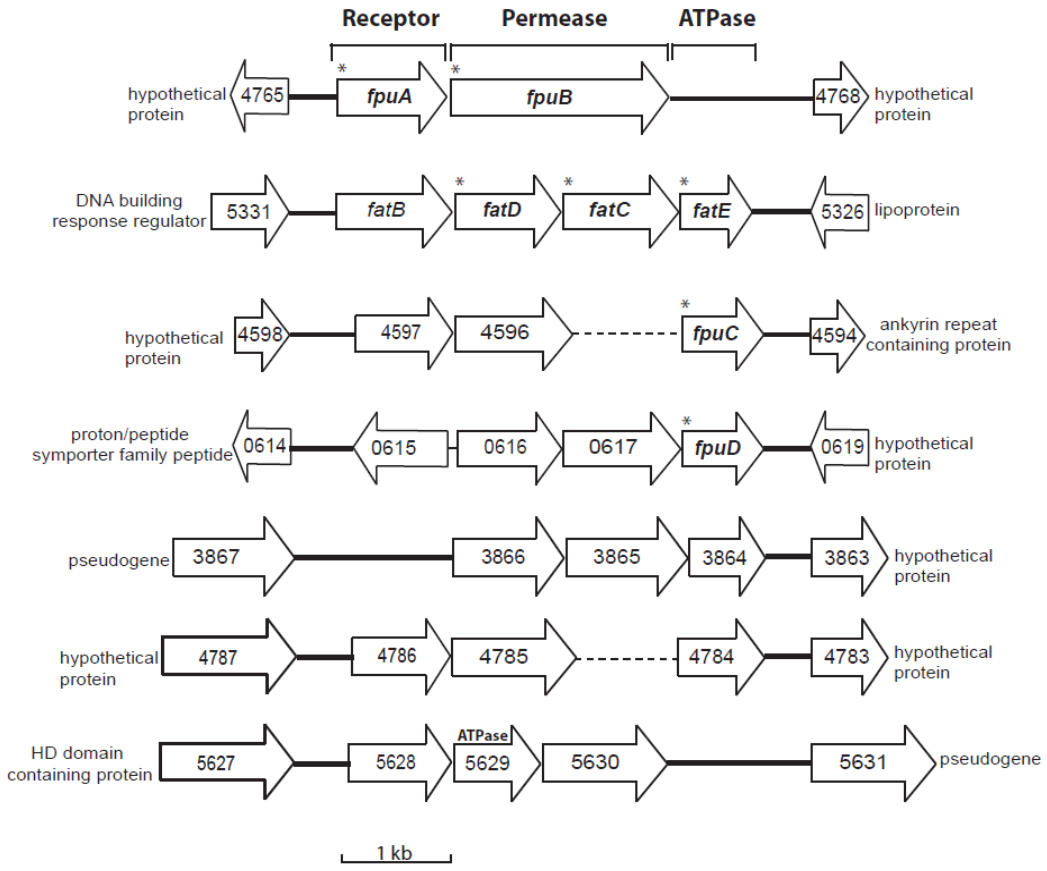

Figure 2-1. Organization of genes investigated in this work. The genes encoding the iron associated ABC transporter components investigated in this work reside in seven separate clusters. Those found to be involved in the reacquisition of petrobactin belong to four of these clusters; individual genes directly involved in this process are marked with asterisks. Gene names for *fpuB* (GBAA4767; previously annotated as *fhuB*)**,** *fpuC* (GBAA4595), *fpuD* (GBAA0618), and *fatE* (GBAA5327) have been updated to reflect their involvement in petrobactin transport. The three other gene clusters investigated here showed no i nvolvement in this process. All clusters are aligned in the order receptor/permease/ATPase, with the exception of GBAA5629, which is labeled separately as this ATPase gene is positioned between the receptor and permease genes in its cluster. Dotted lines between consecutive genes were used for alignment purposes and do not indicate actual space between the genes. The annotated or predicted functions of all genes flanking each cluster are also shown. Intergenic region between the clusters and the flanking genes are not to scale.

exhibited a growth defect in IDM (Fig. 2-2A, solid squares and solid triangles, Fig. 2-S1 and Table 1-S1). It was therefore hypothesized that more than one of the putative permeases could facilitate the import of petrobactin. To test this, a mutant lacking the two most likely candidate permeases, FpuB and FatCD, was generated. The Δ*fpuB*Δ*fatCD* mutant exhibited a severe growth defect in IDM (Fig. 2-2A, open diamonds), similar to that of mutants deficient in both petrobactin transport (Δ*fpuA*) and petrobactin biosynthesis (Δ*asbABCDEF*) (Fig. 2-2A, open squares and open triangles, respectively). These results suggest that these proteins play redundant roles in petrobactin transport. It is important to note that this growth defect was iron dependent, as all mutants tested exhibited wild-type growth levels in rich media (Fig. 2-2B, and data not shown).

To further demonstrate the role of these permeases in petrobactin import, it was necessary to eliminate the possibility that these mutants were unable to produce or secrete the siderophore. There are several phenotypes that can distinguish an import deficient mutant (*e.g*. Δ*fpuA*), from a biosynthetic mutant (*e.g.* Δ*asbABCDEF*), including the inability to be chemically rescued with supplemental petrobactin, accumulation of extracellular catechol, and resistance to gallium toxicity (Carlson *et al*., 2010). The first phenotype tested was the ability to be chemically rescued to wild-type growth levels in IDM by the addition of exogenous petrobactin. This supplementation allows for recovery of growth of petrobactin biosynthetic mutants, while transport deficient mutants are not complemented in this manner. Spores of wild-type, Δ*asbABCDEF*, Δ*fpuA,* or Δ*fpuB*Δ*fatCD* strains were grown in IDM with or without supplemental petrobactin (2.5 μM). As expected, the growth of the petrobactin biosynthetic mutant was fully restored

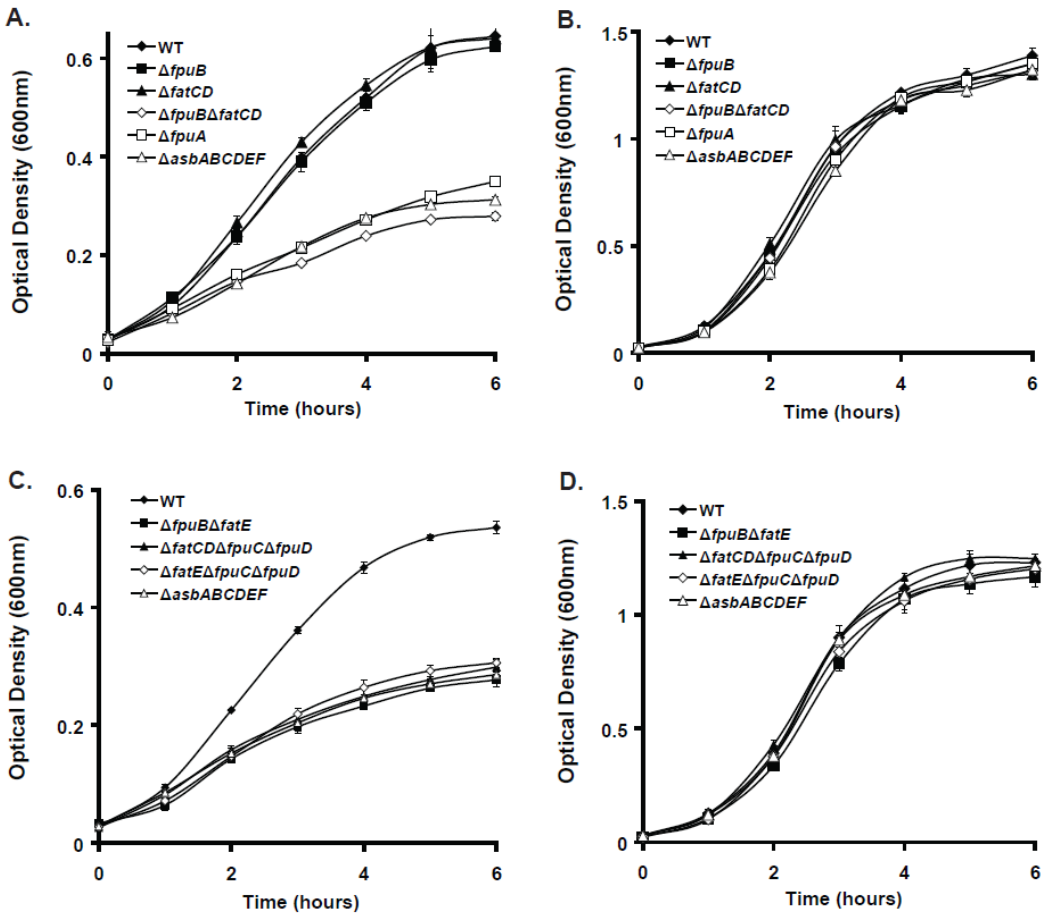

Figure 2-2. Growth phenotypes of *B. anthracis* mutant strains. All cultures were inoculated with actively growing vegetative bacilli at an initial OD_{600} of 0.05. Growth was monitored hourly by measuring OD_{600}. Wild-type and Δ*asbABCDEF* strains were used in all experiments as controls. (A, B) Growth of permease deletion mutants. Wild-type (solid diamonds), Δ*fpuB* (solid squares), Δ*fatCD* (solid triangles), Δ*fpuB*Δ*fatCD* (open diamonds), Δ*fpuA* (open squares), and Δ*asbABCDEF* (open triangles) strains were grown in either IDM media (A) or BHI media (B). (C, D) Growth of ATPase deletion mutants. Wild-type (solid diamonds), Δ*fpuB*Δ*fatE* (solid squares), Δ*fatCD*Δ*fpuC*Δ*fpuD* (solid triangles), Δ*fatE*Δ*fpuC*Δ*fpuD* (open diamonds), and Δ*asbABCDEF* (open triangles) strains were grown in either IDM media (C) or BHI media (D). Data are presented as mean ± standard deviation of triplicate measures from one experiment and represent at least three independent experiments.

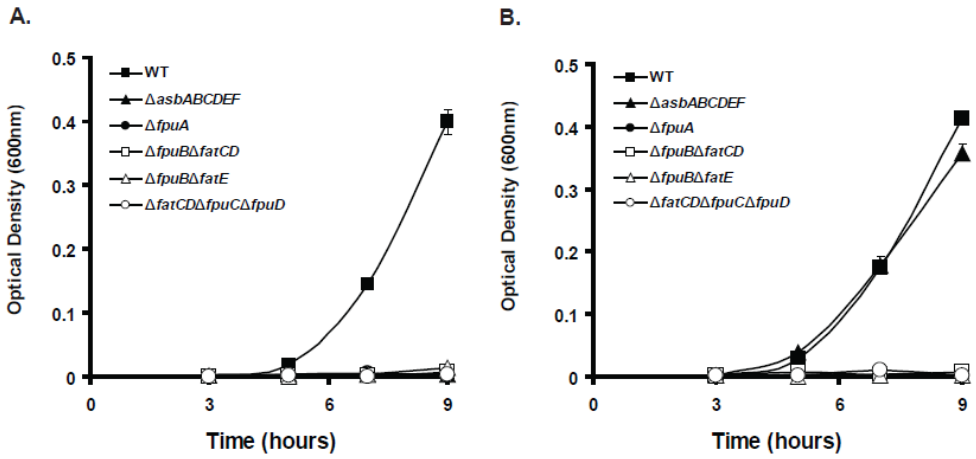

Figure 2-3. Petrobactin supplementation does not restore growth of transport deficient mutants in IDM. Cultures of either IDM (A) or in IDM supplemented with 2.5 µM purified petrobactin (B) were inoculated with 1×10^5 spores of wild-type (solid squares), Δ*asbABCDEF* (solid triangles), Δ*fpuA* (solid circles)**,** Δ*fpuB*Δ*fatCD* (open squares), Δ*fpuB*Δ*fatE* (open triangles), or Δ*fatCD*Δ*fpuC*Δ*fpuD* (open circles). Growth was monitored by measuring OD_{600} over nine hours. Data are presented as mean ± standard deviation of triplicate measures from one experiment and represent at least three independent experiments.

by this supplementation (Fig 2-3. A and B, solid triangles). However, this treatment did not restore growth of the double permease mutant (Δ*fpuB*Δ*fatCD*), indicating an inability to import petrobactin (Fig 2-3. A and B, open squares). This result was identical to that of the known petrobactin transport mutant (Δ*fpuA*) (Fig. 2-3 A and B, solid circles) (Carlson *et al*., 2010, Arnow, 1937).

A second phenotype of mutants unable to import petrobactin is significant accumulation of catechol in the culture supernatant, compared to that seen in wild-type strains (Carlson *et al*., 2010). The individual permease mutants, Δ*fpuB* and Δ*fatCD,* and the double mutant, Δ*fpuB*Δ*fatCD,* were assayed for extracellular catechol using the Arnow assay (Arnow, 1937). The petrobactin biosynthetic mutant was included as a control for non-petrobactin catechols. As reported previously (Carlson *et al*., 2010), culture supernantants from this strain exhibited minimal levels of catechol, indicating that the majority of what was observed is petrobactin (Fig. 2-4, Δ*asbABCDEF*). Catechol levels detected in the supernatants of all single permease mutants were nearly identical to those found in wild-type supernatants (Fig. 2-4). However, extracellular catechol levels in the culture supernatant of Δ*fpuB*Δ*fatCD* were significantly higher than those detected in wild-type (Fig. 2-4). These results are similar to those obtained for Δ*fpuA,* which is unable to import petrobactin (Fig. 2-4 and (Carlson *et al*., 2010)).

The final phenotype tested was resistance to gallium toxicity. Gallium resistance has been used to show siderophore transport in several bacterial systems (Olakanmi *et al.*, 2000, Banin *et al.*, 2008, Ecker & Emery, 1983, Carlson *et al*., 2010). Gallium is able to bind to siderophores with high efficiency (Zawadzka *et al*., 2009b, Banin *et al*., 2008)

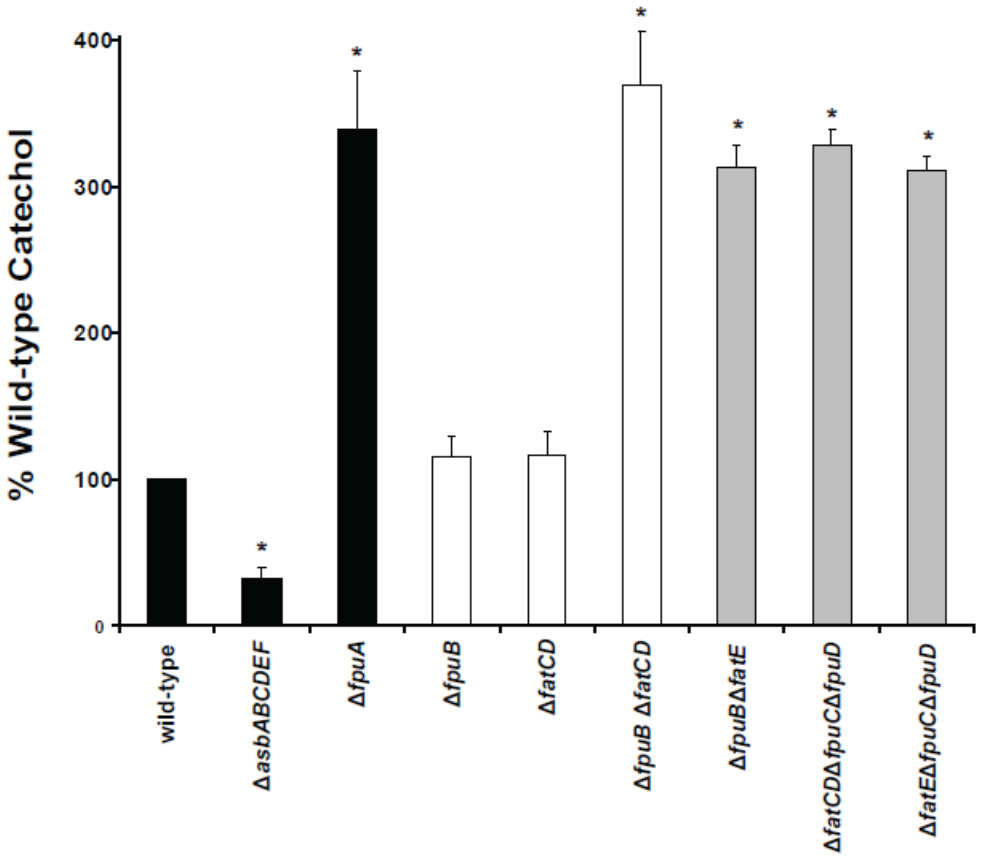

Figure 2-4. Accumulation of extracellular catechols in petrobactin transport deficient strains. Catechols were measured in filtered culture supernatants following six-hour growth of either control strains (black bars), permease mutants (white bars), or ATPase mutants (grey bars) using the Arnow assay. Data were normalized to the OD_{600} of cultures and are presented as percent of wild-type catechol levels. Data are presented as mean ± standard deviation of triplicate measures from one experiment and represent three or more independent experiments. * = $p \leq 0.005$. The level of catechol observed from Δ*fpuB*Δ*fatCD* is not statistically significant ($p = 0.52$) from Δ*fpuA*.

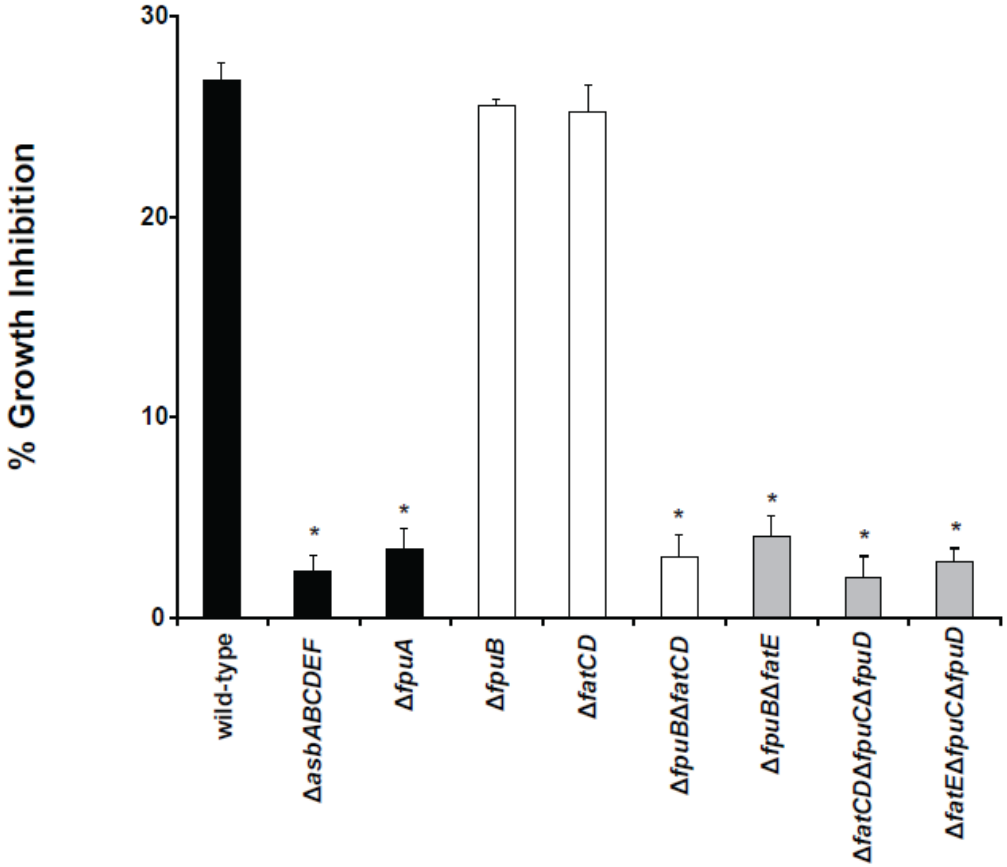

Figure 2-5. Resistance of petrobactin transport deficient strains to gallium toxicity. Control strains (black bars), permease mutants (white bars), or ATPase mutants (grey bars) were grown in IDM with or without 20 μM gallium sulfate and examined for change in OD_{600} after two hours. Results are presented as percent growth inhibition in the presence of 20 μM gallium sulfate. Data are presented as mean ± standard deviation of triplicate measures from one experiment and represent at least three independent experiments. * = $p \leq 0.0001$. Percent growth inhibition was calculated as {[(OD_{600} IDM + gallium)/ (OD_{600} IDM)]*100}.

and is toxic when imported into the bacterial cytoplasm (Banin *et al*., 2008). Previous studies have shown that the addition of 20 μM gallium sulfate to IDM culture media results in a petrobactin-dependent growth defect in wild-type *B. anthracis* (Carlson *et al*., 2010). To further test the ability of Δ*fpuB*Δ*fatCD* to import petrobactin, growth of this strain was examined in the presence of gallium. Wild-type, Δ*asbABCDEF*, Δ*fpuA,* Δ*fpuB,* Δ*fatCD, and* Δ*fpuB*Δ*fatCD* strains were incubated in the presence or absence of gallium sulfate and growth was measured by change in OD_{600} after two hours. The addition of gallium sulfate to wild-type *B. anthracis* resulted in a significant growth inhibition when compared to cultures grown without gallium (Fig. 2-5). In contrast, strains unable to produce or import petrobactin are protected from this toxicity (Fig. 2-5, Δ*fpuA* and Δ*asbABCDEF*) (Carlson et al., 2010, Cendrowski et al., 2004b). As predicted by their ability to grow in IDM, both single permease mutants (Δ*fpuB* and Δ*fatCD*) were significantly inhibited by the presence of gallium (Fig. 2-5). Much like the petrobactin biosynthetic mutant, the double permease mutant, Δ*fpuB*Δ*fatCD*, was not significantly inhibited by the presence of gallium (Fig. 2-5).

The Δfpu*B*Δfat*CD mutant is attenuated for virulence in a murine model of inhalational anthrax

Known petrobactin biosynthetic (Δ*asbABCDEF*) and receptor (Δ*fpuA*) mutants exhibit significant attenuation in murine virulence (Cendrowski et al., 2004b, Carlson et al., 2010). Therefore, it was hypothesized that a strain lacking all permease components of the petrobactin import system would exhibit a similar attenuation. To test this hypothesis, a murine model of inhalational anthrax was used (Cendrowski et al., 2004b). Mice were inoculated intratracheally with either wild-type (n=8) or Δ*fpuB*Δ*fatCD* (n=16)

spores at a dose of approximately 20 times the LD_{50} (1 x 10^5 spores/mouse). Mice were then monitored for 14 days post-infection. As expected, all mice infected with wild-type spores succumbed to infection within four days (Fig. 2-6A, circles) (Cendrowski et al., 2004b). In sharp contrast, mice inoculated with the Δ*fpuB*Δ*fatCD* strain exhibited a significant increase in survival ($p \leq 0.0001$), with the majority of mice (15 of 16) surviving the full two-week experiment (Fig. 2-6A, solid squares).

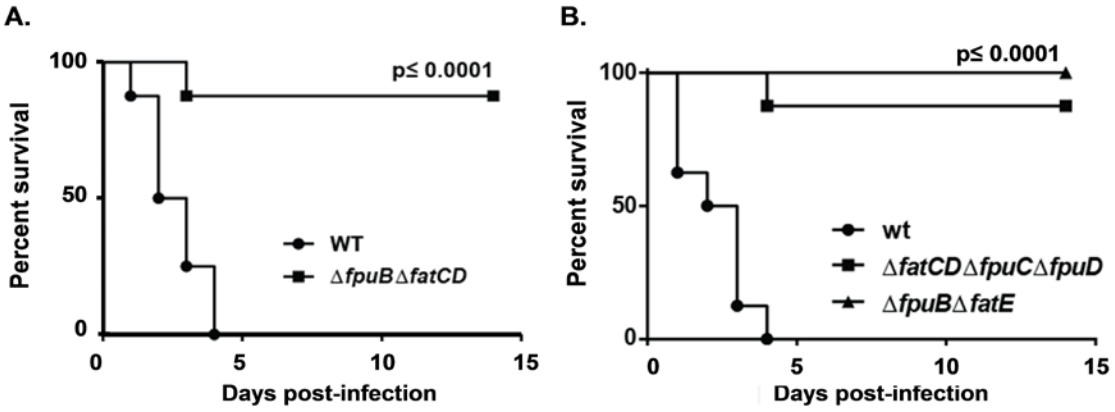

Figure 2-6. Attenuation of double permease mutant and ATPase mutants in murine model of inhalational anthrax. DBA/2J mice were infected via intratracheal inoculation with either wild-type (solid circles, n=8, A and B), Δ*fpuB*Δ*fatCD* (solid squares, n=16, A), Δ*fatCD*Δ*fpuC*Δ*fpuD* (solid squares, n=8, B) or Δ*fpuB*Δ*fatE* (solid triangles, n=8, B) mutant spores at a dose of 1 x 10^5 spores/mouse. Mice were monitored for fourteen days after infection. The survival curve for all mutant strains tested here were significantly different from wild-type by the log-rank test ($p \leq 0.0001$).

Identification of three ATPase components involved in petrobactin transport

Six ATPase proteins were identified as candidates for a role in petrobactin import. These putative ATPases are encoded by GBAA4595, GBAA0618, GBAA5629, GBAA4784, GBAA3864, and GBAA5327 (Fig. 2-1). To assess the putative role of these candidate proteins in petrobactin transport, six single deletion mutants were generated, each lacking one of these genes. Similar to what was observed for the permeases, none of these single mutants exhibited a growth defect in IDM (Fig. 2-S1 and Table 2-S1). These findings, and the identification of two distinct petrobactin-specific permeases as described above, suggested the possibility that distinct ATPases could be functioning individually with each permease. Of the six putative ATPases, *fatE* is located directly downstream of the *fatCD* and was, therefore, the most likely candidate to function with this permease. To determine whether FatE was functioning with the FatCD permease, it was necessary to prevent transport through the other permease, FpuB. Therefore, a mutant lacking the FatE ATPase was generated in the Δ*fpuB* background. This mutant, Δ*fpuB*Δ*fatE,* displayed all of the hallmark characteristics of a petrobactin import mutant including a growth defect in IDM (Fig. 2-2C, solid squares), an inability to be restored to wild-type growth levels by the addition of exogenous petrobactin (Fig. 2-3A and B, open triangles), increased extracellular catechol levels in culture supernatants (Fig. 2-4, grey bars), and resistance to gallium induced growth inhibition (Fig. 2-5, grey bars). These phenotypes combined implicate FatE in petrobactin import through interaction with the FatCD permease.

In order to identify the ATPase(s) functioning with the FpuB permease, an analogous approach was taken. Each of the remaining five putative ATPase genes was

deleted individually in the Δ*fatCD* background. However, none of these mutants exhibited a growth defect in IDM (data not shown). This result suggested that multiple ATPases were functioning with this single permease. To test this, a double ATPase deletion mutant was generated in the Δ*fatCD* background targeting the two genes (GBAA4595 and GBAA0618) having the highest amino acid sequence identity to the FhuC ATPase from *Escherichia coli* (45% and 42% identity, respectively). This mutant, Δ*fatCD*Δ*fpuC*Δ*fpuD*, displayed all of the phenotypic characteristics of a mutant deficient in petrobactin import. These included an inability to grow to wild-type levels in IDM (Fig. 2-2C, solid triangles), an inability to be restored to wild-type growth levels by the addition of exogenous petrobactin (Fig. 2-3A and B, open circles), increased extracellular catechol levels in culture supernatants (Fig. 2-4, grey bars), and protection from gallium induced growth inhibition (Fig. 2-5, grey bars). We therefore propose naming these genes *fpuC* (GBAA4595) and *fpuD* (GBAA0618). A mutant lacking only these two ATPases, but still encoding the FatCD permease (Δ*fpuC*Δ*fpuD*) did not have a growth defect in IDM (data not shown). Indeed, no mutant lacking two of these ATPases (*fatE*, *fpuC*, or *fpuD*) showed any phenotype. Furthermore, to test whether these ATPases were also importance for virulence, mice were inoculated intratracheally with either wild-type (n=8), Δ*fatCD*Δ*fpuC*Δ*fpuD* (n=8), or Δ*fpuB*Δ*fatE* (n=8) spores at a dose of approximately 20 times the LD50 (1×10^5 spores/mouse). Mice were then monitored for 14 days post-infection. All mice infected with wild-type spores succumbed to infection within four days (Fig. 2-6, A and B circles) while, mice inoculated with either Δ*fatCD*Δ*fpuC*Δ*fpuD* or Δ*fpuB*Δ*fatE* strains were highly attenuated for virulence ($p \leq 0.0001$), compared to that of wild-type (Fig. 2-6B, solid squares or solid triangles). All of these data combine to

implicate the ATPases encoded by *fpuC* and *fpuD* in the import of petrobactin through interaction with the FpuB permease.

Finally, a mutant lacking all three ATPase components was constructed (Δ*fatE*Δ*fpuC*Δ*fpuD*). This strain retained wild-type copies of both of the identified petrobactin reacquisition permeases. The triple ATPase mutant exhibited the expected growth defect in IDM (Fig. 2-2C, open diamonds). As expected, the Δ*fatE*Δ*fpuC*Δ*fpuD* mutant also exhibited increased catachol levels (Fig. 2-4, grey bars), and no sensitivity to gallium (Fig. 2-5, grey bars). However, in addition to the growth defect observed in IDM, this mutant grew poorly in sporulation media, and failed to sporulate efficiently. Due to the inability to isolate spores, the petrobactin supplementation assay could not be performed. Although the mutant failed to grow well in sporulation media, it did not exhibit a general growth defect, as it grew as well as wild-type in rich media, (Fig. 2D, open diamonds) or in IDM supplemented with 20 μM ferrous sulfate (data not shown). The growth and sporulation defects observed for the Δ*fatE*Δ*fpuC*Δ*fpuD* mutant could be complemented in *trans*. Growth in IDM was restored to wild-type levels when either *fpuD* or *fatE* was expressed from a plasmid, (Fig. 7, solid triangles and solid circles, respectively). The ability to grow well in sporulation media and produce spores was restored in the complemented strains as well (data not shown). For unknown reasons, attempts to complement *fpuC* are so far unsuccessful.

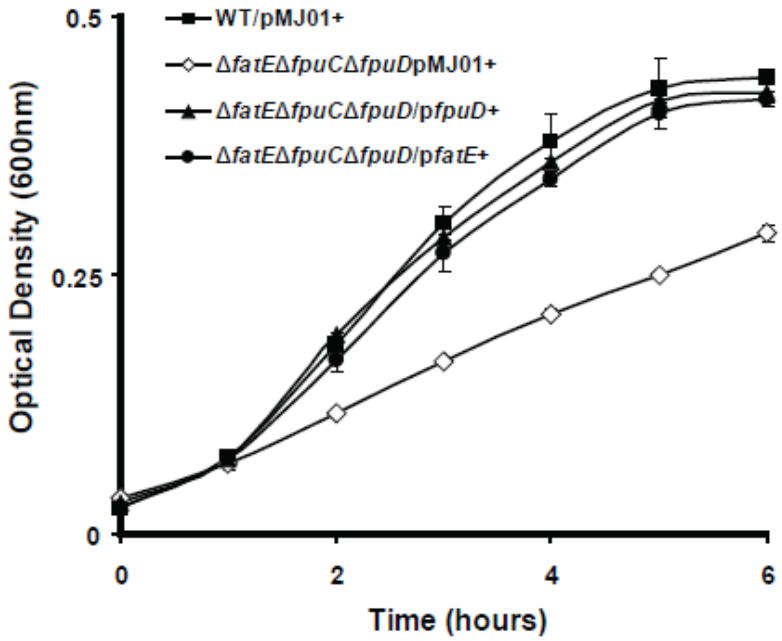

Figure 2-7. Complementation of triple ATPase mutant. All cultures were inoculated with vegetative bacilli at an initial OD_{600} of 0.05 and growth was monitored hourly for six hours by measuring increase in OD_{600}. Wild-type/pMJ01+ and Δ*fatCD*Δ*fpuC*Δ*fpuD*/pMJ01+ strains were used as empty vector controls. Wild-type/pMJ01+ (solid squares), Δ*fatE*Δ*fpuC*Δ*fpuD*/pMJ01+ (open diamonds), Δ*fatE*Δ*fpuC*Δ*fpuD*/p*fpuD*+ (solid triangles), Δ*fatE*Δ*fpuC*Δ*fpuD*/p*fatE*+ (solid circles) strains were grown in IDM media containing 10µg ml^{-1} chloramphenicol. Data are presented as mean ± standard deviation of triplicate measures from one experiment and represent at least three independent experiments.

2.3 Discussion

B. anthracis encodes a number of genes involved in scavenging iron from a variety of sources, including those responsible for the biosynthesis of two siderophores (Carlson *et al*., 2009, Lee *et al*., 2007). However, both murine virulence and the ability to grow in iron depleted medium *in vitro* are only dependent on the ability to produce and reacquire one of these molecules, petrobactin. Previous work established both the importance of petrobactin biosynthesis, and the requirement of the petrobactin receptor FpuA in its utilization (Lee et al., 2007, Carlson et al., 2009, Carlson et al., 2010, Cendrowski et al., 2004b, Garner et al., 2004). The work presented here identifies two permeases and three ATPases that also function in petrobactin import. These proteins appear to function with the petrobactin receptor FpuA, presumably making at least three ABC transporter complexes, each independently sufficient for the reacquisition of petrobactin (Fig. 2-8). Two of these transporter complexes involve association of the receptor, FpuA, with the FpuB permease. In turn, FpuB can function with either of two separate ATPases, FpuC or FpuD (Fig. 2-8, complexes A and B). The third transporter complex consists of FpuA associated with the FatCD permease and the FatE ATPase (Fig. 2-8, complex C).

While it is common for all of the components of a bacterial ABC transporter to be encoded within a single operon, instances exist where the genes encoding these components are located in separate positions on the genome. The genes that encode the components for petrobactin acquisition exhibit this partially unclustered genetic organization. The genes encoding FpuA and FpuB belong to a single operon lacking a gene encoding an ATPase (Fig. 2-1). Two distinct genes (*fpuC* and *fpuD*), found at

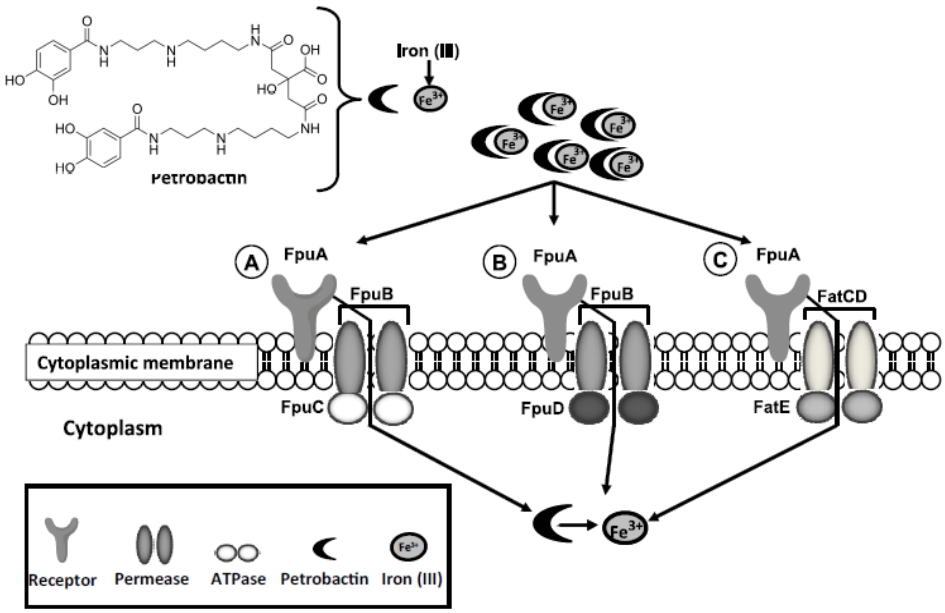

Figure 2-8. Proposed model for *Bacillus anthracis* petrobactin ATP-Binding Cassette (ABC) Import. Extracellular petrobactin (black crescents) binds to ferric iron ions (grey ovals) prior to reacquisition. The proteins required for the import of petrobactin include the substrate-binding receptor protein FpuA (required in all three complexes), two hydrophobic membrane-spanning domains, or permeases, FpuB (complex A and B) and FatCD (complex C), and three cytoplasmic ATPase domains, FatE, and proteins FpuC and FpuD that couple the energy of ATP hydrolysis to import petrobactin. It is presumed that the iron-siderophore complex is imported through the cytoplasmic membrane via one of these three canonical (substrate-binding protein dependent) ABC- transport protein complexes.

separate locations on the chromosome, encode ATPase components that can individually energize import through FpuB (Fig. 2-8, complex A and B). These genes belong to otherwise uncharacterized iron-transport clusters containing both putative receptor and permease genes (Fig. 2-1) that play no apparent role in petrobactin reacquisition. For the FpuA/FatCDE transport complex (Fig.2-8, complex C), the genes encoding the permease and ATPase components are contained within the same operon, *fatBCDE*. FatB, an apparent substrate binding protein, is not required for petrobactin import, but may serve some other undefined role (Carlson *et al*., 2010).

Often the components of ABC transporters are unique to an individual transporter, although some promiscuity, similar to what is reported here for petrobactin import, has been observed. For example, the MsmK ATPase from *Streptococcus pneumoniae* associates with the transmembrane domains of multiple carbohydrate transporters, including those involved in the import of sialic acid (SatABC), raffinose (RafEGF) and maltotetraose (MalXCD) (Marion *et al.*, 2011). Additionally, the FhuC ATPase from *Staphylococcus aureus* functions as the ATPase component of three distinct iron-siderophore transporters, HtsABC, SirABC and FhuCBG. These transporters are required for staphyloferrin A, staphyloferrin B, and hydroxamate-mediated iron acquisition, respectively (Beasley & Heinrichs, 2010). Similarly, the plasmid-encoded anguibactin uptake system of *Vibrio anguillarum* lacks an ATPase, and relies on a yet unidentified enzyme encoded on the chromosome (Koster *et al.*, 1991, Lopez & Crosa, 2007). The work presented here reports an unusual inverse of these configurations in which a single substrate-binding protein, FpuA, presents petrobactin to two distinct permeases and furthermore, these two permease proteins display association with discrete ATPases.

Despite the compelling genetic analysis presented here suggesting three complexes following the canonical model for ABC transporters (Eitinger *et al.*, 2011), we note that protein-protein interaction studies have not been performed. Additional characterizations, including the relative abundance of each transporter on the cell surface and preference of the receptor FpuA for the permeases FpuB or FatCD remain to be determined. Also, the question of when iron is removed from petrobactin, before or after import, remains. Considering the similarity in structure of petrobactin to other well-characterized siderophores including aerobactin (Koster & Braun, 1990a, Koster & Braun, 1990b, Wooldridge *et al.*, 1992) and bacillibactin (Miethke *et al.*, 2006), it is likely that the intact ferric-petrobactin holo-complex is transported across the membrane. According to this model, reduction of the metal (Miethke & Marahiel, 2007) or degradation of the siderophore (Miethke *et al*., 2006, Garénaux *et al.*, 2011) by currently unidentified enzymes would then allow for release of iron in the bacterial cytoplasm. However, the possibility exists that the release of iron from petrobactin occurs prior to internalization. This has been observed in *Salmonella typhimurium* and in *Mycobacterium tuberculosis* where the enzymatic reduction and release of iron from either ferrioxamine or mycobactin, respectively, occurs by extracellular iron reductases (Cowart, 2002, Ratledge, 2004).

We propose that the permeases FpuB and FatCD play redundant roles in petrobactin import, with either protein able to associate with their respective ATPases and the FpuA receptor in the formation of a canonical ABC transport complex. Additional redundancy is observed by the association of FpuB with two ATPases, FpuC or FpuD (Fig. 2-8, Complexes A and B), either of which is sufficient for petrobactin

import. The genes that encode these two ATPases belong to gene clusters that contain both receptor and permease components and have high homology to other ABC transporters involved in ion transport (Fig. 2-1, GBAA4597 and GBAA0615 gene clusters). It seems likely, therefore, that these ATPases are functional components of transporters with roles other than petrobactin acquisition. A possible example of this multi-functionality is demonstrated by the growth defect of the triple mutant (Δ*fatE*Δ*fpuC*Δ*fpuD*) in sporulation media, a defect not present in any other mutant, independent of their growth phenotypes in IDM. This inability to produce spores is most likely the result of the poor growth in the sporulation media, versus a defect in the sporulation machinery. However, the exact nature of this defect is unknown.

Petrobactin-facilitated iron uptake is a determinant of *B. anthracis* virulence. Through this, and previous work, we have completed the identification of components composing the import machinery facilitating this process. The petrobactin import system consists of redundant gene products that interact with specific partners in the formation of three canonical ABC transport complexes (Fig. 2-8, complexes A, B, and C). The description of siderophore uptake systems provides the identification of potential therapeutic targets for combating bacterial infections and creates a more accurate model of steps critical to the life cycle *B. anthracis* during pathogenesis. These findings also highlight the importance of host iron acquisition mechanisms during bacterial infection.

2.4 Experimental Procedures:

Bacterial growth and sporulation conditions

Bacterial strains used for this study are described in Table 2-1. All mutant strains were derived from the *B. anthracis* Sterne $34F_2$ strain ($pXO1^+$, $pXO2^-$). Spores were generated as described previously (Passalacqua & Bergman, 2006), except that growth of the cultures was performed at 37°C and purified by passage through a 3.1 micron glass microfiber filter (National Scientific Company) to increase purity. Spore stocks were stored at room temperature in sterile water and titered using a hematocytometer to the desired concentration for use in mouse infection and petrobactin supplementation studies. All subsequent experiments were performed from these stocks. For experiments performed under low iron conditions, iron-depleted media (IDM) was prepared as previously described (Cendrowski et al., 2004b). For IDM growth experiments, overnight cultures grown in brain heart infusion broth (BHI) were back-diluted 1:50 in fresh medium and allowed to grow for 1 hour at 37°C. Actively growing cells were collected by centrifugation at 1600 ×*g,* and the pellets were washed five times in IDM to remove residual iron. The washed cells were inoculated into IDM at a final optical density at 600 nm (OD_{600}) of 0.05. For complementation experiments, cultures were supplemented with 10 μg ml^{-1} of chloramphenicol where indicated for plasmid maintenance. Cultures were grown at 37°C with aeration, and the OD_{600} was measured hourly for six hours. For experiments performed with supplemental petrobactin, cultures were inoculated with 1 x 10^5 spores of the specified strains in 2 ml IDM with or without the addition of 2.5 μM petrobactin (Carlson *et al*., 2010), and were monitored for change in OD_{600} over nine

Table 2-1. *Bacillus anthracis* strains used in this study

Strain/ Genotype	Relevant Characteristics	Reference
Sterne 34F2	Wild type (pXO1+, pXO2−)	(Sterne, 1939)
34F2, Δ*asbABCDEF*	Petrobactin biosynthesis mutant	(Lee et al., 2007)
34F2, Δ*fpuA*	Petrobactin receptor mutant	(Carlson et al., 2010)
34F2, Δ*fpuB*		This work
34F2, Δ*fatCD*		This work
34F2, Δ*fpuB*Δ*fatCD*	Δ*fatCD* into Δ*fpuB*	This work
34F2, Δ GBAA0616-0617		This work
34F2, Δ GBAA3865-3866		This work
34F2, ΔGBAA4596		This work
34F2, Δ*fpuC*		This work
34F2, Δ*fpuD*		This work
34F2, ΔGBAA5629		This work
34F2, ΔGBAA4784		This work
34F2, ΔGBAA3864		This work
34F2, Δ*fatE*		This work
34F2, Δ*fpuB*Δ*fatE*	Δ*fatE* into Δ*fpuB*	This work
34F2, Δ*fatCD*Δ*fpuC*	Δ*fpuC* into Δ*fatCD*	This work
34F2, Δ*fatCD*Δ*fpuD*	Δ*fpuD* into Δ*fatCD*	This work
34F2, Δ*fatCD*Δ*fpuC*Δ*fpuD*	Δ*fpuD* into Δ*fatCD*Δ*fpuC*	This work
34F2, Δ*fpuC*Δ*fpuD*	Δ*fpuC* into Δ*fpuD*	This work
34F2, Δ*fatE*Δ*fpuC*	Δ*fatE* into Δ*fpuC*	This work
34F2, Δ*fatE*Δ*fpuD*	Δ*fatE* into Δ*fpuD*	This work
34F2, Δ*fatE*Δ*fpuC*Δ*fpuD*	Δ*fatE* into Δ*fpuC*Δ*fpuD*	This work

hours. For gallium sensitivity assays, strains were inoculated into IDM, as described above, with or without the addition of 20 μM gallium sulfate. Results of the gallium sensitivity assay were normalized to culture OD_{600} and are presented as percent growth inhibition and calculated as ([(OD_{600} IDM+gallium)/(OD_{600} IDM)]*100) at two hours (Carlson *et al*., 2010).

Isolation of mutants and construction of complementation plasmids

Mutant strains isolated for this work were all constructed via allelic exchange. Each mutant allele was constructed via PCR using Phusion High Fidelity DNA polymerase (New England Biolabs) according to the manufacturer's instructions. The PCR products were first cloned into the TOPO® cloning vector (Invitrogen), using manufacturer protocols, and the DNA sequence was verified (University of Michigan DNA sequencing core). The mutant allele was then cloned into the NotI site of the allelic exchange vector pBKJ258 (Janes & Stibitz, 2006) using standard methods. Each construct contained approximately 500 bp both upstream and downstream of the target gene with NotI restriction sites on each end for subsequent cloning. Each mutant allele retained the first ten codons, followed by the DNA sequence GGGCCCTCCGGATCCCCCGGG, and then the last nine codons plus the predicted stop codon. A similar strategy was followed for each single gene deletion mutant. For mutations where two sequential genes were deleted, the initial ten codons of the first gene were fused with the final nine codons of the second gene, in the same manner described above. Allelic exchange was performed as described previously (Janes & Stibitz, 2006). The presence of the mutant alleles was verified by PCR, and each resulting mutant was otherwise isogenic to the parental strain. Sequences of all oligonucleotides used in the

creation and screening of these mutants are available upon request. Spore stocks for each mutant were generated and stored as described above.

PCR was used to amplify *fatE* and *fpuD* by standard methods. DNA fragments were cloned and each DNA sequence verified as described above for mutant allele construction. Primers were designed such that an XbaI site was inserted directly upstream of the intiation codon of the gene of interest, and a HindIII site directly downstream of the native stop codon. Each gene was cloned into the XbaI and HindIII sites of pGFP (Wilson *et al.*, 2011a, Wilson *et al.*, 2011b), replacing the *gfpmut3a* allele with the gene of interest, expressed by the *p43* promoter present on the plasmid. The plasmid pMJ01, a version of pGFP lacking the *gfpmut3a* allele was used as a control(Wilson et al., 2011b). Plasmids were passaged through SCS110 (*dam dcm*) and then transferred into the appropriate *B. anthracis* strain via electroporation (Passalacqua & Bergman, 2006).

Measurement of catechol accumulation

The levels of extracellular catechol were measured using the Arnow assay (Arnow, 1937, Carlson *et al*., 2010). Strains were grown as described above for six hours and supernatants were collected and filtered using a 0 .22 μm syringe filter. Culture supernatants were then mixed with equal volumes of 0.5 M HCl, followed by the sequential addition of equal volumes of nitrate-molybdate reagent (10% sodium nitrate and 10% sodium molybdate), 1 N NaOH, and distilled H_2O in 96-well plates. Sample reactions positive for the presence of catechol moieties produced a red color and absorbance was measured at 515 nm. Absorbance values were normalized to OD_{600} of

the original culture. Data are presented as the percentage of wild-type extracellular catechol in culture supernatants at six hours.

Murine virulence assays

DBA/J2 mice (Jackson Laboratories) were infected via intratracheal inoculation as previously described (Heffernan *et al.*, 2007). Groups of eight female mice age 6-8 weeks were infected with either wild-type or Δ*fpuB*Δ*fatCD* mutant spores at a dose of 1.5 x 10^5 spores/mouse. Mice were monitored for 14 days following infection. All mouse experiments were performed using protocols approved by the University of Michigan on the Use and Care of Animals.

2.5 Supplemental Material

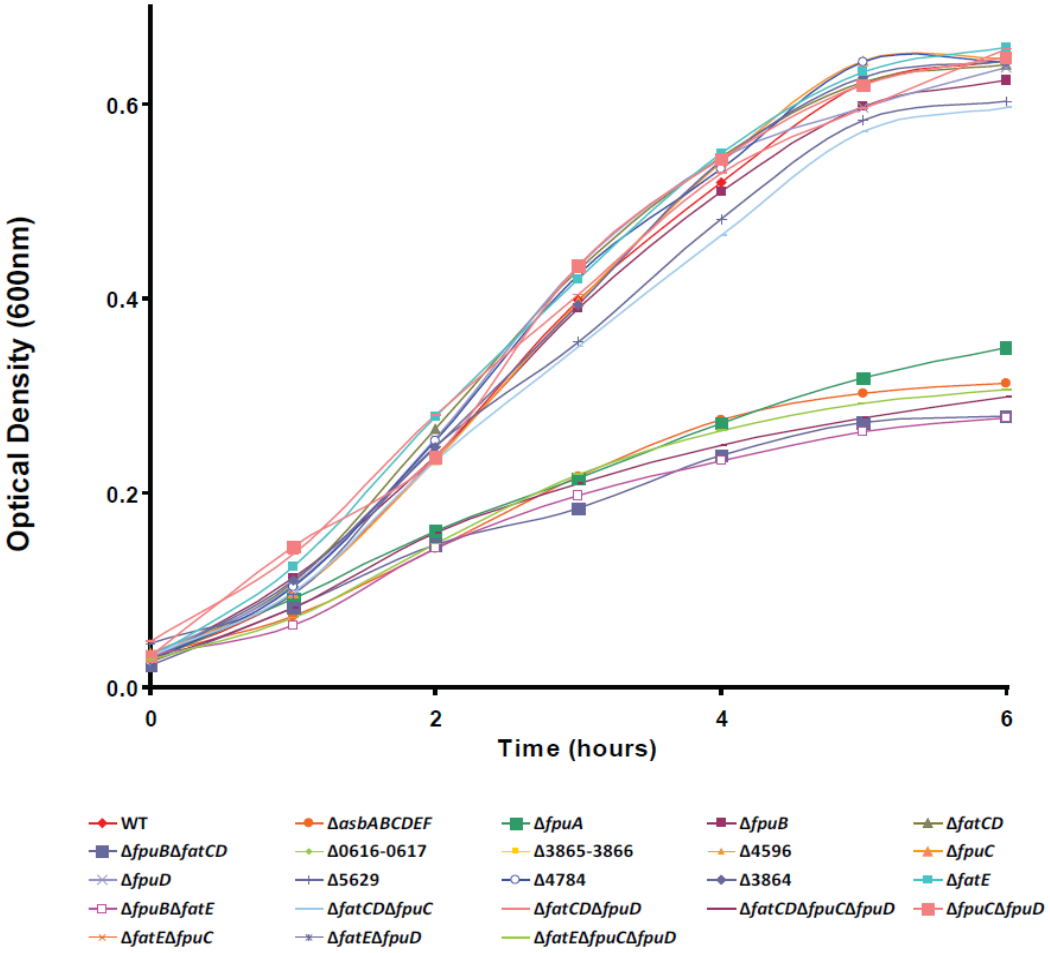

2-S1 and Table 2-S1. Growth patterns of all single and combinatorial *B. anthracis* mutant strains.

This supplemental figure contains all strains described in this work, including those from Figure 2. It should be noted that any mutant strain included here that was not in Figure 2 grew as well as wild-type. All cultures were inoculated with actively growing vegetative bacilli at an initial OD_{600} of 0.05. Growth was measured hourly by measuring OD_{600}. Table S1 contains the optical density (600nm) of all strains tested in this study at 6 hours growth in IDM.

Table S1. Growth of all single and combinatorial *B. anthracis* mutant strains in IDM

Strain/ Genotype	Optical Density (600nm) at 6hours
Sterne 34F2	0.645
34F2, Δ*asbABCDEF*	0.313
34F2, Δ*fpuA*	0.320
34F2, Δ*fpuB*	0.624
34F2, Δ*fatCD*	0.641
34F2, Δ*fpuB*Δ*fatCD*	0.279
34F2, Δ GBAA0616-0617	0.635
34F2, Δ GBAA3865-3866	0.648
34F2, ΔGBAA4596	0.644
34F2, Δ*fpuC*	0.639
34F2, Δ*fpuD*	0.628
34F2, ΔGBAA5629	0.603
34F2, ΔGBAA4784	0.625
34F2, ΔGBAA3864	0.645
34F2, Δ*fatE*	0.659
34F2, Δ*fpuB*Δ*fatE*	0.277
34F2, Δ*fatCD*Δ*fpuC*	0.596
34F2, Δ*fatCD*Δ*fpuD*	0.656
34F2, Δ*fatCD*Δ*fpuC*Δ*fpuD*	0.299
34F2, Δ*fpuC*Δ*fpuD*	0.644
34F2, Δ*fatE*Δ*fpuC*	0.654
34F2, Δ*fatE*Δ*fpuD*	0.607
34F2, Δ*fatE*Δ*fpuC*Δ*fpuD*	0.306

2.6 References

Abergel, R. J., M. K. Wilson, J. E. Arceneaux, T. M. Hoette, R. K. Strong, B. R. Byers & K. N. Raymond, (2006a) Anthrax pathogen evades the mammalian immune system through stealth siderophore production. *Proc Natl Acad Sci U S A* **103**: 18499-18503.

Abergel, R. J., M. K. Wilson, J. E. L. Arceneaux, T. M. Hoette, R. K. Strong, B. R. Byers & K. N. Raymond, (2006b) Anthrax pathogen evades the mammalian immune system through stealth siderophore production. *Proceedings of the National Academy of Sciences* **103**: 18499-18503.

Abergel, R. J., A. M. Zawadzka & K. N. Raymond, (2008) Petrobactin-mediated iron transport in pathogenic bacteria: coordination chemistry of an unusual 3,4-catecholate/citrate siderophore. *J Am Chem Soc* **130**: 2124-2125.

Almeida, J. L., B. Harper & K. D. Cole, (2008) Bacillus anthracis spore suspensions: determination of stability and comparison of enumeration techniques. *J Appl Microbiol* **104**: 1442-1448.

Arnow, L. E., (1937) Colorimetric determination of the components of 3, 4 - dihydroxyphenylalanine-tyrosine mixtures. *J Biol Chem* **118**: 531-537.

Banin, E., A. Lozinski, K. M. Brady, E. Berenshtein, P. W. Butterfield, M. Moshe, M. Chevion & E. P. Greenberg, (2008) The potential of desferrioxamine-gallium as an anti-Pseudomonas therapeutic agent. *Proc Natl Acad Sci U S A* **105**: 16761-16766.

Barbeau, K., G. Zhang, D. H. Live & A. Butler, (2002) Petrobactin, a photoreactive siderophore produced by the oil-degrading marine bacterium Marinobacter hydrocarbonoclasticus. *J Am Chem Soc* **124**: 378-379.

Beasley, F. C. & D. E. Heinrichs, (2010) Siderophore-mediated iron acquisition in the staphylococci. *J Inorg Biochem* **104**: 282-288.

Braun, V. & M. Braun, (2002) Active transport of iron and siderophore antibiotics. *Curr Opin Microbiol* **5**: 194-201.

Carlson, P. E., Jr., K. A. Carr, B. K. Janes, E. C. Anderson & P. C. Hanna, (2009) Transcriptional profiling of Bacillus anthracis Sterne (34F2) during iron starvation. *PLoS ONE* **4**: e6988.

Cendrowski, S., W. MacArthur & P. Hanna, (2004a) Bacillus anthracis requires siderophore biosynthesis for growth in macrophages and mouse virulence. *Molecular Microbiology* **51**: 407-417.

Cendrowski, S., W. MacArthur & P. Hanna, (2004b) Bacillus anthracis requires siderophore biosynthesis for growth in macrophages and mouse virulence. *Mol Microbiol* **51**: 407-417.

Challis, G. L., (2005) A widely distributed bacterial pathway for siderophore biosynthesis independent of nonribosomal peptide synthetases. *Chembiochem* **6**: 601-611.

Cowart, R. E., (2002) Reduction of iron by extracellular iron reductases: implications for microbial iron acquisition. *Arch Biochem Biophys* **400**: 273-281.

Davidson, A. L., E. Dassa, C. Orelle & J. Chen, (2008) Structure, function, and evolution of bacterial ATP-binding cassette systems. *Microbiol Mol Biol Rev* **72**: 317-364, table of contents.

Dixon, T. C., A. A. Fadl, T. M. Koehler, J. A. Swanson & P. C. Hanna, (2000) Early Bacillus anthracis-macrophage interactions: intracellular survival survival and escape. *Cell Microbiol* **2**: 453-463.

Dixon, T. C., M. Meselson, J. Guillemin & P. C. Hanna, (1999) Anthrax. *N Engl J Med* **341**: 815-826.

Doganay, L. & P. D. Welsby, (2006) Anthrax: a disease in waiting? *Postgrad Med J* **82**: 754-756.

Dutz, W. & E. Kohout-Dutz, (1981) Anthrax. *Int J Dermatol* **20**: 203-206.

Dutz, W. & E. Kohout, (1971) Anthrax. *Pathol Annu* **6**: 209-248.

Ecker, D. J. & T. Emery, (1983) Iron uptake from ferrichrome A and iron citrate in Ustilago sphaerogena. *J Bacteriol* **155**: 616-622.

Eitinger, T., D. A. Rodionov, M. Grote & E. Schneider, (2011) Canonical and ECF-type ATP-binding cassette importers in prokaryotes: diversity in modular organization and cellular functions. *FEMS Microbiol Rev* **35**: 3-67.

Faraldo-Gomez, J. D. & M. S. Sansom, (2003) Acquisition of siderophores in gram-negative bacteria. *Nat Rev Mol Cell Biol* **4**: 105-116.

Fox, D. T., K. Hotta, C. Y. Kim & A. T. Koppisch, (2008) The missing link in petrobactin biosynthesis: asbF encodes a (-)-3-dehydroshikimate dehydratase. *Biochemistry* **47**: 12251-12253.

Garénaux, A., M. Caza & C. M. Dozois, (2011) The Ins and Outs of siderophore mediated iron uptake by extra-intestinal pathogenic Escherichia coli. *Veterinary Microbiology* **153**: 89-98.

Garner, B. L., J. E. Arceneaux & B. R. Byers, (2004) Temperature control of a 3,4-dihydroxybenzoate (protocatechuate)-based siderophore in Bacillus anthracis. *Curr Microbiol* **49**: 89-94.

Glanfield, A., D. P. McManus, G. J. Anderson & M. K. Jones, (2007) Pumping iron: a potential target for novel therapeutics against schistosomes. *Trends Parasitol* **23**: 583-588.

Guidi-Rontani, C., M. Weber-Levy, E. Labruyere & M. Mock, (1999) Germination of Bacillus anthracis spores within alveolar macrophages. *Mol Microbiol* **31**: 9-17.

Hanna, P., (1998a) Anthrax pathogenesis and host response. *Curr Top Microbiol Immunol* **225**: 13-35.

Hanna, P., (1998b) How anthrax kills. *Science* **280**: 1671, 1673-1674.

Heffernan, B. J., B. Thomason, A. Herring-Palmer & P. Hanna, (2007) Bacillus anthracis anthrolysin O and three phospholipases C are functionally redundant in a murine model of inhalation anthrax. *FEMS Microbiol Lett* **271**: 98-105.

Hotta, K., C. Y. Kim, D. T. Fox & A. T. Koppisch, (2010) Siderophore-mediated iron acquisition in Bacillus anthracis and related strains. *Microbiology* **156**: 1918-1925.

Inglesby, T. V., D. A. Henderson, J. G. Bartlett, M. S. Ascher, E. Eitzen, A. M. Friedlander, J. Hauer, J. McDade, M. T. Osterholm, T. O'Toole, G. Parker, T. M. Perl, P. K. Russell & K. Tonat, (1999) Anthrax as a biological weapon: medical and public health management. Working Group on Civilian Biodefense. *JAMA* **281**: 1735-1745.

Inglesby, T. V., T. O'Toole, D. A. Henderson, J. G. Bartlett, M. S. Ascher, E. Eitzen, A. M. Friedlander, J. Gerberding, J. Hauer, J. Hughes, J. McDade, M. T. Osterholm, G. Parker, T. M. Perl, P. K. Russell & K. Tonat, (2002) Anthrax as a biological weapon, 2002: updated recommendations for management. *JAMA* **287**: 2236-2252.

Janes, B. K. & S. Stibitz, (2006) Routine markerless gene replacement in Bacillus anthracis. *Infect Immun* **74**: 1949-1953.

Kadi, N. & G. L. Challis, (2009) Chapter 17. Siderophore biosynthesis a substrate specificity assay for nonribosomal peptide synthetase-independent siderophore

synthetases involving trapping of acyl-adenylate intermediates with hydroxylamine. *Methods Enzymol* **458**: 431-457.

Koppisch, A., S. Dhungana, K. Hill, H. Boukhalfa, H. Heine, L. Colip, R. Romero, Y. Shou, L. Ticknor, B. Marrone, L. Hersman, S. Iyer & C. Ruggiero, (2008a) Petrobactin is produced by both pathogenic and non-pathogenic isolates of the Bacillus cereus group of bacteria. *Biometals*.

Koppisch, A. T., C. C. Browder, A. L. Moe, J. T. Shelley, B. A. Kinkel, L. E. Hersman, S. Iyer & C. E. Ruggiero, (2005) Petrobactin is the primary siderophore synthesized by Bacillus anthracis str. Sterne under conditions of iron starvation. *Biometals* **18**: 577-585.

Koppisch, A. T., K. Hotta, D. T. Fox, C. E. Ruggiero, C. Y. Kim, T. Sanchez, S. Iyer, C. C. Browder, P. J. Unkefer & C. J. Unkefer, (2008b) Biosynthesis of the 3,4-dihydroxybenzoate moieties of petrobactin by Bacillus anthracis. *J Org Chem* **73**: 5759-5765.

Koster, W., (2001) ABC transporter-mediated uptake of iron, siderophores, heme and vitamin B12. *Res Microbiol* **152**: 291-301.

Koster, W., (2005) Cytoplasmic membrane iron permease systems in the bacterial cell envelope. *Front Biosci* **10**: 462-477.

Koster, W. & V. Braun, (1990a) Iron (III) hydroxamate transport into Escherichia coli. Substrate binding to the periplasmic FhuD protein. *J Biol Chem* **265**: 21407-21410.

Koster, W. & V. Braun, (1990b) Iron(III) hydroxamate transport of Escherichia coli: restoration of iron supply by coexpression of the N- and C-terminal halves of the cytoplasmic membrane protein FhuB cloned on separate plasmids. *Mol Gen Genet* **223**: 379-384.

Koster, W. L., L. A. Actis, L. S. Waldbeser, M. E. Tolmasky & J. H. Crosa, (1991) Molecular characterization of the iron transport system mediated by the pJM1 plasmid in Vibrio anguillarum 775. *J Biol Chem* **266**: 23829-23833.

Lee, J. Y., B. K. Janes, K. D. Passalacqua, B. F. Pfleger, N. H. Bergman, H. Liu, K. Hakansson, R. V. Somu, C. C. Aldrich, S. Cendrowski, P. C. Hanna & D. H. Sherman, (2007) Biosynthetic analysis of the petrobactin siderophore pathway from Bacillus anthracis. *J Bacteriol* **189**: 1698-1710.

Lee, J. Y., K. D. Passalacqua, P. C. Hanna & D. H. Sherman, (2011) Regulation of Petrobactin and Bacillibactin Biosynthesis in Bacillus anthracis under Iron and Oxygen Variation. *PLoS One* **6**: e20777.

Liu, H., K. Hakansson, J. Y. Lee & D. H. Sherman, (2007) Collision-activated dissociation, infrared multiphoton dissociation, and electron capture dissociation of the Bacillus anthracis siderophore petrobactin and its metal ion complexes. *J Am Soc Mass Spectrom* **18**: 842-849.

Lopez, C. S. & J. H. Crosa, (2007) Characterization of ferric-anguibactin transport in Vibrio anguillarum. *Biometals* **20**: 393-403.

Marion, C., A. E. Aten, S. A. Woodiga & S. J. King, (2011) Identification of an ATPase, MsmK, which energizes multiple carbohydrate ABC transporters in Streptococcus pneumoniae. *Infect Immun* **79**: 4193-4200.

Miethke, M., O. Klotz, U. Linne, J. J. May, C. L. Beckering & M. A. Marahiel, (2006) Ferri-bacillibactin uptake and hydrolysis in Bacillus subtilis. *Mol Microbiol* **61**: 1413-1427.

Miethke, M. & M. A. Marahiel, (2007) Siderophore-based iron acquisition and pathogen control. *Microbiol Mol Biol Rev* **71**: 413-451.

Neilands, J. B., (1995) Siderophores: structure and function of microbial iron transport compounds. *J Biol Chem* **270**: 26723-26726.

Nicholson, W. L., N. Munakata, G. Horneck, H. J. Melosh & P. Setlow, (2000) Resistance of Bacillus endospores to extreme terrestrial and extraterrestrial environments. *Microbiol Mol Biol Rev* **64**: 548-572.

Olakanmi, O., B. E. Britigan & L. S. Schlesinger, (2000) Gallium disrupts iron metabolism of mycobacteria residing within human macrophages. *Infect Immun* **68**: 5619-5627.

Oves-Costales, D., N. Kadi & G. L. Challis, (2009) The long-overlooked enzymology of a nonribosomal peptide synthetase-independent pathway for virulence-conferring siderophore biosynthesis. *Chemical Communications*: 6530-6541.

Oves-Costales, D., N. Kadi, M. J. Fogg, L. Song, K. S. Wilson & G. L. Challis, (2007) Enzymatic logic of anthrax stealth siderophore biosynthesis: AsbA catalyzes ATP-dependent condensation of citric acid and spermidine. *J Am Chem Soc* **129**: 8416-8417.

Oves-Costales, D., N. Kadi, M. J. Fogg, L. Song, K. S. Wilson & G. L. Challis, (2008) Petrobactin biosynthesis: AsbB catalyzes condensation of spermidine with N(8)-

citryl-spermidine and its N(1)-(3,4-dihydroxybenzoyl) derivative. *Chem Commun (Camb)*: 4034-4036.

Passalacqua, K. D. & N. H. Bergman, (2006) Bacillus anthracis: interactions with the host and establishment of inhalational anthrax. *Future Microbiol* **1**: 397-415.

Pfleger, B. F., Y. Kim, T. D. Nusca, N. Maltseva, J. Y. Lee, C. M. Rath, J. B. Scaglione, B. K. Janes, E. C. Anderson, N. H. Bergman, P. C. Hanna, A. Joachimiak & D. H. Sherman, (2008a) Structural and functional analysis of AsbF: Origin of the stealth 3,4-dihydroxybenzoic acid subunit for petrobactin biosynthesis. *Proc Natl Acad Sci U S A*.

Pfleger, B. F., Y. Kim, T. D. Nusca, N. Maltseva, J. Y. Lee, C. M. Rath, J. B. Scaglione, B. K. Janes, E. C. Anderson, N. H. Bergman, P. C. Hanna, A. Joachimiak & D. H. Sherman, (2008b) Structural and functional analysis of AsbF: origin of the stealth 3,4-dihydroxybenzoic acid subunit for petrobactin biosynthesis. *Proc Natl Acad Sci U S A* **105**: 17133-17138.

Pfleger, B. F., J. Y. Lee, R. V. Somu, C. C. Aldrich, P. C. Hanna & D. H. Sherman, (2007) Characterization and analysis of early enzymes for petrobactin biosynthesis in Bacillus anthracis. *Biochemistry* **46**: 4147-4157.

Ratledge, C., (2004) Iron, mycobacteria and tuberculosis. *Tuberculosis (Edinb)* **84**: 110-130.

Ratledge, C. & L. G. Dover, (2000) Iron metabolism in pathogenic bacteria. *Annu Rev Microbiol* **54**: 881-941.

Spencer, R. C., (2003) Bacillus anthracis. *J Clin Pathol* **56**: 182-187.

Sweeney, D. A., C. W. Hicks, X. Cui, Y. Li & P. Q. Eichacker, (2011) Anthrax infection. *Am J Respir Crit Care Med* **184**: 1333-1341.

Wandersman, C. & P. Delepelaire, (2004) Bacterial iron sources: from siderophores to hemophores. *Annu Rev Microbiol* **58**: 611-647.

Wilson, M. J., P. E. Carlson, B. K. Janes & P. C. Hanna, (2011) Membrane topology of the Bacillus anthracis GerH germinant receptor proteins. *J Bacteriol*.

Wilson, M. K., R. J. Abergel, J. E. Arceneaux, K. N. Raymond & B. R. Byers, (2009) Temporal production of the two Bacillus anthracis siderophores, petrobactin and bacillibactin. *Biometals* **23**: 129-134.

Wilson, M. K., R. J. Abergel, K. N. Raymond, J. E. Arceneaux & B. R. Byers, (2006) Siderophores of Bacillus anthracis, Bacillus cereus, and Bacillus thuringiensis. *Biochem Biophys Res Commun* **348**: 320-325.

Wooldridge, K. G., J. A. Morrissey & P. H. Williams, (1992) Transport of ferric-aerobactin into the periplasm and cytoplasm of Escherichia coli K12: role of envelope-associated proteins and effect of endogenous siderophores. *J Gen Microbiol* **138**: 597-603.

Zawadzka, A. M., R. J. Abergel, R. Nichiporuk, U. N. Andersen & K. N. Raymond, (2009a) Siderophore-mediated iron acquisition systems in Bacillus cereus: Identification of receptors for anthrax virulence-associated petrobactin. *Biochemistry* **48**: 3645-3657.

Zawadzka, A. M., Y. Kim, N. Maltseva, R. Nichiporuk, Y. Fan, A. Joachimiak & K. N. Raymond, (2009b) Characterization of a Bacillus subtilis transporter for petrobactin, an anthrax stealth siderophore. *Proc Natl Acad Sci U S A* **106**: 21854-21859.

Chapter 3

A High Throughput Screen for Inhibitors of the *Bacillus anthracis* Petrobactin ABC-Transporter ATPases

3.1 Introduction

Bacillus anthracis is the causative agent of the disease anthrax, a consistently lethal and a proven bioweapon and bioterrorism agent with a limited amount of treatment options (Dixon *et al.*, 1999, Bouzianas, 2009, Frankel *et al.*, 2009, Friedlander, 2001). Current methods for treating anthrax infection require improvement, as the use of antibiotics against infection does not target the early stages of *B. anthracis* colonization and subsequent expression of toxins, mechanisms of nutrient acquisition, and other virulence factors (Bouzianas, 2009). Because of the ability of *B. anthracis* to replicate rapidly in the host once disseminated (Frankel et al., 2009), it is likely that antibiotic treatment targeting later stages in pathogenesis will fail to be effective in preventing the death of the host. Like many bacteria, *B. anthracis* is reliant on biosynthesis, secretion, and re-uptake of small, Fe^{3+}-specific chelators called siderophores for the biologically necessary purpose of iron sequestration (Cendrowski *et al.*, 2004). In *Bacillus anthracis* the siderophore petrobactin is the only siderophore vital for iron acquisition and virulence (Cendrowski et al., 2004). In fact, our lab has shown that mutants deficient in petrobactin biosynthesis are highly attenuated in a murine model of inhalational anthrax infection (Pfleger *et al.*, 2008{Cendrowski, 2004 #13 5). These findings demonstrate the

requirement for petrobactin-mediated iron acquisition in the establishment of infection. Furthermore, recent studies in our laboratory have led to the identification of proteins comprising multiple adenosine triphosphate (ATP)-binding cassette (ABC)-transporters required for the reacquisition of this siderophore. ABC transport systems function by coupling ATP hydrolysis to the translocation of essential solutes across the biological membrane (Carlson *et al.*, 2010, Dixon *et al.*, 2012). Typically, an ABC transporter is composed of four parts: two transmembrane domains, or permeases, and two ATP-hydrolyzing domains, or ATPases (Higgins, 1992). We have found that two distinct permeases, FpuB or FatCD, and three distinct ATPases, FpuC, FpuD, and FatE are sufficient for iron acquisition and play redundant roles in petrobactin transport across the cell membrane. Our studies show that these ABC-transport systems are essential in cell viability in iron depleted conditions, virulence and pathogenicity (Dixon et al., 2012). ABC transporters are required by most bacteria for membrane transport of various small molecules vital for their metabolism (Davidson et al. 2008) and, for pathogenic bacteria, their ability to cause infection. Members of this family have been identified in all three major domains of life including bacteria, archaea, and eukarya (Higgins, 1992, Holland & A. Blight, 1999, Koster, 2001).

The ATPase components of ABC transporters are characterized by the presence of highly conserved sequence motifs involved in ATP binding and hydrolysis with amino acid identities ranging from 25-35% (45-50% similarity) across bacterial species (Holland & A. Blight, 1999). With a well-developed repertoire for studying *B. anthracis* pathogenesis and disease, this system serves as an excellent experimental model for directly exploring ABC transporters, and specifically ATPase enzymes, as targets for new

types of therapeutics for the treatment of both anthrax and potentially many other bacterial infections reliant on these systems for pathogenesis. As mentioned above, humans and other mammals also use a variety of ABC-transport pathways, and while maintaining many features in common with each other, have very few, if any, direct sequence homologies with the bacterial systems (Davidson *et al.*, 2008a, Rosenberg *et al.*, 2005). Of the many inhibitory compounds used against mammalian ABC transport to treat a large variety of diseases in humans, none of these, to the best of our knowledge, have been reported to have anti-bacterial properties. The reciprocal may also be true, in which potential small molecule inhibitors of petrobactin-associated transport or other bacterial ABC transport systems may not readily affect mammalian cells, leading to a low toxicity potential in people.

Because active FpuC, FpuD, and FatE ATPases can be easily purified and only require ATP as a substrate, these proteins are prime candidates as targets for a high-throughput inhibitor search. Furthermore, established biochemical assays are available for the detection of ATPase activity and subsequent inhibition. By investigating methods to inhibit the activity of these ATPases, we hope to devise strategies to shut down import of the vital siderophore petrobactin and thus the necessary act of iron acquisition by *B. anthracis* and other dangerous pathogens. To achieve this goal, a high-throughput assay was developed utilizing the chemical libraries and high-throughput (HTP) facilities at the University of Michigan Center for Chemical Genomics to discover novel molecules in inhibiting the activity of these crucial ATPase enzymes.

3.2 Results

Heterologous Over-Expression and Purification of Three ATPases

To screen for inhibitors of the petrobactin ABC transport ATPases, purified active versions of the enzymes were generated by first cloning the open reading frames of each ATPase into an expression vector that simultaneously incorporated a hexahistidine tag on the N terminus of each of the proteins. Each of the three His_6-ATPase proteins were then over-expressed in *E. coli* and purified via nickel-affinity chromatography. While soluble, functional enzymes were generated for all three ATPases (FpuC, FpuD, and FatE), the most consistently over-expressed of these, FpuD, was selected for transitioning to a HTP screen (HTS). It was hypothesized that due to the high sequence similarity between the three petrobactin import ATPases, candidate inhibitors obtained from a small molecule screen would display some efficacy against the other two ATPases, FpuC and FatE as well. The highly conserved primary structure of these three enzymes, particularly in the canonical ATPase catalytic domains, has been highlighted through primary sequence alignment (Clustal, EMBIO) (Figure 3-1A).

Among the ATPases purified, highly-conserved domains include the Walker A motif (GxxGxGKS/T), the Walker B motif (DEP/AxxxLD) and the Signature sequence (LSGGxxQRV). Both the Walker A and Walker B motifs are common to most ATPases that are involved in the binding and hydrolysis of ATP, while the signature sequence is unique to ABC type ATPases (Holland & A. Blight, 1999, Davidson *et al.*, 2008b). All three of these motifs can be identified in the sequences of the petrobactin ABC-transport ATPases (Figure 3-1A). To determine whether these regions were important for the catalytic function of these ATPases we chose to begin by mutating the highly conserved

E163 of the FpuD Walker B motif to generate FpuD(E163Q). The Walker B motif has been demonstrated to coordinate with Mg^{2+} ions to stabilize attack by H_2O molecules during ATP hydrolysis (Davidson et al., 2008a, Schneider & Hunke, 1998); thus an amino acid change from an acidic glutamic acid (Glu) to a polar glutamine (Gln) residue should hypothetically result in either full or partial loss of the ability of the ATPase to hydrolyze ATP.

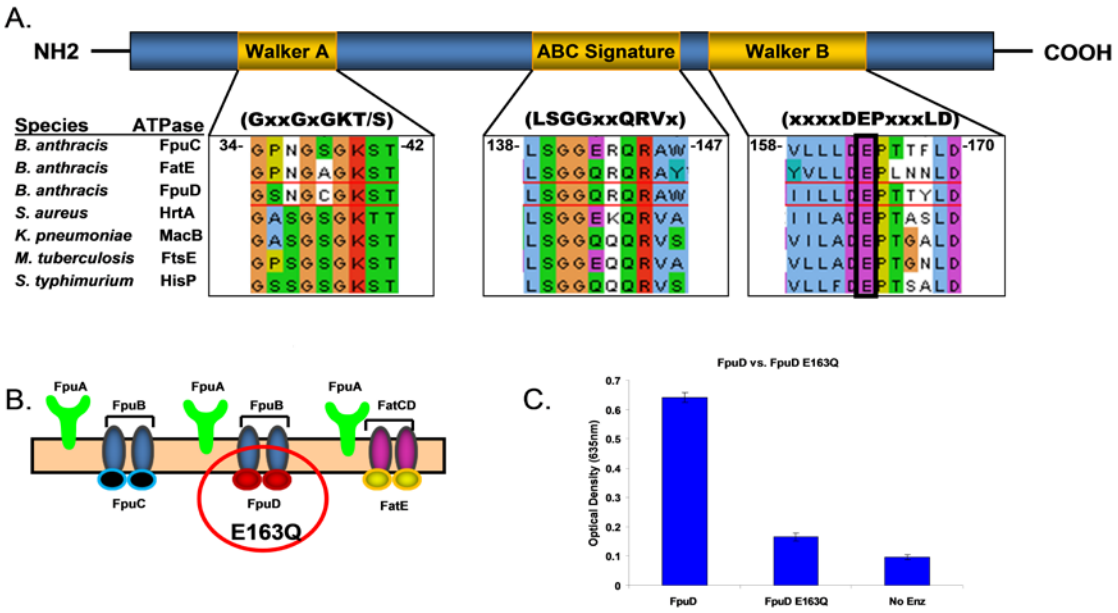

Figure 3-1. Representation of prototypical ABC transporter ATPases and sequence alignment of conserved domains. A)The Walker A, ABC signature, and Walker B motifs can be detected in *B. anthracis* petrobactin uptake ABC transporter ATPases as well as in other well characterized bacterial ABC transporter ATPases. B) The highly conserved Glu 163 of *B. anthracis* petrobactin ABC transporter ATPase, FpuD was mutated to Gln to produce a nonfunctional FpuD(E163Q). The conserved Glu (E) residue is shown boxed in black in panel A. C) Malachite green ATP turnover assay with purified wild type FpuD, FpuD(E163Q), and a no-enzyme control. The single amino acid replacement at E163 in the Walker B site largely abrogates FpuD activity.

Colorimetric Determination of ATPase Activity

Following successful purification of the ATPase enzymes, an assay was developed that would allow for the detection of enzymatic activity. A malachite green-based assay was selected to test for initial activity of the target ATPase FpuD and its mutant FpuD(E163Q). In this reaction, the ATPase catalyzes hydrolysis of the ATP substrate to adenosine diphosphate (ADP) and inorganic phosphate (P_i). The released phosphate will then complex with 12 molecules of molybdate to form a phosphomolybdate complex (Cogan *et al.*, 1999). The complex is then stained with malachite green dye to form a blue-green product which can be detected as an increase in absorbance at 635 nm (McQuade *et al.*, 2009, Pegan *et al.*, 2010). Because increased ATP turnover by FpuD activity is directly proportional to the amount of free inorganic phosphate in the reaction mixture, a nearly linear increase in A_{635nm} is observed with increasing concentration of enzyme, and reaction rate appears consistent up to one hour (Fig. 3-2A). The enzymatic activities of ATPases have been shown to be influenced by their surrounding physiochemical conditions (Holland & Blight, 1999). Therefore, to determine the conditions required for FpuD to display optimal enzymatic activity and to probe the sensitivity of this enzyme to perturbations in the reaction conditions, the effects of temperature, metal cofactor (Mg^{2+}) concentrations, and substrate (ATP) concentrations on the activity of FpuD were tested.

As expected, the enzyme activity of FpuD at 4°C was nearly identical to that of the no enzyme control at 37°C as most ABC ATPases do not display activity at low temperatures (Stauff *et al.*, 2008, Davidson et al., 2008b). FpuD did, however, exhibit robust activity at 25°C with peak activity at 37°C (Fig. 3-2B). This result was not

surprising as several ATPases involved in ABC transport demonstrate maximal activity at physiological temperatures (Koster, 2001, Stauff et al., 2008), and given the function of the FpuD ATPase in the import of petrobactin during infection of the mammalian host, maximal activity at or near 37°C would be expected. An effort was made to determine the optimal reaction conditions allowing for maximal FpuD activity at 25°C. This temperature was chosen for all subsequent enzymatic experiments since measurable FpuD activity could be obtained at this temperature and experimentation near ambient temperature would allow for an easier transition to a high throughput format. Divalent metal cations are critical for the catalytic activity of ATPase enzymes (Davidson et al., 2008b). A range of Mg^{2+} concentrations from 0-2.5 mM was tested showing that a concentration of approximately 0.625 mM supported the maximal catalytic activity of FpuD when ATP was kept at 0.5 mM (Fig. 3-2C). For simplicity, a concentration of 0.5 mM Mg^{2+} was chosen to proceed with the subsequent activity assays. FpuD ATPase activity reached a maximal level with a substrate concentration of 1 mM and began to plateau at 0.5 mM when a range of ATP concentrations from 0 mM to 1 mM was tested at 25°C with 0.5 mM Mg^{2+} for 30 minutes (Fig. 3-2D). Under these conditions, mutation of the residue E163 almost completely eliminated the ability of FpuD to cleave ATP (Fig. 3-1C, 3-2A). These data indicate that the highly conserved E163 residue in the Walker B motif is essential for ATP hydrolysis. Furthermore, the abolished ATPase catalytic activity of the FpuD(E163) ATPase allows this mutant to serve as a positive control for ATPase inhibition in subsequent activity assays.

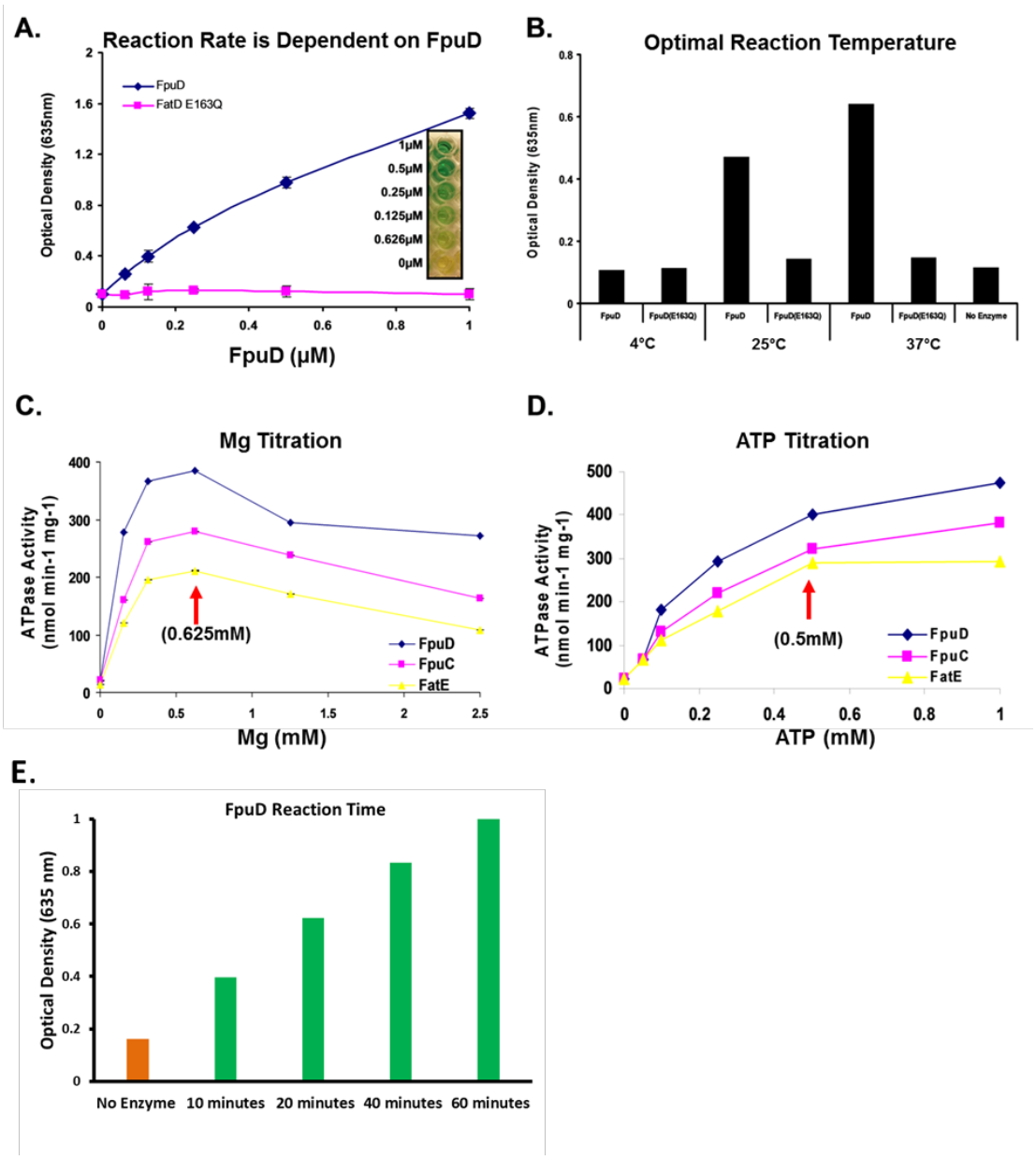

Figure 3-2. Optimization of the malachite green-based ATPase activity assay. A) Under preliminary conditions over one hour, reaction rate is exclusively and directly dependent on FpuD catalysis up to 1 μM (blue line) while the E163Q mutant is largely inactive (pink line). Inset photograph shows the colorimetric readout of increased P_i due to enzymatic activity. B) Temperature dependence of FpuD activity. Only basal P_i release occurs at 4º C for wild-type FpuD or with FpuD(E163Q) and the no-enzyme control at any temperature. C) When 1 mM ATP was used to start the reaction, all three petrobactin uptake associated ATPases displayed peak activity with ~0.5-0.65 mM $MgCl_2$ present. Enzymatic activity was dependent on the presence of Mg^{2+}. D) With 1 μM ATPase present, enzymatic ATP turnover begins to plateau at ~1 mM substrate. Unless otherwise noted, 0.5 mM $MgCl_2$ was used in all activity assays. E.) Timecourse demonstrating a nearly linear reaction rate up to an hour.

Optimization of the Malachite Green Based ATPase Activity Assay

With a suitable assay validated for the initial detection of *in vitro* FpuD activity, the assay underwent further optimization to make it more amenable for HTS format. As an alternative to the absorbance method described above, a recent adaptation by University of Michigan researchers utilizes the aforementioned color change of malachite green dye to quench the inherent fluorescent properties of white plastic 384-well micro-plates (Zuck, 2005). Thus, instead of monitoring an increase in absorbance at 630 nm, a decrease in light emitted off of the plate is measured as inorganic phosphate is released. This is achieved by using an excitation and emission pair where either the excitation or the emission matches the absorbance maximum of the colored sample. In this case, a wavelength of 430 nm was chosen to excite the plate and then measure a decrease in fluorescence at 600nm as emitted light is absorbed in the presence of malachite green stained phosphomolybdate complexes (Fig. 3-3). This reduction in light output is directly proportional to the amount of ATP turnover catalyzed by the FpuD ATPase as shown in our initial experiments where increasing FpuD concentration (0 -1 μM) in a final reaction volume of 12 μL results in a linear decrease in fluorescence intensity at 600 nm (Fig. 3-3). This method permits for a dramatic downsizing of the standard absorbance based malachite green assay allowing for conversion to a HTS format which requires small volumes near 10 μL and increased sample density. The increased sensitivity of this method coupled to the use of plastic 384-well plates allowed for reduction of both purified FpuD enzyme and reagent consumption by 90%.

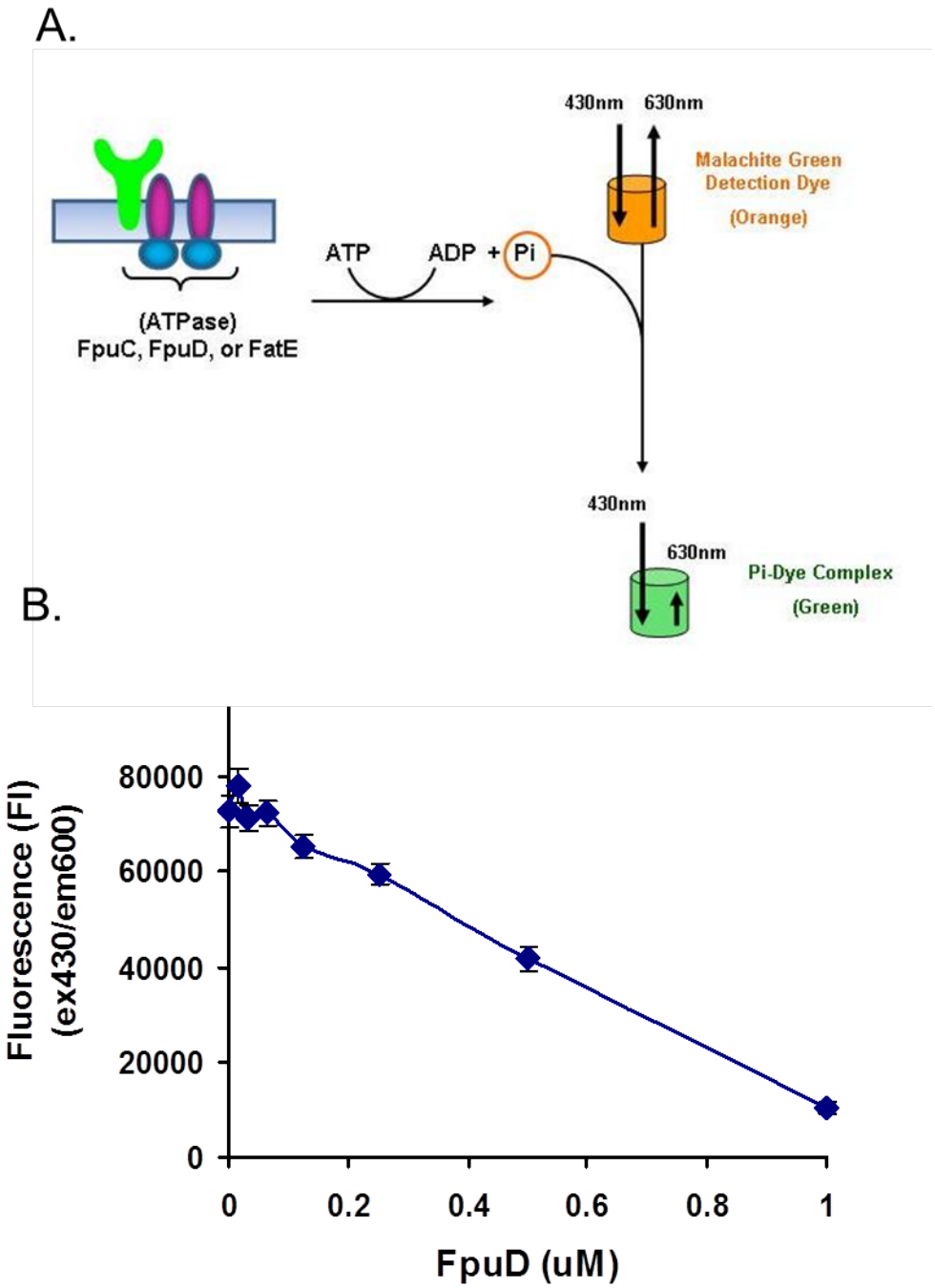

Figure 3-3 Schematic of the malachite-green fluorescence quench ATPase activity assay. A. The malachite green phosphate detection assay is based on the change in absorbance of the dye malachite green in the presence of phosphomolybdate complexes which are formed from inorganic phosphate (P_i) released during ATPase-catalyzed hydrolysis of ATP. When performed in a fluorescing plate, a reduction in emitted light (630 nm) corresponds to this color change. B. The inset graph shows reduced emitted light traveling to the detector with increased FpuD enzymatic activity.

High-Throughput Screen for Small Molecule Inhibitors of FpuD Mediated ATP Hydrolysis

With a reliable malachite green based ATPase activity assay optimized for HTS, a pilot screen for inhibitors of FpuD activity was now possible. Utilizing the facilities at the University of Michigan Center for Chemical Genomics (CCG), a primary screen was devised by selecting roughly 4,000 compounds obtained from four small molecule libraries available at the CCG (MS-Spectrum 2000, BioFocus NIH Clinical Collection, Focused Collections of Natural Products, and Focused Collections of Target Specific compounds). Plate layout and assay flow are outlined in Figure 3-4. Briefly, the "pin" tool on the Biomek FX (Beckman) liquid handling robot was used to rapidly transfer compounds from library stock plates to 384-well assay plates, leaving two rows on either side of the plate empty to allow for the addition of positive and negative controls. Since our assay was designed to identify inhibitors of FpuD ATPase activity, the positive control for inhibition consisted of all reaction components except FpuD, indicating 100% inhibition. The negative control for inhibition consisted of all reaction components, including FpuD, with the addition of DMSO instead of test compound, indicating full enzyme activity with 0% inhibition. Positive and negative controls on each plate allowed for reliable calculation of the percent inhibition exhibited by test compounds against the assay target and were used for scoring compounds with inhibitory action as "hits". Assay buffer containing the FpuD enzyme was added to all wells except the positive control and the reaction was then started by the addition of ATP. Following 30 minute incubation, the Malachite green phosphate detection dye was added to each well. Due to the acidic nature of the malachite green preparation lending to the possibility of non-enzymatic breakdown of ATP (Hohenwallner & Wimmer, 1973), a citrate solution was added to the reaction

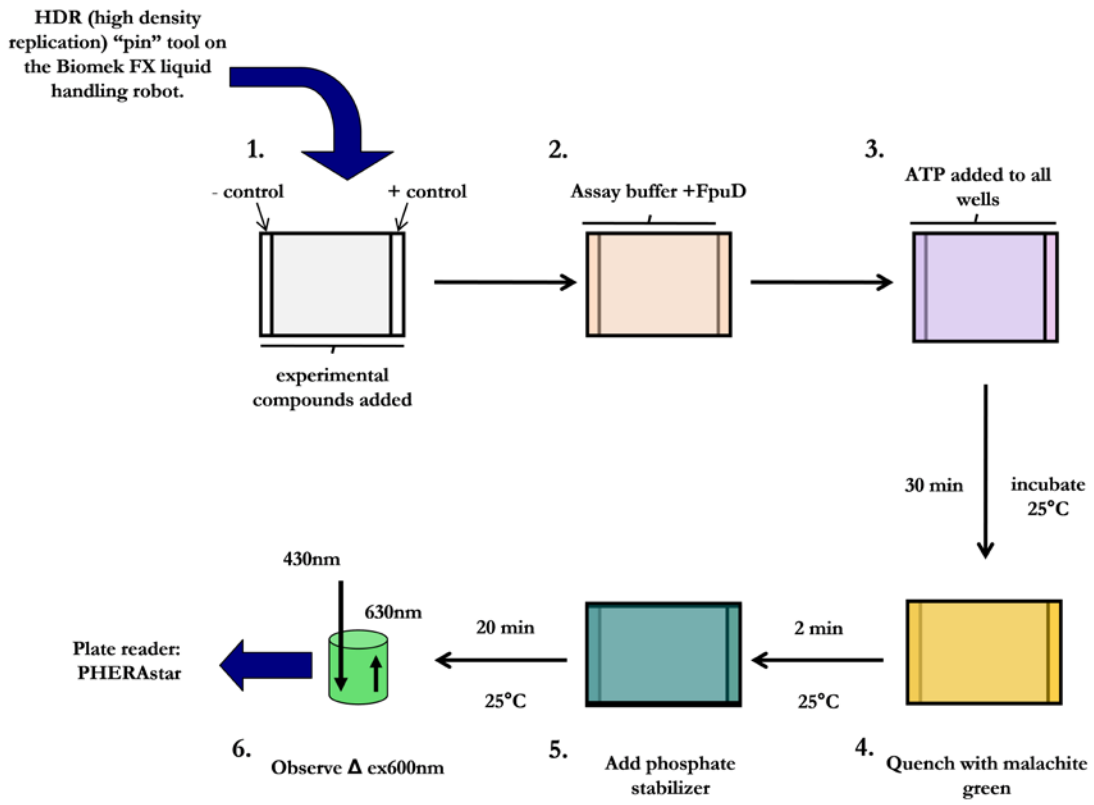

Figure 3-4. HTS Flow Chart. The 384-well plate is filled to half the final reaction volume with assay buffer. Test compounds dissolved in DMSO are added with an automated pin tool (1.). This is with the exception of the two outermost left and right columns, which receive DMSO free of test compound and serve as control wells. Purified FpuD diluted in assay buffer is added to all but the two right-most "positive control" columns, which receive assay buffer alone (2.). ATP dissolved in assay buffer is added to all wells to start the reaction (3.). The reaction is quenched with malachite green development solution after 30 minute room temperature incubation (4.). Development occurs for 2 minutes prior to addition of a reaction stabilizer (5.) to prevent detection of spontaneous ATP hydrolysis. Quenching of plate fluorescence at 600 nm is observed (6.) after an additional 20-minute incubation.

mix as a stabilizer. All assay plates were then monitored for a ei ther a d ecrease in fluorescence intensity or a signal similar to that of the positive control (no enzyme) as an indicator of FpuD inhibition by the test compounds.

The University of Michigan MScreen software, a web-based open source cheminformatics application (Jacob *et al.*, 2012), was used for the management of all data obtained in the primary HTS, secondary screen and dose-response assays presented here. The "campaign view" shown in figure 3-5 displays the results obtained from the primary HTS and presents the data from all 14 assay plates in one scatter plot. The Z' value was calculated for each plate and averaged 0.85, with individual plate Z' values ranging from 0.81 to 0.88. F ollowing the primary screen, a total of 447 compounds were categorized as active hits from the 3892 compounds tested. The initial triage of these hit compounds followed a standard cut-off criteria in which compounds with ≥ 50% inhibition of FpuD and ≥ 3SD from the negative control are selected for further analysis. These criteria limited the number of compounds to be further tested to approximately 60; however, to take advantage of the "per plate" nature of the HTS facility, it was equally cost-efficient to screen double that number of compounds. Therefore, the range of cutoff criteria was increased to include compounds with ≥10% inhibition against FpuD to reach a total 120 compounds for secondary and dose response assays.

To quantify the inhibition of FpuD, dose response curves were generated for the 120 compounds remaining after the initial triage of the primary screen. Each compound

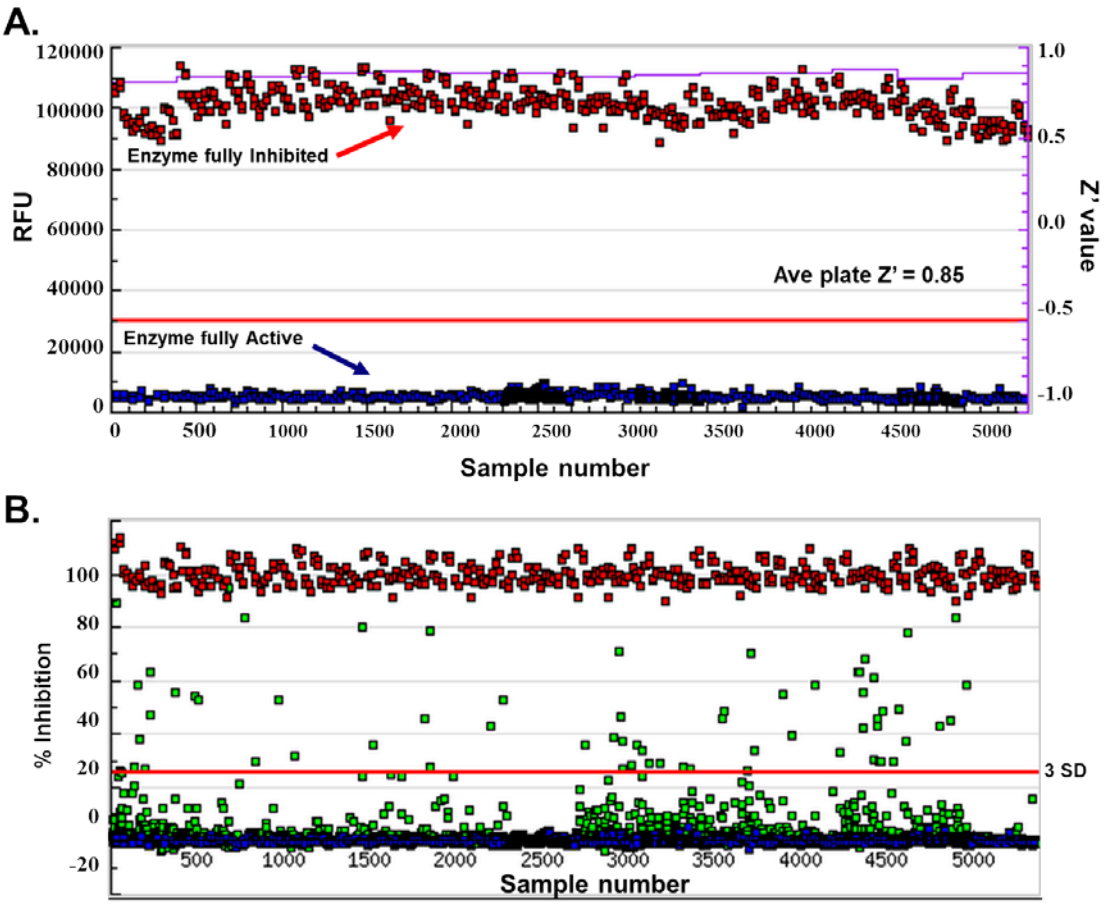

Figure 3-5. HTS results for primary screen of small molecule ATPase inhibitor compounds. A) The y axis represents the relative fluorescence units (RFU) for an equivalent number of positive controls (red squares, n = 448) and negative controls (blue squares, n = 448) for inhibition from all 14 384-well plates assayed in the primary screen. Each plate contained 32 positive controls and 32 negative controls. These data were used to calculate the Z' value of the HTS assay. The calculated average plate Z' for the primary screen was Z' = 0.85. B) The x axis represents the compounds screened (green squares), the positive controls for inhibition (red squares), and the negative controls for inhibition (blue squares). The y axis corresponds to the % inhibition of the test compounds against the FpuD ATPase when compared to the negative and positive controls. The red line represents 3 standard deviations as calculated from the negative controls and potential inhibitory compounds.

was assayed in duplicate in two-fold serial dilutions ranging from 6.9 to 250 μM following the primary assay protocol described above.

This same experiment was performed simultaneously in the presence of excess $MgCl_2$ (10 mM) as a secondary screen to rule out any compounds whose inhibitory activity was a result of general metal chelation. Following the secondary screen, 55 hit compounds were retained after selectively filtering for compounds that maintained inhibitory activity both in the presence and absence of excess $MgCl_2$. Of these 55 remaining compounds, all exhibited sigmoidal dose-response behaviors for which AC_{50} values were calculated, ranging from less than 6 to 95μM. Active concentration, or AC_{50}, is the concentration of a test compound that leads to 50% inhibition of the target's activity. By establishing more stringent cutoff criteria for compounds with AC_{50} values ≤ 30 μM, a maximal efficacy of at least 70% inhibition, and non-magnesium chelators, a manageable number of 16 top hits were selected for further testing (Table 3-1).

Table 3-1 (following page). Key information of the 16 "top hits" from the primary high-throughput FpuD inhibitor screen. An asterisk (*) denotes compounds which have been ordered and retested for inhibitory activity against purified FpuD enzyme and live cell assays with either Δ*fpuC*Δ*fatE* or wild-type *B. anthracis* str. $34F_2$ under iron-depleted conditions.

CCGNumber	Name	CCG Library	pAC50	AC50 (µM)	MaxEfficacy (%activity)	MaxEfficacy_Concentration	MW
CCG-207955*	Tanshinone IIA	Focused_Collections	5.16	6.92	70.7	89.64 µM	294.3
CCG-207993*	Niguldipine	Focused_Collections	4.97	10.72	103.2	149.70 µM	646.2
CCG-208331	I-Apo-Oxytetracycline	Focused_Collections	4.83	14.79	77.7	32.14 µM	442.4
CCG-101287	SB 216763	Focused_Collections	4.81	15.49	275.3	89.64 µM	371.2
CCG-39768*	Hexachlorophene	MS Spectrum 2000	4.77	16.98	90.2	32.14 µM	406.9
CCG-208211*	Gambogic acid	Focused_Collections	4.73	18.62	90.1	53.67 µM	628.8
CCG-101049	Montelukast Na	BioFocus NCC	4.66	21.88	217.4	250 µM	608.2
CCG-208771	4Br-AHX	Focused_Collections	4.63	23.44	105.3	250 µM	512.5
CCG-39365	Homidium Bromide	MS Spectrum 2000	4.61	24.55	273.5	149.70 µM	394.3
CCG-39023*	Meclocycline Sulfosalicylate	MS Spectrum 2000	4.56	27.54	75.4	89.64 µM	695
CCG-100881*	Triclabendazole	BioFocus NCC	4.54	28.84	94.9	250 µM	359.7
CCG-39955	Dipyrocetyl	MS Spectrum 2000	4.54	28.84	284.7	149.70 µM	238.2
CCG-208399	Shikonin	Focused_Collections	4.51	30.90	71.1	53.67 µM	370.4
CCG-208117	BML285 (Diaminoquinazoline)	Focused_Collections	4.51	30.90	109.6	149.70 µM	401.4
CCG-100935*	Naftopidil	BioFocus NCC	4.45	35.48	89	250 µM	392.5
CCG-39772*	Dichlorophene	MS Spectrum 2000	4.44	36.31	76.1	32.14 µM	269.1

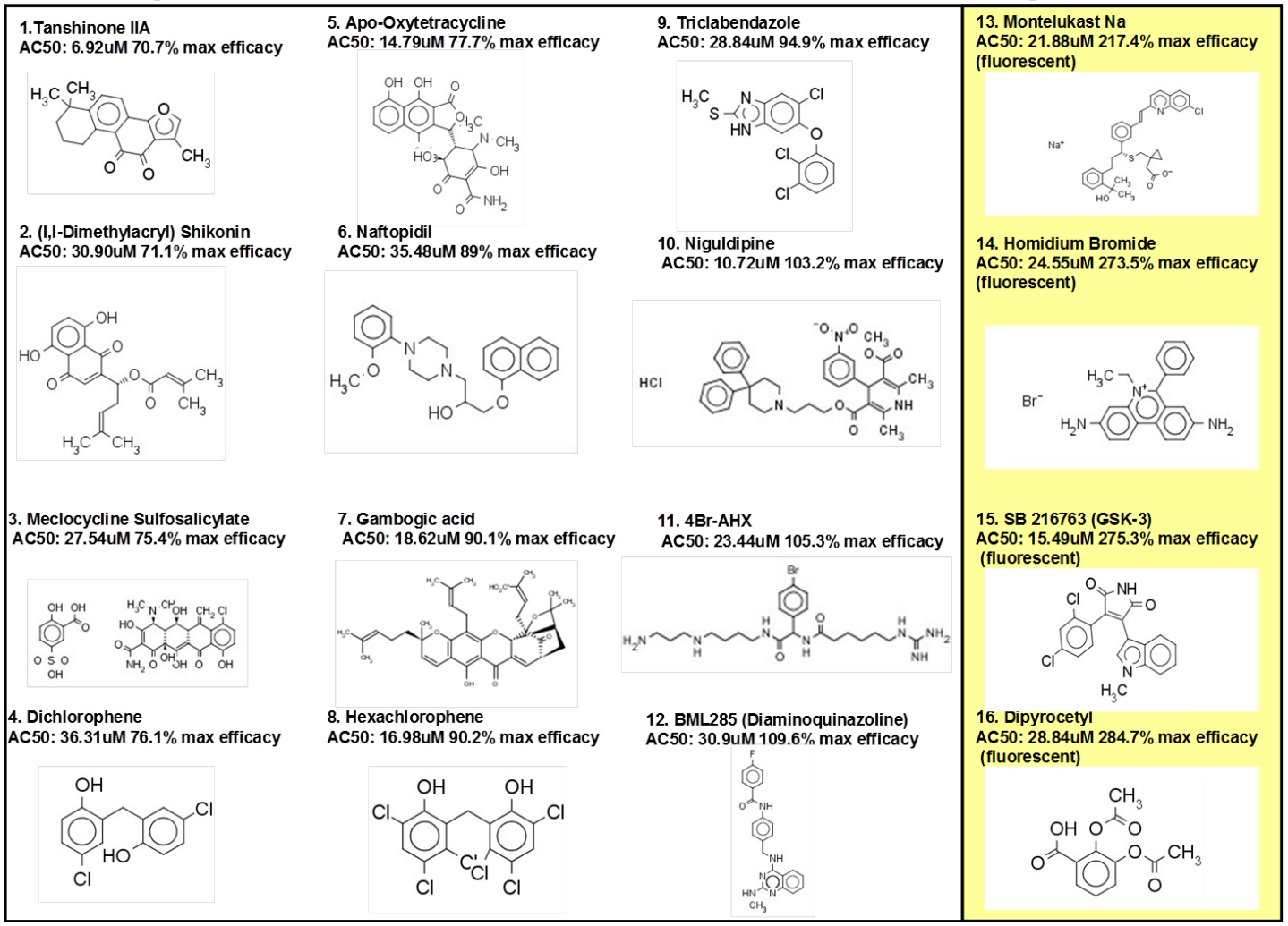

Figure 3-6. Top 16 hit compounds from the FhuD inhibitor pilot screen.

Reconfirmation of Inhibitory Activity of Hit Compounds

The top 16 lead compounds from the HTS were re-ordered from their respective distributors; however, due to supply issues, only eight could be obtained for follow-up testing. Using the original bench-top malachite green assay described previously, these eight compounds were tested to reconfirm inhibitory activity against FpuD. A similar degree of inhibition of the target enzyme was expected in this "low-throughput" version of the assay. Indeed some target compounds displayed dose-dependent efficacy, including meclocycline, dichlorophene, hexachlorophene, naftopidil, gambogic acid, and niguldipine; however, tanshinone and triclabendazole lost apparent efficacy during this reconfirmation experiment (Fig. 3-7). This is not without precedent, as hits from HTS screens occasionally fail to reconfirm. Often, this is explained by the actual inhibitory agent being a degradation product of the catalogued chemical. Future experiments including elucidating the structures of purchased compounds using NMR and mass spectrometry as well as high-temperature incubations to induce compound degradation will resolve the observed inconsistency between the HTS data and reconfirmation screens.

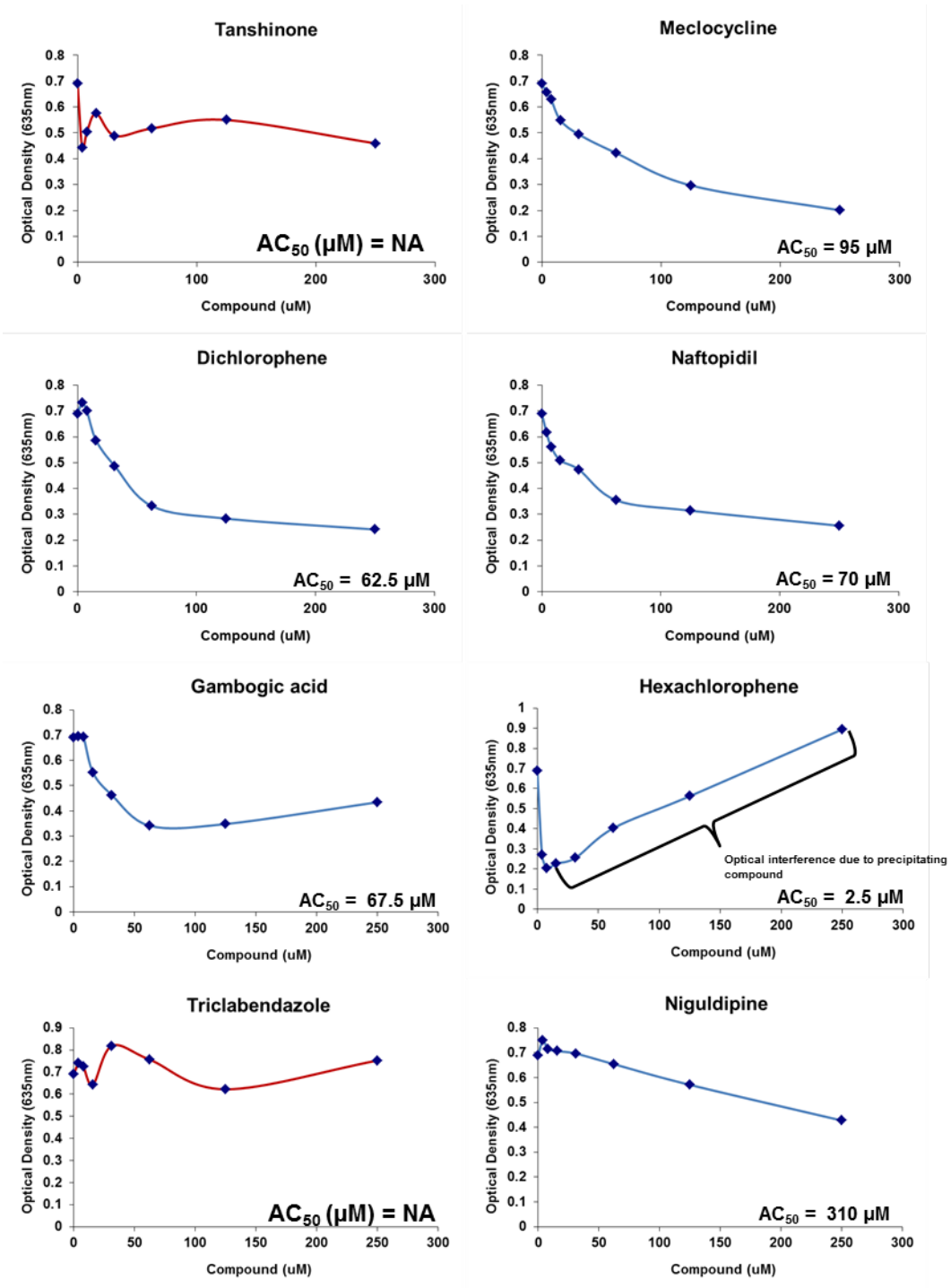

Figure 3-7. Reconfirmation of top hits from the primary screen. Dose response curves of lead compounds using the bench-top malachite green assay in 96-well plate format recapitulate enzyme inhibition by six of the eight compounds tested.

In vitro Antimicrobial Activity of Top FpuD Inhibitors

Live cell assays in iron-depleted medium were conducted with the *B. anthracis* Sterne $34F_2$ Δ*fpuC*,Δ*fatE* mutant. This strain expresses only one of the 3 petrobactin uptake ATPase genes, the target of the HTP screen, *fpuD*. This would ensure any effects of test compounds on cell replication could be more reliably related to the inhibition of the individual ATPase. Serial dilutions of the available 8 hit compounds were prepared for a final concentration ranging from 250 to 1.79 µM in 200 µl iron depleted medium (IDM) cultures using a 96-well plate format. Wells were inoculated with $1x10^4$ spores/ml and monitored over 18 hours. Because spore outgrowth in IDM is reliant on petrobactin production, it was hypothesized significant inhibition of petrobactin uptake should result in delayed or abrogated bacterial growth, with the minimum inhibitory concentration (MIC) for each test compound being defined as the minimum concentration required to completely prevent outgrowth from spores. Raw data is presented in figure 3-8 with all compounds indeed displaying a dose-dependent inhibition of bacterial growth in IDM.

A question remained whether or not the redundancy of ATPases in a wild type genetic background would affect the efficacy of the above compounds on live, iron-depleted cultures. For the majority of the compounds, no significant increase in minimal inhibitory concentration (MIC) was noted when tested on WT as opposed to Δ*fpuC*,Δ*fatE* *B. anthracis* str. Sterne $34F_2$. In some instances, the lowest concentration tested (1.79 µM) still completely inhibited growth; therefore a secondary dose-response experiment with a smaller range of test compound concentrations was also applied where appropriate to approximate MIC. Representative curves showing dose-response inhibition of bacterial growth are shown in Figure 3-9. A higher MIC was observed for gambogic acid and

tanshinone IIA against wild type Sterne $34F_2$ with the capacity to express all three petrobactin uptake ATPases than against a strain with the Δ*fpuC*,Δ*fatE* background. MICs for all compounds tested under iron depleted conditions are given in Table 3-2.

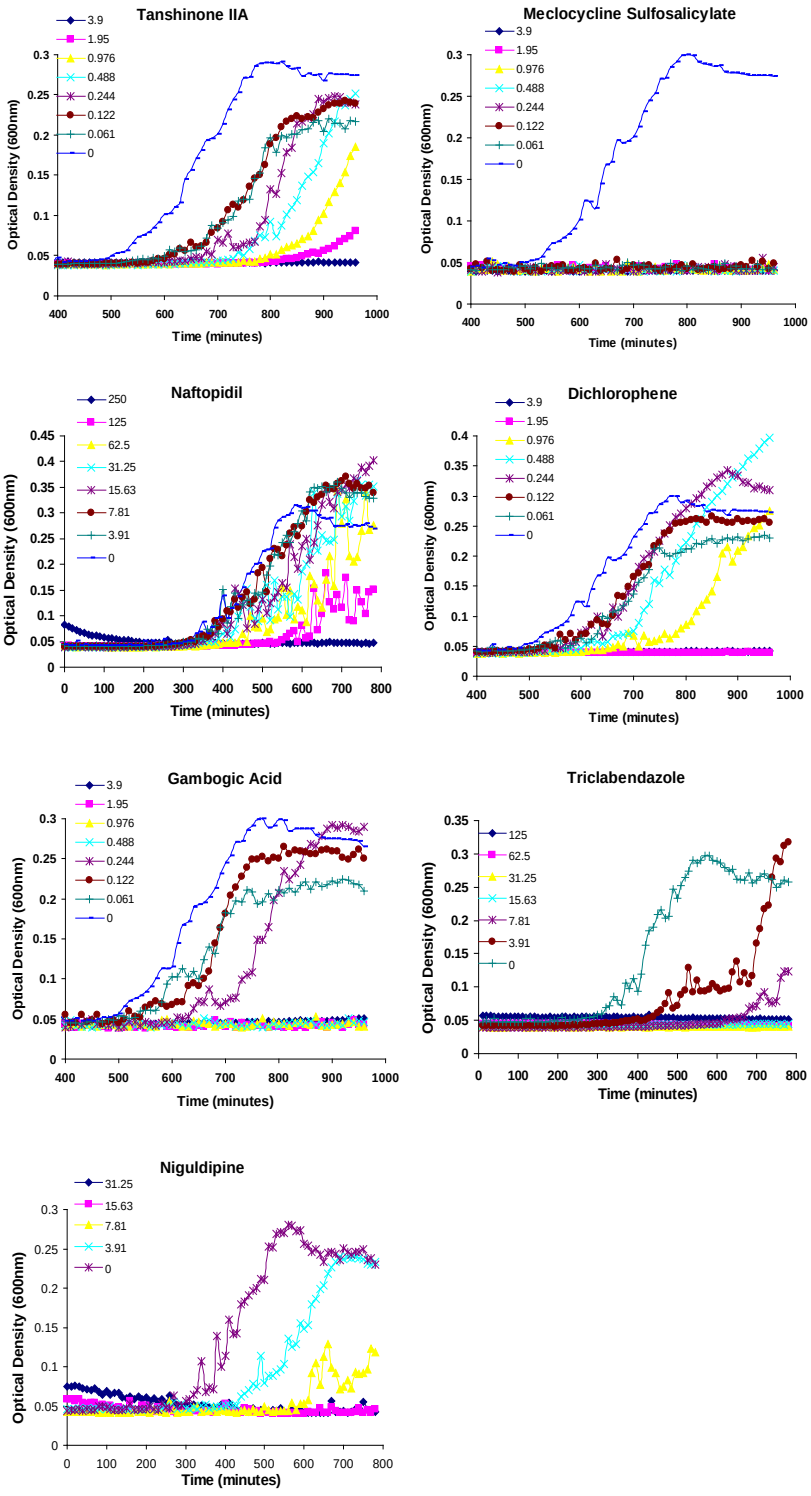

Figure 3-8. Live cell dose-response assay with the Δ*fpuC*Δ*fatE* mutant. IDM containing two-fold serial dilutions of 0-250 µM test compound was inoculated with spores ($1x10^4$ spores/ml) of *B. anthracis* possessing only one (*fpuD*) of the three petrobactin import ATPase genes. OD_{600} was observed every 10 minutes.

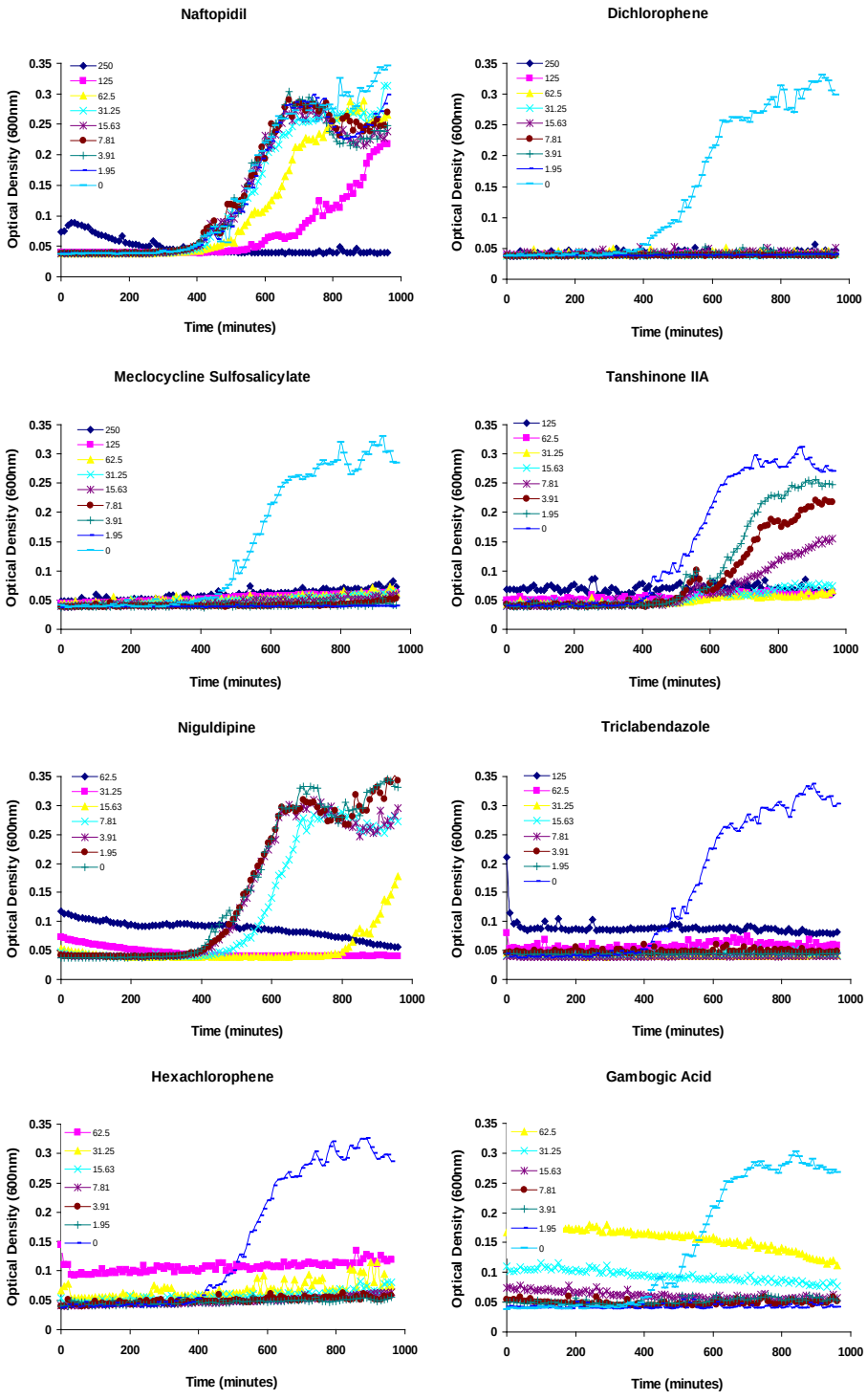

Figure 3-9 Live cell dose-response assay with Sterne 34F$_2$. IDM containing two-fold serial dilutions of 0-250 µM test compound was inoculated with wild type spores (1x10^4 spores/ml) of *B. anthracis* str. 34F$_2$ possessing all three petrobactin import ATPase genes. OD_{600} was observed every 10 minutes.

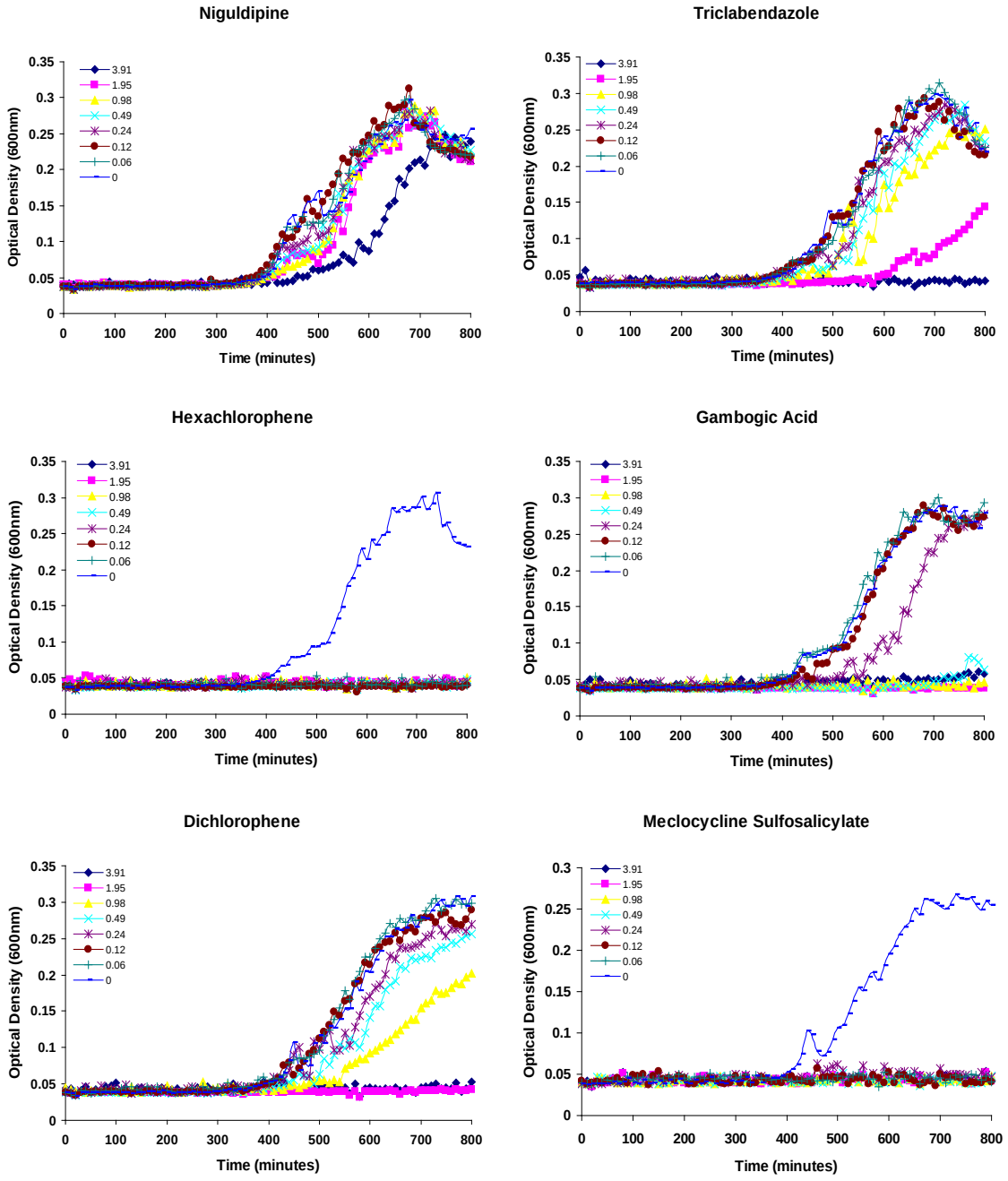

Figure 3-10 Live cell dose-response assay with Sterne 34F$_2$ using reduced concentrations. IDM containing two-fold serial dilutions of 0-3.9 µM test compound was inoculated with wild type spores (1x10^4 spores/ml) of *B. anthracis* str. 34F$_2$ possessing all three petrobactin import ATPase genes. OD_{600} was observed every 10 minutes.

Compound	MIC (μM)	
	wild-type	ΔfpuCΔfatB
Naftopidil	250	250
Dichlorophene	1.95	1.95
Meclocycline Sulfosalicylate	0.06	0.06
Tanshinone IIA	15.63	3.9
Niguldipine	7.9	7.9
Triclabendazole	3.9	3.9
Hexachlorophene	0.06	Not Tested
Gambogic Acid	0.49	0.244

Table 3-2 Minimal Inhibitory Concentration (MIC) Values for Inhibitor Compounds tested in live cell assays with Sterne 34F$_2$ or *ΔfpuCΔfatE*.

3.3 Conclusion and Future Directions

Aside from the challenges faced in identifying potential outbreaks and infected individuals, antibiotic resistant strains of *B. anthracis* engineered for deployment as a weapon is a looming biodefense concern (Inglesby *et al.*, 1999, Jernigan *et al.*, 2001). Although naturally occurring antibiotic resistant *B. anthracis* strains are rare, partially due to the decreased prevalence of these infections compared to that of other organisms, the possibility of resistance arising due to the extended lengths of time required for antibiotic treatment remains (Aldred *et al.*, 2012, Beierlein & Anderson, 2011). The increasing likelihood that bacteria are exposed to sub-lethal doses of antibiotics, and the long standing problem of patient compliance in chemotherapeutic regimens can also play a major role in the rise of resistant strains of *B. anthracis* as well as several other pathogenic bacteria including MRSA and *Mycobacterium tuberculosis* (Calfee, 2012, Morris *et al.*, 2005). Current vaccines used to induce immunity to anthrax infection have several inherent problems of their own and require much improvement. Currently, an acellular vaccine using protective antigen produced from the avirulent non-encapsulated Sterne strain called Anthrax Vaccine Adsorbed (AVA, also known as Biothrax®) is the only FDA approved vaccine used to prevent anthrax infection in the US (Chitlaru *et al.*, 2011). Yet, as mentioned above, the lack of patient compliance and the extended nature of administration of this vaccine, lends to the burdensome and ineffectual nature of this method. Such concerns with current vaccines and therapies along with the recognition of *B. anthracis* as not only a bioterrorist threat but also a model organism for studying Gram positive bacterial infections, highlights the need for research and identification of new targets for small molecule drug design to treat both anthrax and many other diseases.

One of the best avenues to more effectively combat future biological threats like anthrax is by developing strategies that more selectively target factors and pathways exclusively involved in virulence. Almost without exception, current antimicrobials target pathways required for general survival of a cell in both environmental and host niches like cell wall synthesis, DNA replication, or translation of polypeptides (Sanyal & Doig, 2012, Fischbach & Walsh, 2009). By creating new chemotherapeutics that would exclusively target virulence factors, the time in which selective pressure is applied to an invading strain (only during infection, and not within the environment) to develop a resistance *de novo* or acquire one by horizontal gene transfer is significantly reduced. Furthermore, this strategy holds the potential to more directly target invading microbes, and not commensal strains, reducing the likelihood of side-effects associated with depletion of beneficial microbiota with broad-spectrum antibiotics. On the vaccine side, surface-associated proteins up-regulated during host infection would likely serve as prime candidates for formulations with higher immunogenicity than those currently on the market. In both areas, siderophore-facilitated iron acquisition pathways serve as logical targets to explore as they are often only active during infection and require transport mechanisms with several surface-associated components easily targeted by the immune system and chemotherapeutics. Examples of successes in this area have already been reported in *E. coli* and *S. aureus*, with regard to vaccines, and in *M. tuberculosis* with small molecule inhibitors (Arimitsu *et al.*, 2012, Mariotti *et al.*, 2012, Mishra *et al.*, 2012, Miller *et al.*, 2011, Ji *et al.*, 2012).

It stands to reason that petrobactin utilization is an ideal pathway for developing new anti-infectives. Recent identification of the permease and ATPase components of

the petrobactin import system have revealed two distinct permeases, FpuB or FatCD, and three distinct ATPases, FpuC, FpuD, and FatE (Dixon et al., 2012). These proteins are sufficient for iron acquisition and play redundant roles in petrobactin transport across the bacterial cell membrane. Not only are these ABC-transport proteins essential in cell viability, virulence and pathogenicity, but they also share conserved sequences across all bacterial species, making these proteins intriguing targets for therapeutics that can potentially treat a wide range of bacterial infections. The results presented here represent the first effort to employ HTS to identify small molecule inhibitors of petrobactin ABC-import machinery. Because active ABC transporter ATPases can be easily purified and require a single substrate for activity, these enzymes are prime candidates for a high-throughput inhibitor search. Novel molecules capable of inhibiting these crucial ATPase proteins in the petrobactin transport system have been identified using an adapted malachite green assay. A pilot screen was conducted using select small libraries consisting of 3892 chemically diverse and biologically active compounds at the CCG. The results of the pilot screen showed a robust assay with a Z' = 0.85.

Follow-up dose-response and metal chelation experiments were performed in HTS format and allowed 120 selected hits to be filtered down to 16 target compounds (Fig. 3-6). Among the compounds depicted in figure 3-6, some structural similarities are apparent, including the naphthalene-like functionalities on compounds 6, 12, and 13 and the tetracyclic cores of 3 and 7. Resemblance to the nucleoside of ATP seen in apo-oxytetracycline, triclabendazole, homidium bromide, and GSK-3 suggests that some of the hit compounds may be competing with the ATPase's natural substrate at the active site. Future studies testing inhibitory activity under varying concentrations of ATP may

delineate whether the top hits are acting as competitive inhibitors or having an allosteric effect on enzymatic activity. An idea of how specific FpuD inhibitors are will only be garnered from empirical observation of screen hit activity on other purified ATPases, including FatE and FpuC. The nature of the chemical collections used for the pilot screen means that most hits possess previously known modes of action or targets that must be taken into consideration when moving forward with drug design (Table 3-3). One compound in particular, gambogic acid, appears to be potent in the sub-micromolar range, and has already shown relatively low side effects when used as an antitumor chemotherapeutic in mice (Pandey *et al.*, 2007)- a desirable trait when moving forward with SAR and other medicinal chemistry.

Of the eight "top hits" used in subsequent whole cell assays, all showed some degree of inhibition of bacterial growth. Interestingly, a compound's MIC was generally lower than the corresponding AC_{50} when incubated with purified FpuD. Perhaps inhibitory compounds are accumulating intracellularly so that the local concentration surrounding a native ATPase is higher than that administered to the culture. It is also likely that multiple targets, and not just petrobactin import, are being affected by some test compounds, thus conferring higher-than-expected sensitivity. Repetition of live-cell experiments in iron-rich media may help determine if this is in fact occurring. With this pilot screen now validated, we aim to screen larger libraries for further inhibitors. The long term goal is to perform medicinal chemistry on lead hits of this and larger future screens to design druggable compounds that inhibit siderophore-facilitated iron uptake, or more broadly, ABC transport systems required by *B. anthracis* and other dangerous pathogens.

Eight Top ATPase Inhibitor Compounds Re-tested at the Bench				
Compound	Vendor	Catalogue #	Lot #	Current Use / Target
Tanshinone IIA	Sigma Life Sciences	T4952	091M1917V	Anticoagulant, prevention of liver fibrosis, alpha glucosidase inhibitor
R-(-)- Nigulidipine Hydrochloride	Sigma Life Sciences	N162	118H4621V	Calcium channel blocker, α1-adrenergic receptor antagonist
Hexachlorophene	Sigma Life Sciences	45526	SZ138042XV	Disinfectant
Gambogic Acid	Sigma Life Sciences	G8171	111M4710V	Anti-tumor, N-FκB repressor
Meclocycline Sulfosalicylate	Sigma Life Sciences	M1388	050H0682V	Topical antibiotic
Triclabendazole	Sigma Life Sciences	32802	SZBA29ZXV	Anthelmenthic, binds β-tubulin
Naftopidil	Sigma Life Sciences	N158	099K1235V	Antihypertensive α1-adrenergic receptor antagonist
Dichlorophene	Sigma Life Sciences	35992	SZB8121XV	Disinfectant, antiparasitic

Table 3-3. Ordering information and know activities of the eight “top hits” tested at the bench.

3.4 Experimental Procedures

Bacterial Strains and Plasmids

Bacillus anthracis strain Sterne 34F2 (Turnbull, 1991, Sterne, 1946) and its derivatives were used in all experiments unless specified otherwise. Brain heart infusion media (BHI), iron depleted media (IDM), and iron replete media (IRM) were used for growth of *B. anthracis*. Luria broth (LB) (for genetic manipulations) and terrific broth (TB) (for protein purification) were used for growth of *Escherichia coli*; for plasmid selection kanamycin sulfate was used at a concentration of 50 μg/mL.

Cloning and Over-Expression of B. anthracis ABC Transport ATPases and ATPase Mutants

The genes for each of the FpuC, FpuD, and FatE ATPases were PCR amplified from *B. anthracis* chromosomal DNA and introduced into expression vector pET-28a (+) (Novagen; Madison, WI) using restriction sites XbaI and XhoI to produce N-terminally 6-histidine-tagged ATPases. The recombinant pET-28a plasmids were transformed into One Shot® Mach1™-T1^{R} Chemically Competent *E. coli* non-expression cells. Positive clones were identified by selection of kanamycin resistant colonies on LB agar plates containing 50μg/mL kanamycin and each reading frame was verified by sequencing with a T7 terminator primer. For over-expression of the His_6-tagged ATPases, confirmed plasmids were transformed into competent BLR expression host cells carrying T7 RNA polymerase gene (λDE3 lysogen). Flasks containing 50 mL of TB (Terrific Broth) media supplemented with 4% glycerol and 25 μg/mL kanamycin were inoculated individually with 500 μL overnight culture of BLR pET-28a-His_6-ATPase (FpuC, FpuD, or FatE) and incubated at 37°C to an optical density (600nm) of ~0.6-1.0, about 3-4 hours. At this

point the culture was cooled to 18°C with shaking for 30 minutes and expression of the His_6-ATPase was induced for 16hrs with 0.25 mM IPTG at 18°C, the optimal temperature for the yield of soluble protein. Cells were then harvested by centrifugation at 8,000 x g for 20 minutes.

The *fpuD*(E163Q) insert was constructed using internal PCR primers that changed codon 167 from GAG (coding for Glu) to CAG (coding for Gln) to generate two fragments of the final insert gene. These fragments were purified by a gel electrophoresis cleanup kit (Qiagen) and served together as the template to be stitched together as the product of a second round of PCR. Cloning and overexpression of the pET-28a–His_6-*fpuD*(E163Q) construct was achieved using the same protocol as described above for the wild-type ATPases.

Purification of B. anthracis ABC Transport ATPase-His and ATPase-E167Q-His Mutants

Cells over-expressing His_6-ATPase were resuspended in 5 mL lysis buffer containing 20mM HEPES buffer, pH 8, containing 300 mM sodium chloride, 20 mM imidazole, 1 mM (tris(2-carboxyethyl)phosphine) TCEP, and 10% glycerol. The cell suspension was transferred to a sonication-safe container kept within an ice water slurry. Cells were sonicated using a ½" disruptor horn at 60% intensity for 10 seconds on, 30 seconds off for 2 minutes total "on" time. Crude cell lysate was then transferred to chilled high-speed centrifuge tubes for removal of insoluble material by ultracentrifugation at 40,000 x g for 45 minutes at 4°C. The soluble lysate supernatant was transferred to a tube containing ~500µL Ni^{2+}-NTA resin (Qiagen) that had been pre-equilibrated with lysis buffer and was mixed gently on a rocker for 2 hr at 4°C to allow binding of His_6-ATPase

proteins to the Ni^{2+}-NTA resin. Lysate-resin slurry was then centrifuged at 2,000 x g for 2 minutes at 4°C, and supernatant was decanted by aspiration. Two subsequent washes were conducted by resuspending pelleted His_6-ATPase bound Ni^{2+}-NTA resin in wash buffer containing 20mM HEPES, pH 8, 250 mM sodium chloride, 40 mM imidazole, 1 mM TCEP, and 10% glycerol and rocking at 4°C for 30 min. The Ni^{2+}-NTA resin was eluted by rocking for 20 min. with 4 mL elution buffer containing 20mM HEPES, pH 8, 50 mM sodium chloride, 300 mM imidazole, 1 mM TCEP, and 10% glycerol and centrifuged for 5 minutes at 4,000 x g . Supernatant containing eluted protein was removed and combined with an equal volume of storage buffer containing 50mM HEPES, pH 8, 150 mM sodium chloride, 1 mM TCEP, and 20% glycerol. The eluate was concentrated and exchanged into ~90% storage buffer using an Amicon centrifugation filter, 10 kDa MWCO (Amicon Ultra, Millipore). Aliquots of purified ATPases-His proteins were flash frozen in a liquid nitrogen/ethanol bath and stored immediately at -80°C until further use.

ATPase Activity Assay

ATPase activities were determined using the P_i ColorLock Gold ATPase assay system (Innova Biosciences) according to the manufacturer's recommendations. This is a malachite green-based assay for the colorimetric detection of free phosphate. Reaction components were kept at 4° C or on ice until directly prior to experimentation. Initial characterization of all ATPases was performed in 96-well clear bottom plates (Corning). Unless specified differently, conditions were as follows: an enzyme reaction solution (76µL) containing 50 mM HEPES, 150 mM NaCl2, 0.5 mM MgCl2, 1.0 mM DTT, and 0.5 µM purified ATPase (FpuC, FpuD, or FatE) was added to all wells except the

positive control for inhibition (no enzyme). The ATPase activity reaction was started by the addition of 4 µl 10 mM ATP for a final concentration of 0.5 mM ATP and was then incubated at 25° C for 30 minutes. The reaction was quenched and developed with the addition of 1:4 the initial volume (20 µl) Innova Biosciences Gold Mix. Quenched reaction mixtures were incubated for 2 min, after which 1:10 the initial volume (8µl) of stabilizer reagent was added. Reaction mixtures were allowed to incubate an additional 20 minutes after which an increase in absorbance at 635nm was measured on a SpectraMax m2 plate reader (Molecular Devices) and compared to that observed with the no-enzyme positive control reactions.

For high-throughput screening, the following changes were made to the assay conditions: briefly, recombinant FpuD was diluted to a final concentration of 1 µM in 10 µl of assay buffer described above, and was added to all but the positive control (no enzyme). The reaction is then started by the addition of 2.0 µl 3.5 mM ATP and is then incubated at 25° C for 30 minutes. The screen is quenched and developed with the addition of 2.5 µl Innova Biosciences Gold Mix (1:100 dilution of Accelerator into PiColorLock Gold). Quenched reaction mixtures were incubated for 2 min, after which 1 µl of stabilizer reagent is added. Reaction mixtures were incubated an additional 20 mins after which a decrease in fluorescence (Ex430nm/EmA630nm) compared to that observed with no-enzyme positive control reactions indicates enzymatic activity. Alternatively, an increase in fluorescence (Ex430nm/EmA630nm) upon quenching compared to that observed with no-compound negative control suggests a reduction in enzymatic activity.

Small-Molecule Libraries

Four small molecule libraries available at the University of Michigan Center for Chemical Genomics (CCG) were utilized for use in a primary high-throughput screen consisting of approximately 4000 compounds. These libraries included the MicroSource MS2000, BioFocus National Institutes of Health (NIH) Clinical Collection (NCC), Focused Collections Natural Products, and the Focused Collections Target Specific libraries. Briefly, the MicroSource MS2000 library contains approximately 2000 bioactive compounds exceeding 95% purity. The collection includes 958 known therapeutic drugs, 629 natural products and derivatives, 343 compounds with reported biological activities, and 70 compounds that have been approved for use in agriculture. The BioFocus NIH Clinical Collection and NIH Clinical Collection 2 are plated arrays of 446 and 281, respectively, small molecules that have a history of use in human clinical trials. The Focused Collections Natural Products library consists of over 30,000 crude natural product extracts and the Focused Collections Target Specific libraries contain pure natural products, epigenetic/autophagy/redox compounds, and protease and proteostasis inhibitors. The activity of promising compounds was confirmed using repurchased samples from Sigma Aldrich (St. Louis, MO). All purchased compounds were tested without further purification.

High Throughput Screening Protocol and Determination of Z'

The high-throughput screen was conducted using a malachite green based fluorescence quench assay with all reagents prepared exactly as described above in "ATPase activity assay". All components other than test compounds were added using a

Multidrop dispenser (Thermo Fisher Scientific, Inc.), and were kept at 4° C or on ice directly prior to experimentation. The FpuD ATPase stock solution was prepared as described above so that the final concentration of FpuD was 1 μM in assay buffer. The FpuD/buffer solution (10μL) was then added to each well of opaque, white, low-volume, non-sterile, polystyrene 384-well plates (Grenier Bio-One, Monroe, NC) except for the last two outer columns on the right of the plate which were filled with assay buffer containing no FpuD enzyme to serve as a positive control for enzyme inhibition. The library screened consisted of ~ 4000 compounds selected from the libraries listed above in "*Small Molecule Libraries*". Stock compounds (~30μM) or DMSO (left two outer columns) were then delivered by the HDR (high density replication) "pin" tool on the Biomek FX (Beckman) liquid handling robot from the library plates to the 384-well assay plates (containing FpuD/buffer solution) at the rate of one plate/minute at ambient temperature at a volume 0.2 μL. To avoid false positives, the plates were read after the addition of compounds to identify any compounds that are inherently fluorescent. Finally, 2 μL of a 3.5 mM ATP solution (final concentration of 0.5 mM ATP) was added to start the reaction. The plates were then incubated for 30 minutes at 25°C. After incubation, each well received 3 μL of Innova Biosciences Gold Mix, allowing 2 minutes for development of the reaction, followed by the addition of 2 μL stabilizer reagent to quench the non-enzymatic release of inorganic phosphate. Plates were then incubated for an additional 20 minutes at 25°C and the fluorescence intensity was measured (excitation 430 nm, emission 600 nm) on a PHERAstar plate reader. Any compounds with inhibitory activity against FpuD resulted in a higher fluorescence reading compared to the negative control containing only DMSO. To evaluate the signal window and signal-to-noise ratio

of the assay, a test for Z' factor calculation was performed for every 384-well plate based on the negative and positive control. Z' was calculated using the following formula: $Z' = 1-(|3SD_+ + 3SD_-|)/ |Ave_+ - Ave_-|$ where Ave_+ = the average fluorescence units of the positive controls, Ave_- = the average fluorescence units of negative controls, and SD_+ and SD_- is the standard deviation of the positive and negative controls, respectively.

Dose Response Assays and Determination of AC_{50} for Inhibitors

To determine the AC_{50} values for the selected compounds, reactions were performed as described under the "*ATPase Activity Assay*" section above, with the exception that compounds were added using a TTP Labtech Mosquito X1 with "cherry-picking" ability to transfer specific compounds from library plates to the 384-well assay plates. A Biomek FX serial dilution head was then used to sequentially dilute the compounds to desired concentrations ranging from 250 μM – 6.9 μM. Activity was normalized to uninhibited controls containing only DMSO performed alongside these reactions. Each reaction was performed in duplicate. Data analysis was performed using MScreen software, a high-throughput screening data storage and analysis system at the University of Michigan Center for Chemical Genomics (Jacob et al., 2012).

Secondary Screen Against Metal Chelating Compounds

To investigate whether inhibitors were Mg^{2+}-competitive and eliminate any compounds whose inhibitory activity was due to metal chelation, reactions were run in the presence of 10mM excess $MgCl_2$. Compounds resulting in loss of inhibitory activity

in the presence of 10mM excess $MgCl_2$ were considered general metal chelators and were eliminated from the "hit" selection pool.

Cytotoxicity Assays and Determination of MIC Values for Inhibitors

MIC values of eight of the 16 top hit compounds were obtained using a standard microdilution assay in clear 96-well tissue culture plates (Costar®, Corning Inc.). Compounds were diluted in iron depleted media (IDM, prepared as described previously) ranging from 0-250 μM as indicated. Cultures started from spores ($1x10^4$ spores/ml) of either Δ*fpuC*Δ*fatE* mutant strain or *B. anthracis* str. $34F_2$ in a final volume of 200 μl IDM and were grown at 37°C for 18 hours. Optical density (600nm) was monitored every ten minutes with 5 seconds of shaking prior to each read on a SpectraMax M2 plate reader (Molecular Devices). The MIC is defined as the lowest concentration of compound that resulted in no detectable growth.

3.7 References

Aldred, K.J., S.A. McPherson, P. Wang, R.J. Kerns, D.E. Graves, C.L. Turnbough, Jr. & N. Osheroff, (2012) Drug interactions with Bacillus anthracis topoisomerase IV: biochemical basis for quinolone action and resistance. *Biochemistry* **51**: 370-381.

Arimitsu, H., K. Sasaki, T. Shimizu, K. Tsukamoto & T. Tsuji, (2012) Large-scale preparation of Shiga toxin 2 i n Escherichia coli for toxoid vaccine antigen production. *Microbiol Immunol*.

Beierlein, J.M. & A.C. Anderson, (2011) New developments in vaccines, inhibitors of anthrax toxins, and antibiotic therapeutics for Bacillus anthracis. *Curr Med Chem* **18**: 5083-5094.

Bouzianas, D.G., (2009) Medical countermeasures to protect humans from anthrax bioterrorism. *Trends in Microbiology* **17**: 522-528.

Calfee, D.P., (2012) Methicillin-resistant Staphylococcus aureus and vancomycin-resistant enterococci, and other Gram-positives in healthcare. *Curr Opin Infect Dis* **25**: 385-394.

Carlson, P.E., Jr., S.D. Dixon, B.K. Janes, K.A. Carr, T.D. Nusca, E.C. Anderson, S.E. Keene, D.H. Sherman & P.C. Hanna, (2010) Genetic analysis of petrobactin transport in Bacillus anthracis. *Molecular microbiology* **75**: 900-909.

Cendrowski, S., W. MacArthur & P. Hanna, (2004) Bacillus anthracis requires siderophore biosynthesis for growth in macrophages and mouse virulence. *Mol Microbiol* **51**: 407-417.

Chitlaru, T., Z. Altboum, S. Reuveny & A. Shafferman, (2011) Progress and novel strategies in vaccine development and treatment of anthrax. *Immunol Rev* **239**: 221-236.

Cogan, E.B., G.B. Birrell & O.H. Griffith, (1999) A robotics-based automated assay for inorganic and organic phosphates. *Anal Biochem* **271**: 29-35.

Davidson, A.L., E. Dassa, C. Orelle & J. Chen, (2008a) Structure, Function, and Evolution of Bacterial ATP-Binding Cassette Systems. *Microbiology and Molecular Biology Reviews* **72**: 317-364.

Davidson, A.L., E. Dassa, C. Orelle & J. Chen, (2008b) Structure, function, and evolution of bacterial ATP-binding cassette systems. *Microbiol Mol Biol Rev* **72**: 317-364, table of contents.

Dixon, S.D., B.K. Janes, A. Bourgis, P.E. Carlson, Jr. & P.C. Hanna, (2012) Multiple ABC transporters are involved in the acquisition of petrobactin in Bacillus anthracis. *Molecular microbiology* **84**: 370-382.

Dixon, T.C., M. Meselson, J. Guillemin & P.C. Hanna, (1999) Anthrax. *N Engl J Med* **341**: 815-826.

Fischbach, M.A. & C.T. Walsh, (2009) Antibiotics for emerging pathogens. *Science* **325**: 1089-1093.

Frankel, A.E., S.R. Kuo, D. Dostal, L. Watson, N.S. Duesbery, C.P. Cheng, H.J. Cheng & S.H. Leppla, (2009) Pathophysiology of anthrax. *Front Biosci* **14**: 4516-4524.

Friedlander, A.M., (2001) Microbiology: Tackling anthrax. *Nature* **414**: 160-161.

Higgins, C.F., (1992) ABC Transporters: From Microorganisms to Man. *Annual Review of Cell Biology* **8**: 67-113.

Holland, I.B. & M. A. Blight, (1999) ABC-ATPases, adaptable energy generators fuelling transmembrane movement of a variety of molecules in organisms from bacteria to humans. *Journal of Molecular Biology* **293**: 381-399.

Holland, I.B. & M.A. Blight, (1999) ABC-ATPases, adaptable energy generators fuelling transmembrane movement of a variety of molecules in organisms from bacteria to humans. *J Mol Biol* **293**: 381-399.

Inglesby, T.V., D.A. Henderson, J.G. Bartlett, M.S. Ascher, E. Eitzen, A.M. Friedlander, J. Hauer, J. McDade, M.T. Osterholm, T. O'Toole, G. Parker, T.M. Perl, P.K. Russell & K. Tonat, (1999) Anthrax as a biological weapon: medical and public health management. Working Group on Civilian Biodefense. *JAMA* **281**: 1735-1745.

Jacob, R.T., M.J. Larsen, S.D. Larsen, P.D. Kirchhoff, D.H. Sherman & R.R. Neubig, (2012) MScreen: an integrated compound management and high-throughput screening data storage and analysis system. *J Biomol Screen* **17**: 1080-1087.

Jernigan, J.A., D.S. Stephens, D.A. Ashford, C. Omenaca, M.S. Topiel, M. Galbraith, M. Tapper, T.L. Fisk, S. Zaki, T. Popovic, R.F. Meyer, C.P. Quinn, S.A. Harper, S.K.

Fridkin, J.J. Sejvar, C.W. Shepard, M. McConnell, J. Guarner, W.J. Shieh, J.M. Malecki, J.L. Gerberding, J.M. Hughes & B.A. Perkins, (2001) Bioterrorism-related inhalational anthrax: the first 10 cases reported in the United States. *Emerg Infect Dis* **7**: 933-944.

Ji, C., P.A. Miller & M.J. Miller, (2012) Iron transport-mediated drug delivery: practical syntheses and in vitro antibacterial studies of tris-catecholate siderophore-aminopenicillin conjugates reveals selectively potent antipseudomonal activity. *J Am Chem Soc* **134**: 9898-9901.

Koster, W., (2001) ABC transporter-mediated uptake of iron, siderophores, heme and vitamin B12. *Research in microbiology* **152**: 291-301.

Mariotti, P., E. Malito, M. Biancucci, P. Lo Surdo, R.P. Mishra, V. Nardi-Dei, S. Savino, M. Nissum, G. Spraggon, G. Grandi, F. Bagnoli & M.J. Bottomley, (2012) Structural and functional characterization of the Staphylococcus aureus virulence factor and vaccine candidate FhuD2. *Biochem J*.

McQuade, T.J., A.D. Shallop, A. Sheoran, J.E. Delproposto, O.V. Tsodikov & S. Garneau-Tsodikova, (2009) A nonradioactive high-throughput assay for screening and characterization of adenylation domains for nonribosomal peptide combinatorial biosynthesis. *Anal Biochem* **386**: 244-250.

Miller, M.J., A.J. Walz, H. Zhu, C. Wu, G. Moraski, U. Mollmann, E.M. Tristani, A.L. Crumbliss, M.T. Ferdig, L. Checkley, R.L. Edwards & H.I. Boshoff, (2011) Design, synthesis, and study of a mycobactin-artemisinin conjugate that has selective and potent activity against tuberculosis and malaria. *Journal of the American Chemical Society* **133**: 2076-2079.

Mishra, R.P., P. Mariotti, L. Fiaschi, S. Nosari, S. Maccari, S. Liberatori, M.R. Fontana, A. Pezzicoli, M.G. De Falco, F. Falugi, E. Altindis, D. Serruto, G. Grandi & F. Bagnoli, (2012) Staphylococcus aureus FhuD2 is involved in the early phase of staphylococcal dissemination and generates protective immunity in mice. *J Infect Dis* **206**: 1041-1049.

Morris, R.P., L. Nguyen, J. Gatfield, K. Visconti, K. Nguyen, D. Schnappinger, S. Ehrt, Y. Liu, L. Heifets, J. Pieters, G. Schoolnik & C.J. Thompson, (2005) Ancestral

antibiotic resistance in Mycobacterium tuberculosis. *Proc Natl Acad Sci U S A* **102**: 12200-12205.

Pandey, M.K., B. Sung, K.S. Ahn, A.B. Kunnumakkara, M.M. Chaturvedi & B.B. Aggarwal, (2007) Gambogic acid, a novel ligand for transferrin receptor, potentiates TNF-induced apoptosis through modulation of the nuclear factor-κB signaling pathway. *Blood* **110**: 3517-3525.

Pegan, S.D., Y. Tian, V. Sershon & A.D. Mesecar, (2010) A universal, fully automated high throughput screening assay for pyrophosphate and phosphate release from enzymatic reactions. *Comb Chem High Throughput Screen* **13**: 27-38.

Pfleger, B.F., Y. Kim, T.D. Nusca, N. Maltseva, J.Y. Lee, C.M. Rath, J.B. Scaglione, B.K. Janes, E.C. Anderson, N.H. Bergman, P.C. Hanna, A. Joachimiak & D.H. Sherman, (2008) Structural and functional analysis of AsbF: Origin of the stealth 3,4-dihydroxybenzoic acid subunit for petrobactin biosynthesis. *Proceedings of the National Academy of Sciences of the United States of America*.

Rosenberg, M.F., R. Callaghan, S. Modok, C.F. Higgins & R.C. Ford, (2005) Three-dimensional Structure of P-glycoprotein: THE TRANSMEMBRANE REGIONS ADOPT AN AS YMMETRIC CONFIGURATION IN THE NUCLEOTIDE-BOUND STATE. *Journal of Biological Chemistry* **280**: 2857-2862.

Sanyal, G. & P. Doig, (2012) Bacterial DNA replication enzymes as targets for antibacterial drug discovery. *Expert Opin Drug Discov* **7**: 327-339.

Schneider, E. & S. Hunke, (1998) ATP-binding-cassette (ABC) transport systems: functional and structural aspects of the ATP-hydrolyzing subunits/domains. *FEMS Microbiol Rev* **22**: 1-20.

Stauff, D.L., D. Bagaley, V.J. Torres, R. Joyce, K.L. Anderson, L. Kuechenmeister, P.M. Dunman & E.P. Skaar, (2008) Staphylococcus aureus HrtA is an ATPase required for protection against heme toxicity and prevention of a transcriptional heme stress response. *Journal of bacteriology* **190**: 3588-3596.

Sterne, M., (1946) Avirulent anthrax vaccine. *Onderstepoort J Vet Sci Anim Ind* **21**: 41-43.

Turnbull, P.C., (1991) Anthrax vaccines: past, present and future. *Vaccine* **9**: 533-539.

Chapter 4

Discussion of Research

4.1 Summary

Work in the previous chapters describes the great majority of what is currently understood regarding petrobactin-associated iron uptake in *Bacillus anthracis*. Chapter 1 has highlighted the importance of iron to all living organisms, provides an even deeper understanding of the essentiality of the siderophore petrobactin during mammalian infection by *B. anthracis*, and highlights the general structure and utility of ABC transporters in many bacterial processes. Chapter 2 outlines the identification and first description of the multiple ABC transport systems that are required for the reacquisition of iron-bound petrobactin following the sequestration of iron from mammalian proteins during infection. The third chapter in this thesis takes a step further to investigate the utility of the ATPase components of the petrobactin ABC transport system as potential targets for the identification of inhibitors of petrobactin-associated iron acquisition.

This chapter aims to discuss the implications and future directions of this research, including a re-exploration of the fate of the siderophores petrobactin and bacillibactin during inhalational anthrax infection and a discussion of new avenues in the discovery of novel small molecule compounds that can serve as probes in the development of inhibitors against siderophore-associated iron acquisition.

4.2 Iron Release

Though ferri-petrobactin recognition and import has now been thoroughly studied, questions remain surrounding how the iron atom is released prior to usage by the bacterial cell (Carlson *et al.*, 2010, Dixon *et al.*, 2012, Zawadzka *et al.*, 2009a, Zawadzka *et al.*, 2009b). The strategy employed for iron removal largely depends on the affinity the chelator has for ferric iron (Miethke & Marahiel, 2007). Reduced ferrous iron is not bound strongly to siderophores, thus the overall reductive environment of the cytoplasm is sufficient for dissociation of iron from relatively weaker siderophores ($K_f \sim 10^{20}$) (Miethke & Marahiel, 2007, Harrington & Crumbliss, 2009). This mechanism has been speculated for desferrioxamine in which iron dissociation can be facilitated by general cellular reducing agents like FADH (Harrington & Crumbliss, 2009). In some instances, specific ferri-siderophore reductases have been identified, including FhuF and YqjH, which interact with hydroxamates and catecholates respectively in *E. coli* (Miethke *et al.*, Matzanke *et al.*, 2004). A unique example of reductases is found in *Mycobacterium* species in which iron reduction occurs extracellularly, and only the dissociated ion, as opposed to the siderophore-iron complex, is internalized (Ratledge, 2004). Tris-catecholate siderophores like bacillibactin and enterobactin (and its salmochelin derivatives) have the highest affinity for ferric iron of any known natural compounds, thus creating a redox potential unfavorable for conversion of bound iron to the ferrous ion, even enzymatically. In these instances, the siderophore must first be degraded by a specific hydrolase—FesA in *E. coli* and YuiI in *Bacillus* spp.—before iron liberation can occur (Miethke & Marahiel, 2007). Interestingly, specific siderophore degradation enzymes have also been observed in some cases that are not required for iron utilization,

and thus seemingly serve another unknown metabolic function (Tomisic *et al.*, 2008). The structure of petrobactin includes both carboxylate and catechol chelation points which combine to confer a unique, intermediate binding affinity for iron (Abergel *et al.*, 2008), thus the methods employed by *Bacillus* spp. for petrobactin iron release remain enigmatic as does the fate of the siderophore after interaction with the ABC transporter (Fig. 4-1, 4-2A). Future experiments to probe this are straight-forward in theory: whole cell extracts of *B. anthracis* grown under different conditions could be incubated anaerobically with petrobactin pre-complexed with iron. Because Fe^{3+}-catechol complexes are chromophores, iron release or reduction may be tracked colorimetrically while possible breakdown of petrobactin could be tracked via mass spectrometry. If iron release from petrobactin is reliant on enzymatic activity, this may represent yet another target in shutting down bacterial growth.

In an attempt to identify enzymes that are involved in petrobactin degredation, I have identified candidate siderophore esterase/peptidase and reductase genes in *B. anthracis*. In *Escherichia coli* and *Salmonella typhymurium*, iron is removed from their siderophore following breakdown of the molecule by the esterases Fes and IroD respectively. Multiple candidate genes have been identified based on sequence identity to these two esterases. The most attractive of these candidates is GBAA2694 which is upregulated under iron limiting conditions and has ~25% sequence identity to the separate proteins encoded by both *fes and iroD*. Gene products with high homology to canonical *E. coli* reductases have also been targeted for deletion. Often genes serving a concerted cellular function, like iron acquisition, are in close proximity on the bacterial genome. This is possibly the case with GBAA_1859-1860, encoding both a putative

degradation enzyme and a reductase that binds catechol chemical groups like those on petrobactin. The generation of mutant strains harboring deletions of all genes described is underway. O nce obtained, these strains await further testing in iron-depleted conditions.

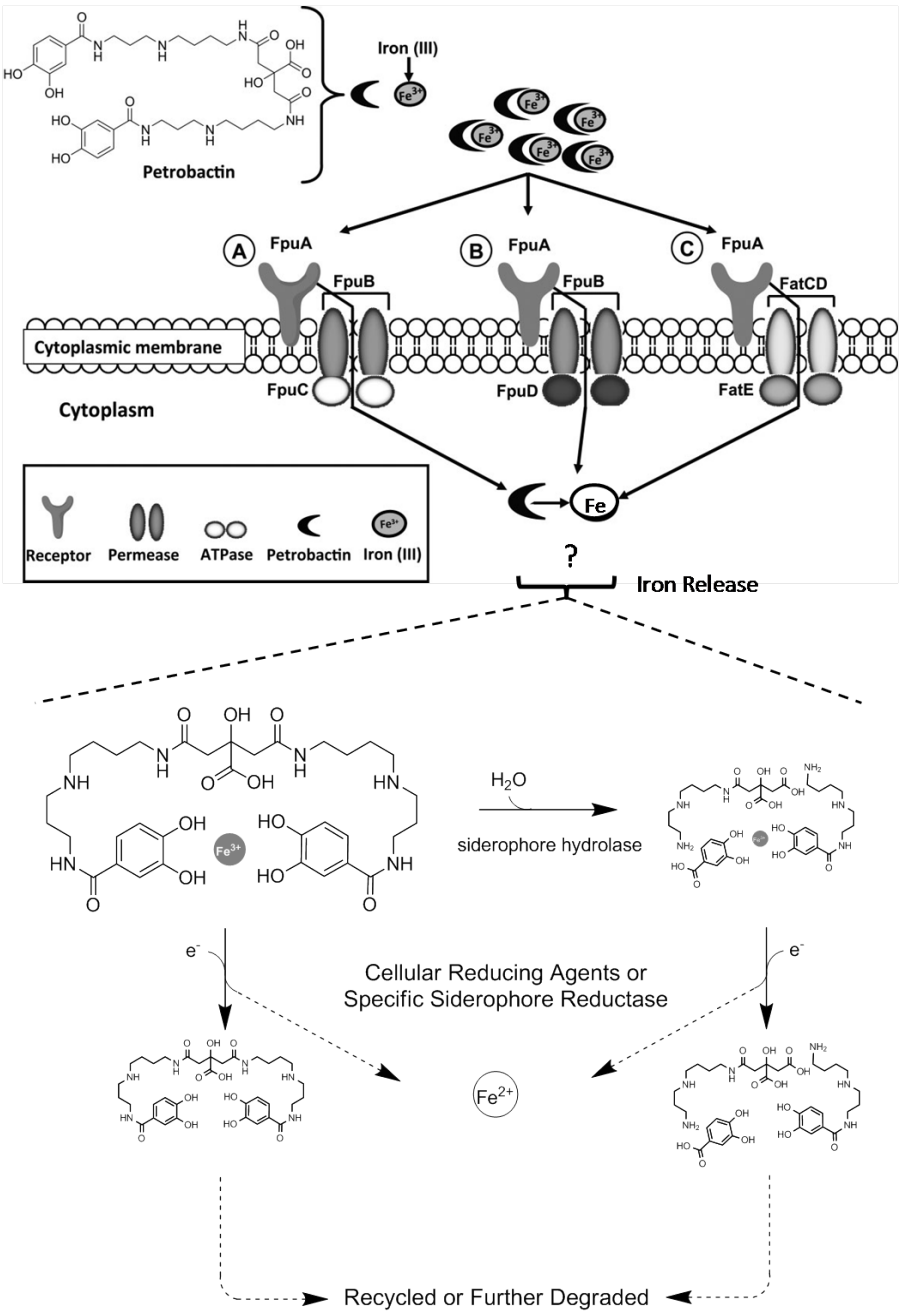

Figure 4-1. Hypothetical Iron Release Mechanisms of Petrobactin. Upon internalization of ferri-petrobactin via the ABC importers described in Chapter 2, iron must be released from the siderophore for use by the cell. The factors required for this have not been identified but may include hydrolytic enzymes as well as specific reducing agents.

4.3 Petrobactin Efflux and Cycling

While the preceding chapters have comprehensively outlined the process of ferri-petrobactin import, and previous reports have characterized biosynthesis of this siderophore, how petrobactin is secreted into the extracellular space to scavenge iron is still unknown (Fig 4-2A). There are a few examples of individual major facilitator superfamily (MFS) transporters previously identified as multi-drug resistance efflux pumps to also serve as siderophore exporters including NorA in the case of *S. aureus* (Deng *et al.*, 2012) and YmfE of *B. subtilis* (Miethke et al., 2008). Alternatively, iron response operons in *Azotobacter vinelandii* (CsbX), and *Bordetella pertussis* (AlcS) encode MFS exporters specific for their operons (Brickman & Armstrong, 2005, Page *et al.*, 2003). While no functional gene annotated as an exporter is associated with the petrobactin *asb* operon in *B. anthracis*, remnants of a downstream pseudogene resembling an ABC exporter component remain. Because it appears the capacity for petrobactin production was acquired by *B. anthracis* via horizontal gene transfer, it stands to reason that the ancestral *asb* operon was associated with an exporter of its own; however, its functionality over time could have been lost if compensated for by a functional homolog elsewhere on the *Bacillus* genome. Figure 4-2B depicts genes in *B. anthracis* str. Ames Ancestor with sequence homology to siderophore exporters of other species or genes annotated as exporters found in close association with *asb*-like clusters from marine microbes. Of these candidate genes, some are moderately up-regulated during iron starvation (Carlson *et al.*, 2009). Problematically, both ABC and MFS-type genes appear to be associated with petrobactin excretion in different species, and the

A

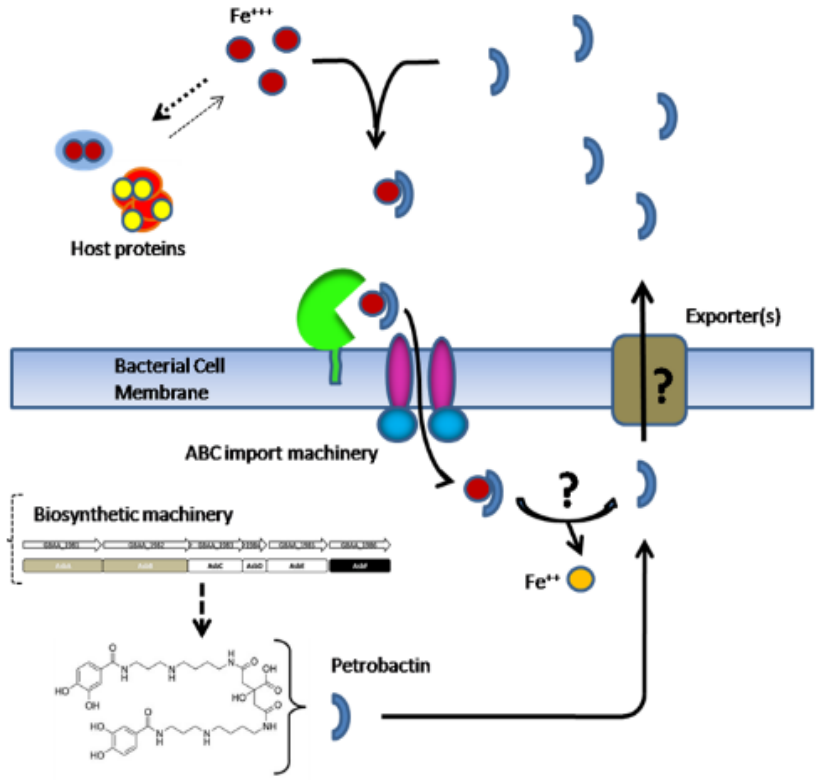

B

Locus #	Iron Starved Expression Change	NCBI Annotation	Homology to Known Siderophore Exporters
GBAA0528		ABC Exporter	asb-associated ABC transporter in Oceanimonasspp.
GBAA0787	upregulated 1.5-fold	MFS protein	NorA from S. aureus
GBAA0835		BIT, putative polyamine exporter	NorA from S. aureus
GBAA1642		MFS protein	asb-associated MFS in Marinobacter and Verrucomicrobium spp.
GBAA1858	upregulated 2-fold	MFS protein	NorA from S. aureus
GBAA2004		Multidrug Resistance Protein	CsbX from A. vinelandii and AlcS from B. pertussis
GBAA3296		MFS protein	asb-associated MFS in Marinobacter and Verrucomicrobium spp.
GBAA5411	upregulated 4-fold	ABC Exporter	asb-associated ABC transporter in Oceanimonas spp.

Figure 4-2. The Petrobactin Iron-Acquisition Pathway. A. Biosynthesis, iron-scavenging, and now uptake of petrobactin has been well studied. The mechanisms for iron release from the siderophore and its initial export from the *Bacillus* cell have yet to be elucidated. B. Candidate petrobactin exporter genes from *B. anthracis* str. Ames Ancestor based on homology to known siderophore exporters or genes associated with *asb*-like operons in other species.

inherent redundancy of Bacillus proteins, exemplified by the multiple importers in previous chapters, may make finding all exporters responsible for petrobacitn excretion via reverse genetics alone a daunting task.

Biosynthesis of siderophores is a metabolically costly activity. Looking past the depletion of primary metabolites like citrate and spermidine, *Bacillus* still expends at least 4 ATP in the construction of petrobactin (Nusca *et al.*, 2012, Oves-Costales *et al.*, 2009, Oves-Costales *et al.*, 2007, Pfleger *et al.*, 2007). Only a fraction of this expensive metabolite is taken back into the cytoplasm at the expense of another 2 ATP for re-uptake of the siderophore, accounting for import of a single iron atom (Dixon et al., 2012, Koster, 2001). Considering this, there is a clear advantage to a bacterial cell recycling imported petrobactin for another round of iron acquisition as opposed to solely relying on siderophore produced *de novo*. Indeed this strategy has already been suggested for pyoverdin in *P. aeruginosa* (Schalk et al., 2002) and aerobactin in *E. coli* (Braun et al., 1984). Affinity for iron is relatively low for aerobactin, thus its degradation is not necessary for release of the metal into the cytoplasm, allowing the intact aerobactin to be re-secreted to scavenge additional iron. Preliminary studies I conducted showed that growth rate of the siderophore-deficient strain Δ*asb* in iron-depleted medium was directly dependent on concentration of supplemented petrobactin when in the sub-micromolar range (Fig. 4-3A). Under these conditions, supplementation with as low as 10 nM exogenous petrobactin eventually restored growth of Δ*asb* to wild type levels (Fig. 4-3B). Considering the K_d of the SBP FpuA for ferri-petrobactin in *B. cereus* is an order of magnitude higher (175±35 nM), it is likely that the retarded growth is in part a result of slower binding of the siderophore just prior to ABC import (Zawadzka et al., 2009a). It is

hard to imagine how such a low concentration of petrobactin could facilitate the iron uptake necessary to drive cell division to the point of a saturated culture without recycling occurring, but this idea is partially contradicted by a decrease in extracellular petrobactin detected by mass spectrometry over time during the same experiment (Fig. 4-3C); however, this decrease does not account for the intracellular or surface bound-pool of petrobactin as cell-density increases in culture. It is likely that elucidation of the specific exporters and iron release mechanism for petrobactin utilization in *B. anthracis* will provide additional tools in determining whether or not petrobactin recycling occurs.

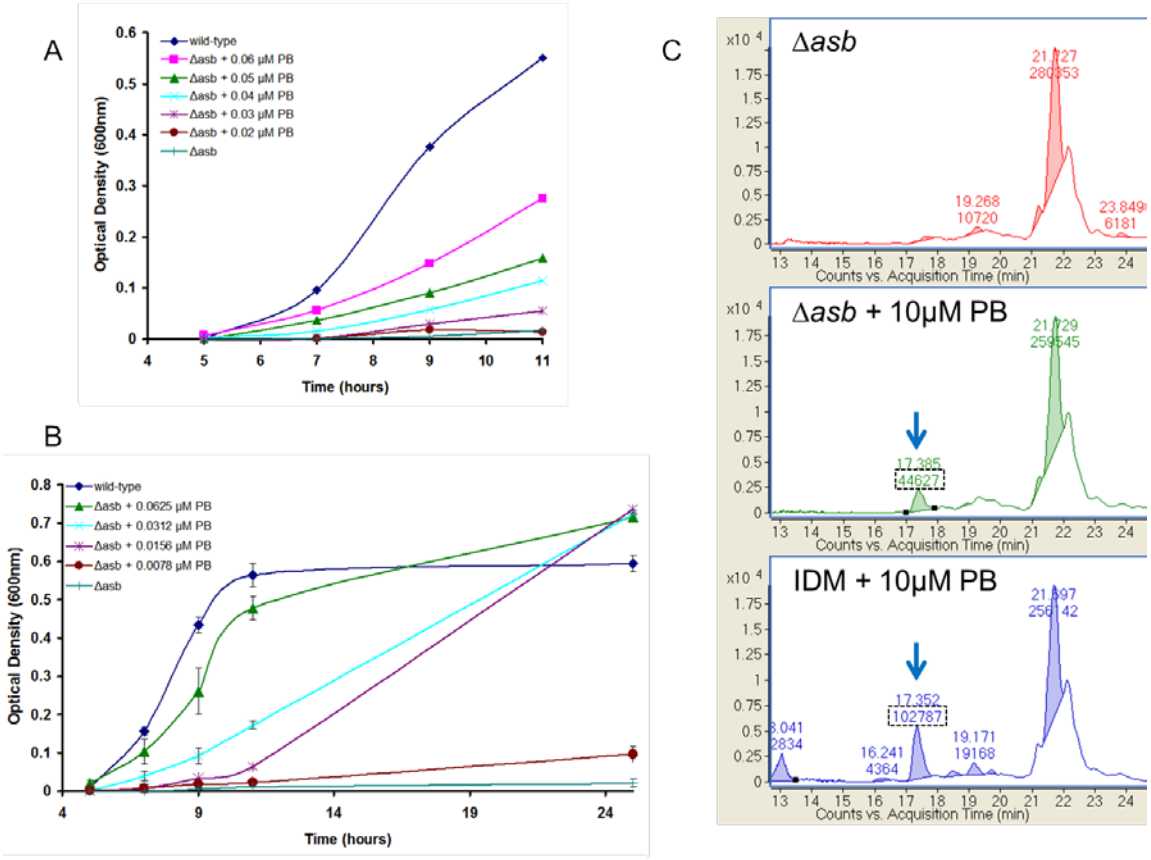

Figure 4-3. Sub-Micromolar Levels of Exogenous Petrobactin Restore growth of Iron-Depleted *B. anthracis* Cultures. A. A growth curve showing petrobactin-dependent recovery of Δ*asb* during iron-depleted growth. B. Under iron-depleted conditions, as low as ~16 nM of supplemental petrobactin recovers liquid Δ*asb* cultures to saturated levels. C. LC-MS analysis of culture supernatants at 6 hours show that the extracellular level of supplemented petrobactin (peak under arrow) diminishes compared to a no-cell control (IDM)

4.4 The Role of Bacillibactin

Previous microarray analysis in iron-depleted conditions shows one of the most up-regulated transcriptional units in *B. anthracis* is the *dhb* operon, responsible for biosynthesis of the ubiquitous *Bacillus* siderophore bacillibactin (Hotta *et al.*, 2010, May *et al.*, 2001). However, in the context of host infection and iron-depleted growth, *B. anthracis* has been shown to require petrobactin to facilitate necessary iron acquisition (Cendrowski *et al.*, 2004). The *asb* operon of petrobactin biosynthesis in turn is only transcriptionally upregulated ~1.5-fold during iron starvation (Carlson et al., 2009). Adding to this, despite the clear abundance of *dhb* mRNA, bacillibactin is not detected in cellular supernatant until many hours after cells have entered latent growth in liquid culture, and even then at relatively low levels (Wilson *et al.*, 2010, Lee *et al.*, 2011).

These observations raise the question of why the capacity to biosynthesize bacillibactin is conserved in *B. anthracis* despite its dispensability in infection. One possibility is that low levels of cytoplasmic bacillibactin are serving as a high-affinity shuttle or storage molecule for metals in the cell, perhaps even involved in handoff of iron from lower-affinity petrobactin. While not apparent in low-iron conditions, perhaps additional environmental stressors will demonstrate a phenotype for a Δ*dhb* mutant. These stressors may include high metal concentrations that would be sequestered by bacillibactin or infection via a gastrointestinal model, an environment shown to harbor trilactone siderophores analagous to bacillibactin (Henderson *et al.*, 2009). In the closely related soil microbes *B. cereus* and *B. thuringiensis*, bacillibactin is the exclusive siderophore and likely plays an important role for iron acquisition in the environment as well as infection of insects (Wilson *et al.*, 2006). In contrast, relatively little is known

about iron uptake of *B. anthracis* in non-dormant life cycles outside the mammalian host, but conserved genes not shown to be essential for infection may still have more importance in this context.

One unique aspect of the *dhb* operon in *B. anthracis* is the inclusion of three additional genes (GBAA_2374-2376) not typically present in other species (Fig. 4-4). These include an MFS family exporter typically involved in drug resistance or secondary metabolite excretion; a phosphopantetheinyl transferase for activating biosynthetic carrier proteins; and a gene of unknown function whose translated polypeptide has closest sequence homology to mRNA stabilizing cold-shock proteins. The function of these genes could be traced to bacillibatin utilization, especially considering that close homologs of the *sfp* gene required for biosynthesis and *ymfE* implicated in export of bacillibactin in *B. subtilis* are not found within the *B. anthracis* genome (Ollinger *et al.*, 2006, Miethke et al., 2008). Because bacillibactin production and utility is so low during mammalian infection though, a separate theory arises, in which the products of GBAA_2374-2376 are contributing to petrobactin up-regulation instead. Indeed, petrobactin biosynthesis is also reliant on the presence of a phosphopantetheinyl transferase and an efflux mechanism of the siderophore has yet to be elucidated. Furthermore, the lack of transcriptional change observed in the *asb* operon from high- to low-iron conditions suggest a post transcriptional step regulates the accumulation of petrobactin observed during this transition. Stabilization of *asb* mRNA by uncharacterized factors like GBAA_2376 or as of yet undefined sRNAs may contribute. Genetic analysis is now underway to probe any functionality the appended *dhb* operon of *B. anthracis* has in contributing to petrobactin production and survival in low-iron

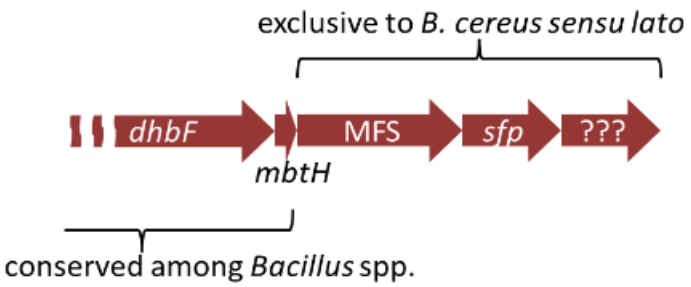

GBAA #	Annotation	Explanation
2372	*dhbF*	encodes the NRPS responsible for bacillibactin biosynthesis
2373	*mbtH*	shown in *Mycobacterium* spp. to stabilize NRPS adenylation domains
2374	major facilitator superfamily (MFS)	EmrB/QacA-like drug resistance exporter
2375	*sfp*	phosphopantetheinyl transferase for activating NRPS carrier domains
2376	unknown function	46% similarity to Af1396 in *Archaeoglobum spinosum*, located directly downstream of petrobactin importer orthologs in this organism

Figure 4-4. Unique Genes Associated with the Bacillibactin-Producing *dhb* Operon of *B. anthracis*. NCBI database annotation and putative function are noted.

conditions. If a connection can be found, it may in part explain the heightened transcription of *dhb* observed in *B. anthracis* str. Sterne despite the fact that very little actual bacillibactin is detected or required for circumstances mimicking host infection.

4.5 Xenosiderophore Recognition

Some organisms have the capacity to use siderophores produced by neighboring species in the environment. Certain species of plants are reliant on siderophore producing soil bacteria for optimal growth (Dudeja *et al.*, 2012). Meanwhile, many previously "unculturable" strains have been shown to be reliant on so-called "xenosiderophores" from symbiotic species (D'Onofrio *et al.*, 2010). More broadly, the genomes of many organisms have been isolated that encode no functional siderophore biosynthetic systems but still contain ABC genes homologous to well-characterized siderophore import (Stewart, 2012, Miethke & Marahiel, 2007, Abergel et al., 2008). Within crowded bacterial environments like soil or the gut, siderophore piracy is documented, as are biosynthetic countermeasures to prevent it (Traxler *et al.*, 2012, Indiragandhi *et al.*, 2008). An example of this is recognition of the triscatechol siderophore produced by *Enterobacteriace*, enterobactin, being recognized by its origin species as well as *Bacillus* spp.; meanwhile, ornate methylation of the analogous *Bacillus* siderophore bacillibactin allows this molecule to only be recognized by a narrow range of species (Peuckert *et al.,* 2011).

It is likely promiscuity for siderophore compounds is facilitated by the binding pocket of receptor domains on the siderophore ABC importers. While previous research by the Raymond group demonstrated two surface-associated lipoproteins, FpuA and

FatB, to be used in the *B. cereus sensu lato* group for petrobactin recognition (Zawadzka et al., 2009a), they appeared to have well-tuned affinities for different portions of the siderophore; FpuA, the only receptor shown to facilitate petrobactin import in *B. anthracis* (Carlson et al., 2010), interacts most tightly with the citryl moiety of petrobactin, suggesting analogous compounds with a similar central structure may also interact with the petrobactin import system (Zawadzka et al., 2009a). Preliminary data from a crossfeeding experiment in which supernatant from an aerobactin-producing strain of *E. coli* rescued iron-depleted growth of Δ*asb B. anthracis* supports this (Table 4-1). Considering the metabolic cost of synthesizing siderophores, there are many heterogeneous microbial environments that would make evolving promiscuous siderophore uptake machinery advantageous; this promiscuity may also confer more freedom in the design of siderophore-like compounds with additional antimicrobial activity.

	Strain tested				
Supernatant	**wild-type**	**Δ*asb***	**Δ*fpuA***	**Δ*fatB***	**Δ*fpuA*/Δ*fatB***
wild-type	1.0 cm	0.5 cm	0.6 cm	1.0 cm	ND
Δ*asb*	ND	ND	ND	ND	ND
CFT073 entF::kan	1.3 cm	1.0 cm	1.3 cm	1.2 cm	ND

Table 4-1. Evidence for Exogenous Siderophore Usage Mediated by the Petrobactin Receptors of *Bacillus*. *B. anthracis* strains grown on iron-deficient plates were supplemented with 20 µl supernatant collected at 6 hours from an iron-starved culture of *E. coli* CFT073 *entF*::kan . This strain produces the NIS-derived siderophore aerobactin, hypothesized to be recognized by the petrobactin SBP FpuA, which has an affinity for the citryl moiety shared by the two siderophores. While the catecholate sideorphore enterobactin is not present, the supernatant still contains the enterobactin precursor 2,3-DHBA, likely recognized by FatB, which has an affinity for catecholate moieties. Values are zone of growth diameters surrounding supernatant-soaked filter discs. ND = none detected.

4.6 Targeting *B. anthracis* Iron Import; The Search for a New Therapeutic

Siderophore production in pathogenic bacteria has gained considerable attention due to its often-crucial function in iron uptake and the relevance of siderophore-associated proteins as molecular markers of various infectious agents (Andrews *et al.*, 2003). Among catecholate siderophores from pathogenic microbes, eliminating petrobactin is particularly important as it escapes sequestration by the mammalian immune protein siderocalin (Abergel *et al.*, 2006, Fischbach *et al.*, 2006) and is required for virulence.

As touched upon in chapter 3, bacterial ABC-transport systems involved in the uptake of iron-siderophore complexes like petrobactin may serve as new targets for antibiotics that can treat anthrax infections and potentially many other bacterial infections. Importantly, eukaryotic ABC transporters have some structural deviations from bacterial systems (Rosenberg *et al.*, 2005, Higgins, 1992, Holland & A. Blight, 1999). For that reason, inhibitors of bacterial ABC transport components have a reduced likelihood of harmfully affecting mammalian cells, hence resulting in low toxicity when used therapeutically. The high level of attenuation observed with the *Bacillus anthracis* petrobactin ABC import mutants detailed herein further implicate the petrobactin ABC-transport system proteins as prime targets for the discovery of druggable inhibitors.

In the future, there will probably be many ways to improve upon this strategy. Further testing is required to truly determine the cross-reactivity of compounds analogous to the prelimiary FpuD inhibitor hits from Chapter 3, as there are both drawbacks and benefits to a broad-range inhibitor of bacterial ATPases. A drug's efficacy and indications may be more appealing from a pharmaceutical standpoint if many processes

or many different strains of bacteria are affected; however with a broad-spectrum drug, the specificity for only pathogenic bacteria is diminished and the likelihood of resistances arising is elevated.

One strategy to improve specificity for compounds targeting petrobactin import, is to take into account the specialized receptor lipoprotein of the ABC transport complexes in the system described in Chapter 2, FpuA. While not enzymatic, and therefore more difficult to characterize, interaction of purified FpuA with small molecules has been tracked with fluorescence polarization (Zawadzka et al., 2009a), and this may be utilized in a high-throughput screen to look for potent blockers of siderophore recognition. Alternatively, success has been had with "Trojan horse" antibiotics against other pathogens, including *M. tuberculosis*, *K. pneumonia*, and *Plasmodium* spp., in which analogs of desired compounds for import (e.g. ferri-siderophores) are used, but contain an antimicrobial "warhead" functionality (Miethke & Marahiel, 2007, Miller *et al.*, 2011). This encourages specific uptake by the target pathogen and a reduced MIC from that of the parent antimicrobial compound. With regard to inhibiting ABC importer ATPases like FpuD, this strategy is even more practical as the target protein for inhibitor delivery is in the same cellular location as where the Trojan horse compound would be internalized if analogous to petrobactin.

4.7 References

Abergel, R. J., M. K. Wilson, J. E. L. Arceneaux, T. M. Hoette, R. K. Strong, B. R. Byers & K. N. Raymond, (2006) Anthrax pathogen evades the mammalian immune system through stealth siderophore production. *Proc Natl Acad Sci U S A* **103**: 18499-18503.

Abergel, R. J., A. M. Zawadzka & K. N. Raymond, (2008) Petrobactin-mediated iron transport in pathogenic bacteria: coordination chemistry of an unusual 3,4-catecholate/citrate siderophore. *Journal of the American Chemical Society* **130**: 2124-2125.

Andrews, S. C., A. K. Robinson & F. Rodriguez-Quinones, (2003) Bacterial iron homeostasis. *FEMS microbiology reviews* **27**: 215-237.

Braun, V., C. Brazelfaisst & R. Schneider, (1984) Growth-Stimulation of Escherichia-Coli in Serum by Iron(Iii) Aerobactin - Recycling of Aerobactin. *FEMS microbiology letters* **21**: 99-103.

Brickman, T. J. & S. K. Armstrong, (2005) Bordetella AlcS transporter functions in alcaligin siderophore export and is central to inducer sensing in positive regulation of alcaligin system gene expression. *Journal of bacteriology* **187**: 3650-3661.

Carlson, P. E., Jr., K. A. Carr, B. K. Janes, E. C. Anderson & P. C. Hanna, (2009) Transcriptional profiling of Bacillus anthracis Sterne (34F2) during iron starvation. *PLoS One* **4**: e6988.

Carlson, P. E., Jr., S. D. Dixon, B. K. Janes, K. A. Carr, T. D. Nusca, E. C. Anderson, S. E. Keene, D. H. Sherman & P. C. Hanna, (2010) Genetic analysis of petrobactin transport in Bacillus anthracis. *Mol Microbiol* **75**: 900-909.

Cendrowski, S., W. MacArthur & P. Hanna, (2004) Bacillus anthracis requires siderophore biosynthesis for growth in macrophages and mouse virulence. *Molecular microbiology* **51**: 407-417.

D'Onofrio, A., J. M. Crawford, E. J. Stewart, K. Witt, E. Gavrish, S. Epstein, J. Clardy & K. Lewis, (2010) Siderophores from neighboring organisms promote the growth of uncultured bacteria. *Chemistry & biology* **17**: 254-264.

Deng, X., F. Sun, Q. Ji, H. Liang, D. Missiakas, L. Lan & C. He, (2012) Expression of multidrug resistance efflux pump gene norA is iron responsive in Staphylococcus aureus. *Journal of bacteriology* **194**: 1753-1762.

Dixon, S. D., B. K. Janes, A. Bourgis, P. E. Carlson, Jr. & P. C. Hanna, (2012) Multiple ABC transporters are involved in the acquisition of petrobactin in Bacillus anthracis. *Molecular microbiology* **84**: 370-382.

Dudeja, S. S., R. Giri, R. Saini, P. Suneja-Madan & E. Kothe, (2012) Interaction of endophytic microbes with legumes. *Journal of Basic Microbiology* **52**: 248-260.

Fischbach, M. A., H. Lin, D. R. Liu & C. T. Walsh, (2006) How pathogenic bacteria evade mammalian sabotage in the battle for iron. *Nat Chem Biol* **2**: 132-138.

Harrington, J. & A. Crumbliss, (2009) The redox hypothesis in siderophore-mediated iron uptake. *Biometals : an international journal on the role of metal ions in biology, biochemistry, and medicine* **22**: 679-689.

Henderson, J. P., J. R. Crowley, J. S. Pinkner, J. N. Walker, P. Tsukayama, W. E. Stamm, T. M. Hooton & S. J. Hultgren, (2009) Quantitative Metabolomics Reveals an Epigenetic Blueprint for Iron Acquisition in Uropathogenic <italic>Escherichia coli</italic>. *PLoS Pathog* **5**: e1000305.

Higgins, C. F., (1992) ABC Transporters: From Microorganisms to Man. *Annual Review of Cell Biology* **8**: 67-113.

Holland, I. B. & M. A. Blight, (1999) ABC-ATPases, adaptable energy generators fuelling transmembrane movement of a variety of molecules in organisms from bacteria to humans. *Journal of Molecular Biology* **293**: 381-399.

Hotta, K., C. Y. Kim, D. T. Fox & A. T. Koppisch, (2010) Siderophore-mediated iron acquisition in Bacillus anthracis and related strains. *Microbiology* **156**: 1918-1925.

Indiragandhi, P., R. Anandham, M. Madhaiyan, G.-H. Kim & T. Sa, (2008) Cross-utilization and expression of outer membrane receptor proteins for siderophore uptake by Diamondback moth Plutella xylostella (Lepidoptera: Plutellidae) gut bacteria. *FEMS microbiology letters* **289**: 27-33.

Koster, W., (2001) ABC transporter-mediated uptake of iron, siderophores, heme and vitamin B12. *Research in microbiology* **152**: 291-301.

Lee, J. Y., K. D. Passalacqua, P. C. Hanna & D. H. Sherman, (2011) Regulation of petrobactin and bacillibactin biosynthesis in Bacillus anthracis under iron and oxygen variation. *PloS one* **6**: e20777.

Matzanke, B. F., S. AnemÃ¼ller, V. SchÃ¼nemann, A. X. Trautwein & K. Hantke, (2004) FhuF, Part of a Siderophoreâ''Reductase Systemâ€ *Biochemistry* **43**: 1386-1392.

May, J. r. J., T. M. Wendrich & M. A. Marahiel, (2001) The dhb Operon of Bacillus subtilisEncodes the Biosynthetic Template for the Catecholic Siderophore 2,3-Dihydroxybenzoate-Glycine-Threonine Trimeric Ester Bacillibactin. *The Journal of biological chemistry* **276**: 7209-7217.

Miethke, M., J. Hou & M. A. Marahiel, The Siderophore-Interacting Protein YqjH Acts as a Ferric Reductase in Different Iron Assimilation Pathways of Escherichia coli. *Biochemistry* **50**: 10951-10964.

Miethke, M. & M. A. Marahiel, (2007) Siderophore-Based Iron Acquisition and Pathogen Control. *Microbiol. Mol. Biol. Rev.* **71**: 413-451.

Miethke, M., S. Schmidt & M. A. Marahiel, (2008) The major facilitator superfamily-type transporter YmfE and the multidrug-efflux activator Mta mediate bacillibactin secretion in Bacillus subtilis. *J Bacteriol* **190**: 5143-5152.

Miller, M. J., A. J. Walz, H. Zhu, C. Wu, G. Moraski, U. Mollmann, E. M. Tristani, A. L. Crumbliss, M. T. Ferdig, L. Checkley, R. L. Edwards & H. I. Boshoff, (2011) Design, synthesis, and study of a mycobactin-artemisinin conjugate that has selective and potent activity against tuberculosis and malaria. *Journal of the American Chemical Society* **133**: 2076-2079.

Nusca, T. D., Y. Kim, N. Maltseva, J. Y. Lee, W. Eschenfeldt, L. Stols, M. M. Schofield, J. B. Scaglione, S. D. Dixon, D. Oves-Costales, G. L. Challis, P. C. Hanna, B. F. Pfleger, A. Joachimiak & D. H. Sherman, (2012) Functional and structural analysis of the siderophore synthetase AsbB through reconstitution of the petrobactin biosynthetic pathway from Bacillus anthracis. *The Journal of biological chemistry* **287**: 16058-16072.

Ollinger, J., K. B. Song, H. Antelmann, M. Hecker & J. D. Helmann, (2006) Role of the Fur regulon in iron transport in Bacillus subtilis. *J Bacteriol* **188**: 3664-3673.

Oves-Costales, D., N. Kadi & G. L. Challis, (2009) The long-overlooked enzymology of a nonribosomal peptide synthetase-independent pathway for virulence-conferring siderophore biosynthesis. *Chemical Communications*: 6530-6541.

Oves-Costales, D., N. Kadi, M. J. Fogg, L. Song, K. S. Wilson & G. L. Challis, (2007) Enzymatic logic of anthrax stealth siderophore biosynthesis: AsbA catalyzes ATP-dependent condensation of citric acid and spermidine. *Journal of the American Chemical Society* **129**: 8416-8417.

Page, W. J., E. Kwon, A. S. Cornish & A. E. Tindale, (2003) The csbX gene of Azotobacter vinelandii encodes an MFS efflux pump required for catecholate siderophore export. *FEMS microbiology letters* **228**: 211-216.

Peuckert, F., Ana A. L. Ramos-Vega, M. Miethke, Clemens J. Schworer, Alexander G. Albrecht, M. Oberthur & Mohamed A. Marahiel, (2011) The Siderophore Binding

Protein FeuA Shows Limited Promiscuity toward Exogenous Triscatecholates. *Chemistry & Biology* **18**: 907-919.

Pfleger, B. F., J. Y. Lee, R. V. Somu, C. C. Aldrich, P. C. Hanna & D. H. Sherman, (2007) Characterization and analysis of early enzymes for petrobactin biosynthesis in Bacillus anthracis. *Biochemistry* **46**: 4147-4157.

Ratledge, C., (2004) Iron, mycobacteria and tuberculosis. *Tuberculosis* **84**: 110-130.

Rosenberg, M. F., R. Callaghan, S. Modok, C. F. Higgins & R. C. Ford, (2005) Three-dimensional Structure of P-glycoprotein: THE TRANSMEMBRANE REGIONS ADOPT AN AS YMMETRIC CONFIGURATION IN THE NUCLEOTIDE-BOUND STATE. *Journal of Biological Chemistry* **280**: 2857-2862.

Schalk, I. J., M. A. Abdallah & F. Pattus, (2002) Recycling of Pyoverdin on the FpvA Receptor after Ferric Pyoverdin Uptake and Dissociation in Pseudomonas aeruginosa†. *Biochemistry* **41**: 1663-1671.

Stewart, E. J., (2012) Growing Unculturable Bacteria. *Journal of bacteriology* **194**: 4151-4160.

Tomisic, V., S. Blanc, M. Elhabiri, D. Expert & A.-M. Albrecht-Gary, (2008) Iron(III) Uptake and Release by Chrysobactin, a Siderophore of the Phytophatogenic Bacterium Erwinia chrysanthemi. *Inorganic chemistry* **47**: 9419-9430.

Traxler, M. F., M. R. Seyedsayamdost, J. Clardy & R. Kolter, (2012) Interspecies modulation of bacterial development through iron competition and siderophore piracy. *Molecular microbiology* **86**: 628-644.

Wilson, M. K., R. J. Abergel, J. E. Arceneaux, K. N. Raymond & B. R. Byers, (2010) Temporal production of the two Bacillus anthracis siderophores, petrobactin and bacillibactin. *Biometals : an international journal on the role of metal ions in biology, biochemistry, and medicine* **23**: 129-134.

Wilson, M. K., R. J. Abergel, K. N. Raymond, J. E. Arceneaux & B. R. Byers, (2006) Siderophores of Bacillus anthracis, Bacillus cereus, and Bacillus thuringiensis. *Biochem Biophys Res Commun* **348**: 320-325.

Zawadzka, A. M., R. J. Abergel, R. Nichiporuk, U. N. Andersen & K. N. Raymond, (2009a) Siderophore-mediated iron acquisition systems in Bacillus cereus: Identification of receptors for anthrax virulence-associated petrobactin. *Biochemistry* **48**: 3645-3657.

Zawadzka, A. M., Y. Kim, N. Maltseva, R. Nichiporuk, Y. Fan, A. Joachimiak & K. N. Raymond, (2009b) Characterization of a Bacillus subtilis transporter for petrobactin, an anthrax stealth siderophore. *Proceedings of the National Academy of Sciences of the United States of America* **106**: 21854-21859.